

ABSTRACT

Title of Thesis: DETERMINATION OF THE DYNAMICS OF FELINE FOLLICLE METABOLISM

Jennifer L. Colvin, Master of Science, 2013

Thesis Directed By: Associate Professor Brian J. Bequette,
Department of Animal and Avian Sciences

The metabolism of feline follicles has been largely overlooked in reproductive science. The primary objective of this study was to determine differences in metabolite profiles and glucose carbon fluxes in feline follicles of different developmental stages and subjected to different developmental environments. Glycolytic flux, cholesterol (P <0.0001), pyruvic acid (P <0.0001), myo-Inositol (P =0.0003) and proline (P <0.0001) were higher in late versus early antral follicles. Serine (P =0.0085), threonine (P <0.0001), and valine (P =0.0025) were significantly higher in early antral follicles cultured *in vitro* than those derived directly from feline ovaries; however, glucose carbon flux was not significantly different. The current study suggests that early antral follicles undergo significant metabolic changes before progressing to the late antral stage. While it appears that early antral follicles have diminished capacity to progress to the late antral stage *in vitro*, it does not appear to be due to fundamental metabolic differences.

DETERMINATION OF THE DYNAMICS OF FELINE FOLLICLE METABOLISM

by

Jennifer L. Colvin

Thesis submitted to the Faculty of the Graduate School of the
University of Maryland, College Park in partial fulfillment
Of the requirements for the degree of
Master of Science
2013

Advisory Committee:

Dr. Brian J. Bequette, Chair (UMD)

Dr. Carol L. Keefer (UMD)

Dr. Nucharin Songsasen (NZI)

© Copyright by
Jennifer L. Colvin
2013

ACKNOWLEDGEMENTS

The successful completion of this project was due in large part to the collaborative efforts of several individuals. I would like to extend my sincerest thanks to my mentors and lab members whose continued attention was essential to the accomplishment of this Masters research project:

To my advisor Dr. Bequette, for his unfailing guidance;

To Dr. Keefer and Dr. Songsasen for the use of their facilities and knowledge;

To my lab members, Qiong Hu, Leslie Juengst, and Umang Agarwal, for their help with instrumentation and analysis;

To Marie Iwaniuk for her patience and help with the SAS program;

Finally, to my family whose constant support allowed me to achieve this goal.

TABLE OF CONTENTS

Acknowledgements.....	ii
Table of Contents.....	iii
List of Tables.....	vi
List of Figures.....	viii
Chapter 1: Literature Review.....	1
1.1. Introduction.....	1
1.2. Overview of Reproduction and the Reproductive Cycle in <i>felis catus</i>	3
1.2.1. The Follicular Phase: Proestrus & Estrus.....	4
1.2.2. The Luteal Phase: Metestrus and Diestrus.....	5
1.2.3. Interestrus.....	6
1.2.4. Anestrus.....	6
1.3. Embryonic Development of the Ovary and Primordial Follicles.....	6
1.4. Follicular Classification and Cell Types in Domestic Cats.....	8
1.4.1. Primordial Follicles.....	9
1.4.2. Primary Follicles.....	9
1.4.3. Secondary Follicles.....	10
1.4.4. Tertiary Follicles.....	11
1.5. Folliculogenesis and Oocyte Growth and Development.....	12
1.5.1. General Patterns of Folliculogenesis and Oocyte Growth.....	12
1.5.2. Dominance in the Domestic Cat.....	14
1.5.3. Additional Proposed Coordination Strategies.....	15
1.6. Historical Understanding of Follicle and Oocyte Metabolism.....	17
1.6.1. Follicle and Cumulus-Oocyte Complex Metabolism.....	17
1.6.1.1. Glucose Metabolism.....	18
1.6.1.2. Lactate Metabolism.....	19
1.6.1.3. Pyruvate Metabolism.....	20
1.6.1.4. Amino Acid Metabolism.....	20
1.6.1.5. Fatty Acids, Triglycerides, and Lipids.....	20
1.6.1.6. Additional Metabolic Markers.....	21
1.6.2. Oocyte Metabolism.....	22
1.7 Assisted Reproductive Technologies.....	23
1.7.1. Techniques Available.....	23
1.7.2. Issues with ART.....	27
1.7.3. Selection of Viable Follicles, Oocytes, and Embryos for Use in ART.....	29
1.7.3.1. Oocytes and Follicles.....	29
1.7.3.2. Embryos.....	30

1.8. Metabolomic Technologies.....	32
1.8.1. Measurement and Identification of Compounds.....	32
1.8.2. Metabolomics Applications.....	35
1.8.3. Metabolomics Applications in Reproduction.....	36
1.8.3.1. Follicle and Oocyte Evaluation.....	36
1.8.3.2. Embryo Evaluation.....	40
1.9. Fluxomic Technologies.....	42
1.9.1. Stable Isotope Tracers.....	43
1.9.2. Central Carbon Metabolism.....	45
1.9.2.1. Pyruvate.....	48
1.9.2.2. α -Ketoglutarate.....	49
1.9.2.3. Oxaloacetate.....	49
1.9.2.4. Acetyl CoA.....	49
1.9.3. Fluxomic Applications.....	50
1.9.4. Fluxomic Applications in Reproduction.....	52
1.10. Discussion.....	52
 Chapter 2: Metabolomic Analysis of Feline Follicles.....	 53
2.1 Introduction.....	53
2.2 Rationale and Hypotheses.....	55
2.3 Materials and Methods.....	55
2.3.1. Study Design.....	55
2.3.2. Follicle Collection and Storage.....	56
2.3.3. Sample Processing.....	58
2.3.4. Gas Chromatography-Mass Spectrometry Analysis.....	59
2.3.5. Metabolite Abundance Calculations.....	60
2.3.6. Statistical Analysis.....	60
2.4. Results.....	61
2.4.1. Metabolomics of <i>in vivo</i> derived follicles.....	62
2.4.2. Differences Between Follicles Derived <i>in vivo</i> and those cultured <i>in vitro</i>	67
2.4.3. <i>In vivo</i> Late Antral versus <i>in vitro</i> Cultured Early Antral Follicles.....	71
2.5 Discussion.....	75
2.5.1. Lipids: Fatty Acids, Cholesterol.....	76
2.5.2. Lactate and Pyruvate.....	77
2.5.3. Amino Acids.....	78
2.5.4. Myo-Inositol.....	81
2.5.5. TCA Cycle Intermediates.....	82
2.5.6. Partial Least Squares-Discriminant Analysis.....	82
 Chapter 3: Fluxomic Analysis of Feline Follicles.....	 84
3.1 Introduction.....	84
3.2 Rationale and Hypotheses.....	86
3.3 Materials and Methods.....	87
3.3.1. Study Design.....	87
3.3.2. Follicle Collection and Storage.....	88
3.3.3. Sample Processing.....	92

3.3.4. Gas Chromatography-Mass Spectrometry Analysis of Media and Follicles Samples.....	93
3.3.5. Flux Calculations.....	95
3.3.6. Statistical Analysis.....	98
3.4 Results.....	98
3.4.1. Differences Across Developmental Stages of Follicles Derived <i>in vivo</i> , Assessed via Spent Media.....	99
3.4.2. Differences Between Follicles Derived <i>in vivo</i> and Those Cultured <i>in vitro</i> , Assessed via Spent Media.....	104
3.4.3. Differences Between Late Antral Follicles Derived <i>in vivo</i> and <i>in vitro</i> cultured Early Antral Follicles.....	109
3.4.4. Differences Among Follicle Stages and Environmental Conditions, Through Direct Assessment of Follicles.....	114
3.5. Discussion.....	124
3.5.1. Non-Invasive Analysis of Follicles Metabolism.....	125
3.5.1.1. Glycolysis.....	125
3.5.1.2. Urea Cycle.....	129
3.5.1.3. TCA Cycle, PPP, and PEPCK-c.....	130
3.5.1.4. Partial Least Square Analysis Based on Results from Spent Media.....	137
3.5.2. Direct Analysis of Follicle Metabolism.....	137
Chapter 4: Concluding Remarks and Future Directions.....	139
Appendices.....	142
References.....	145

LIST OF TABLES

Table 1.1: Outcomes of ART cycles using fresh embryos derived from non-donor oocytes in 2003 and 2011 for different age groups in the United States.....	2
Table 1.2: Amino acid uptake and release corresponding to viable embryos in humans.....	41
Table 1.3: Crude mass isotopomer abundances (moles of tracer per 100 moles of tracee) for D-glucose.....	44
Table 1.4: Anapleurotic and catapleurotic amino acids related to krebs cycle intermediates.....	46
Table 2.1: Composition and company source information for follicle collection media.....	57
Table 2.2: Composition and company source information for calcium chloride solution.....	57
Table 2.3: Composition and company source information for maintenance media.....	57
Table 2.4: Composition and company source information for follicle culture media.....	58
Table 2.5: Metabolites identified in follicles by comparison to established metabolite libraries.....	61
Table 2.6: Relative proportions of metabolites in early and late antral follicles (n=9 per group) derived <i>in vivo</i>	63
Table 2.7: Relative proportions of metabolites in early antral follicles (n=9 per group) derived <i>in vivo</i> and cultured <i>in vitro</i>	68
Table 2.8: Relative proportions of metabolites in <i>in vitro</i> cultured early antral follicles and late antral follicles derived <i>in vivo</i> (n=9 per group).....	72
Table 2.9: Physiological and Media concentrations of selected amino acids.....	79
Table 2.10: Percent abundance of detected amino acids from the current study.....	81
Table 3.1: Composition and company source information for follicle collection media..	90
Table 3.2: Composition and company source information for follicle tracer culture media.....	90

Table 3.3: Composition and company source information for calcium chloride solution.....	91
Table 3.4: Composition and company source information for maintenance media.....	91
Table 3.5: Composition and company source information for follicle culture media.....	91
Table 3.6: Ions monitored for given metabolites in media and follicle samples	94
Table 3.7: Amino & Carboxylic Acids monitored via SIM and those compounds with which they are in equilibrium with.....	97
Table 3.8: Calculated flux through pathways of central carbon metabolism and glucose carbon contributions to selected intermediate pools, as calculated from Spent Media.....	100
Table 3.9: Calculated flux through pathways of central carbon metabolism and glucose carbon contributions to selected intermediate pools, as calculated from Spent Media.....	105
Table 3.10: Calculated flux through pathways of central carbon metabolism and glucose carbon contributions to selected intermediate pools, as calculated from Spent Media.....	110
Table 3.11: Calculated flux through pathways of central carbon metabolism and glucose carbon contributions to selected intermediate pools, as calculated from Follicles.....	115
Table 3.12: Calculated flux through pathways of central carbon metabolism and glucose carbon contributions to selected intermediate pools, as calculated from Follicles.....	118
Table 3.13: Calculated flux through pathways of central carbon metabolism and glucose carbon contributions to selected intermediate pools, as calculated from Follicles.....	121
Table 3.14: (a) Moles of tracer per 100 moles of tracee, as detected in early and late antral follicles.....	126
(b): Moles of tracer per 100 moles of tracee, as detected in early follicles derived <i>in vivo</i> and <i>in vitro</i>	126
(c): Moles of tracer per 100 moles of tracee, as detected in late antral follicles derived <i>in vivo</i> and <i>in vitro</i> cultured early antral follicles.....	127

LIST OF FIGURES

Figure 1.1: Morphology of a Secondary Follicle (Schematic).....	10
Figure 1.2: Morphology of a Graafian Follicle (Schematic).....	11
Figure 1.3: Connected pathways of carbon metabolism including glycolysis, gluconeogenesis, pentose phosphate cycle (PPP), and the krebs cycle (TCA Cycle).....	47
Figure 2.1: Metabolite Abundances in early versus late antral follicles (A), <i>in vivo</i> derived early antral follicles versus <i>in vitro</i> cultured early antral follicles (B), and <i>in vitro</i> cultured early antral follicles versus <i>in vivo</i> derived late antral follicles.....	64
Figure 2.2: Two-dimensional PLS-DA of early and late antral follicles	65
Figure 2.3: Three-dimensional PLS-DA of early and late antral follicles.....	66
Figure 2.4: Two-dimensional PLS-DA of early antral follicles collected directly from feline ovaries and early antral follicles cultured <i>in vitro</i>	69
Figure 2.5: Three-dimensional PLS-DA of early antral follicles collected directly from feline ovaries and early antral follicles cultured <i>in vitro</i>	70
Figure 2.6: Two-dimensional PLS-DA of late antral follicles collected directly from feline ovaries and early antral follicles cultured <i>in vitro</i>	73
Figure 2.7: Three-dimensional PLS-DA of late antral follicles collected directly from feline ovaries and early antral follicles cultured <i>in vitro</i>	74
Figure 3.1: Ion spectra of a sample of stock Tracer Culture Media with uncorrected APE's calculated.....	96
Figure 3.2: Ion spectra of a sample containing unlabeled (A) and a mixture of labeled and unlabeled (B) alanine with uncorrected APE's calculated.....	97
Figure 3.3: [M+3] alanine enrichment and pyruvate sources in early and late antral follicles derived <i>in vivo</i>	101
Figure 3.4: Two-dimensional PLS-DA of spent tracer media from early and late antral follicles.....	102
Figure 3.5: Three-dimensional PLS-DA of spent tracer media from early and late antral follicles.....	103
Figure 3.6: [M+3] alanine enrichment and pyruvate sources in early antral follicles derived <i>in vivo</i> and cultured <i>in vitro</i>	106

Figure 3.7: Two-dimensional PLS-DA of spent tracer media for early antral follicles collected directly from feline ovaries and early antral follicles cultured <i>in vitro</i>	107
Figure 3.8: Three-dimensional PLS-DA of spent tracer media from early antral follicles collected directly from feline ovaries and early antral follicles cultured <i>in vitro</i>	108
Figure 3.9: [M+3] alanine enrichment and pyruvate sources in late antral follicles derived <i>in vivo</i> and early antral follicles cultured <i>in vitro</i>	111
Figure 3.10: Two-dimensional PLS-DA of spent tracer media for late antral follicles collected directly from feline ovaries and early antral follicles cultured <i>in vitro</i>	112
Figure 3.11: Three-dimensional PLS-DA of spent tracer media from late antral follicles collected directly from feline ovaries and early antral follicles cultured <i>in vitro</i>	113
Figure 3.12: Two-dimensional PLS-DA of early and late antral follicles after incubation in tracer media.....	116
Figure 3.13: Three-dimensional PLS-DA of early and late antral follicles after incubation in tracer media.....	117
Figure 3.14: Two-dimensional PLS-DA of early antral follicles derived <i>in vivo</i> and cultured <i>in vitro</i> after incubation with tracer media.....	119
Figure 3.15: Three-dimensional PLS-DA of early antral follicles derived <i>in vivo</i> and cultured <i>in vitro</i> after incubation with tracer media.....	120
Figure 3.16: Two-dimensional PLS-DA of late antral follicles derived <i>in vivo</i> and early antral follicles cultured <i>in vitro</i> after incubation with tracer media.....	122
Figure 3.17: Three-dimensional PLS-DA of late antral follicles derived <i>in vivo</i> and early antral follicles cultured <i>in vitro</i> after incubation with tracer media.....	123
Figure 3.18: [M+2] glutamate and [M+2] proline enrichments in early and late antral follicles derived <i>in vivo</i>	130
Figure 3.19: Summary of metabolic shifts between early and late antral follicles derived <i>in vivo</i>	134
Figure 3.20: Summary of metabolic shifts between early antral follicles derived <i>in vivo</i> and those cultured <i>in vitro</i>	135
Figure 3.21: Summary of metabolic shifts between late antral follicles derived <i>in vivo</i> and early antral follicles cultured <i>in vitro</i>	136

Chapter 1: Literature Review

1.1. Introduction

A deeper understanding of mammalian reproduction has become a major focus in research and in modern society. While assisted reproductive efforts in humans, livestock, and endangered species are on the rise, challenges with assisted reproduction technologies (ARTs), in particular their overall low efficiency rates and paradoxically high number of multiple birth rates, continue to persist (**Table 1**). According to the Society for Assisted Reproductive Technology (2011), in the United States only 46% of ART cycles in humans less than 35 years of age resulted in a pregnancy. Of those pregnancies, nearly 40% resulted in twin, triplet, or higher order births. Low efficiencies are due to a combination of problems that can be encountered during ART in humans as well as in livestock and wild species. For example, low gamete quality, cryopreservation of gametes, suboptimal culture techniques or media, low embryo quality, compromised recipients, amongst other factors all contribute. Multiple births with ARTs are a result of widespread multiple embryo transfers, in order to increase the chance of a successful pregnancy.

Table 1.1: Outcomes of ART cycles using fresh embryos derived from non-donor oocytes in 2003 and 2011 for different age groups in the United States (Society for Reproductive Technology, 2003 and 2011).

	<35		35-37		38-40		41-42		>42	
	2003	2011	2003	2011	2003	2011	2003	2011	2003	2011
Number of Cycles Initiated	36178	39721	18508	19930	17396	20130	7635	10277	3213	6033
Pregnancy Rate (% of Cycles)	43.3	46.2	36.4	38.5	27.1	29.3	18.6	19.5	9.8	9.1
Live Birth Rate (% of Cycles)	37.5	40.1	30.4	31.9	20.2	21.6	11.2	12.2	4.5	4.2
Multiple Pregnancy Rate (% of Pregnancies)	39.9	32	34	28	28.3	22.4	17.6	15.6	7.9	10.6

Assessment of gamete quality for use in *in vitro* fertilization has remained limited, and fairly subjective, relying heavily on morphological markers. While the metabolism of gametes has been explored as a potential benchmark for quality in the past, a thorough understanding through direct measure has yet to be realized. Attaining a better understanding of the metabolism of gametes and embryos could lead to an improvement in outcomes of ARTs in mammalian species, achieved through better selection of oocytes and sperm for use in ART and through improved culture procedures. Using the domestic cat (*felis catus*) as the animal model, the aim of this research was to define developmental shifts in follicle metabolism by employing state-of-the-art metabolomic and ¹³C-fluxomic technologies. Ultimately, this basic information can be used to identify metabolic markers

of “healthy” follicles. Specific aims were to refine current protocols to optimize extraction of metabolites from follicles, to facilitate elucidation of the metabolic profile and pathway fluxes (^{13}C -fluxome) of follicles at different developmental stages and under differing environmental conditions. Future studies could use this metabolic information to refine culture protocols (e.g., media composition) to support the essential metabolic requirements of developing follicles (and oocytes). Overall, the procedures utilized in and results obtained from this research can be employed in practice to improve current ART approaches for successful culture and selection of viable gametes.

1.2. Overview of Reproduction and the Reproductive Cycle in *felis catus*

Female domestic cats, queens, become sexually mature between four and twelve months of age. Factors affecting the onset of puberty include the breed of cat, body weight of the animal, as well as time of year (Jemmett and Evans, 1977; Lofstedt, 1982). They are seasonally polyestrous animals who have several estrous cycles during spring and summer, when the hours of daylight per day increases (long day breeders). Cats are classified as induced or reflex ovulators, typically requiring the physical stimulation of a tom’s penile barbs during coitus to induce ovulation (Malandain *et al.*, 2011; Goodrowe *et al.*, 1989). However, it has been shown that external, environmental cues can also induce ovulation. Visual cues, such as the presence of other cats, and pheromonal cues have triggered ovulation in the domestic cat and in some wild felid species (Lawler *et al.*, 1993; Gudermuth *et al.*, 1997; Feldman and Nelson, 1996).

The estrous cycle of queens consists of several phases including the anovulatory follicular phases (proestrus and estrus), metestrus and diestrus if ovulation occurs, or interestrus if ovulation does not occur, and anestrus.

1.2.1. The Follicular Phase: Proestrus & Estrus

The proestrus period of the queen's estrous cycle is marked by affectionate behaviors that can also be observed during estrus, such as rubbing the head and neck on surrounding objects. In contrast to estrus, proestrus is not accompanied by receptiveness to breeding with toms (Feldman, 1996). This period is short in domestic cats and typically lasts only one or two days. Progesterone levels drop drastically during this period, allowing for an increase in production of gonadotropin releasing hormone (GnRH) from the hypothalamus. GnRH release is affected by a number of factors in addition to progesterone, including indirect affect by leptin, stimulation of release by kisspeptin, and in response to changes in photoperiod (d'Anglemont de Tassigny and Colledge, 2010; Quennell *et al.*, 2005; Hidahl *et al.*, 2013). GnRH causes increased release of follicle stimulating hormone (FSH) and luteinizing hormone (LH) from the anterior lobe of the pituitary. The increase in FSH stimulates the onset of follicular recruitment and allows for a continuing wave of follicle development from the activated reserves in the ovary. As the early antral follicles begin to enlarge and develop, LH acts on thecal cells to induce androgen production. The increase in androgens stimulates granulosa cell proliferation, causing an accompanying rise in estradiol levels in the blood as androgens are released. The rise in estradiol sparks behavioral estrus in the female, and begins vaginal cornification (Feldman, 1996; Shille *et al.*, 1979).

As estrus approaches, many of the follicles which had been recruited become atretic, while few are selected to continue development. As opposed to monotocous species, where one of the selected follicles becomes dominant, in cats three to seven selected follicles go on to become dominant, while the others become atretic (Feldman, 1996).

During estrus, which lasts approximately seven days, affectionate behaviors persist. Rubbing, vocalizing, presenting the hindquarters, expressing lordosis, and travelling rhythmically with the hind legs are all physical and behavioral signs of estrus which culminate in receptivity to breeding (Tsutsui and Stabenfeldt, 1993). Peak estradiol secretion is reached during the estrus phase, allowing for a surge in LH release (Feldman, 1996). The physical stimulus during mating (intensity and frequency) determines the level of LH release, and if adequate, results in the ovulation of oocytes from the preovulatory (dominant) follicles.

1.2.2. The Luteal Phase: Metestrus and Diestrus

If the queen is mated during estrus and ovulation occurs, she will enter a period of metestrus at which time the corpus luteum develops and progesterone secretion increases (Shille *et al*, 1979). During diestrus, functional corpora lutea (CL) are present, and progesterone reaches peak serum concentrations. If pregnancy results, progesterone levels remain high, and diestrus persists for approximately 60 days. If pregnancy does not result, the queen will experience a period of pseudopregnancy, which lasts about 40 days (Bristol-Gould and Woodruff, 2006).

1.2.3. Interestrus

If the queen does not ovulate during estrus, either due to a lack of mating or failure to ovulate during mating, she enters a period of interestrus, which lasts about seven days. At the completion of this period, the follicular phase of the estrous cycle begins again (Lofstedt, 1982).

1.2.4. Anestrus

During the periods of the year in which the queen is not actively cycling (winter and fall), the queen is in a period of anestrus. This period is marked by low concentrations of both estradiol and progesterone in the blood (Feldman, 1996).

1.3. Embryonic Development of the Ovary and Primordial Follicles

During embryonic development, mitotically active primordial germ cells migrate from the epithelium of the yolk sac to the genital ridge, drawn by chemotactic signals (Aerts and Bols, 2010). This invasion induces the formation of the gonadal cords, which further differentiate into the rete ovarii (Byskov, 1975). Mitotically active germ cells, upon arrival to the gonad and embedment, are termed oogonia (Aerts and Bols, 2010).

The oogonia, now surrounded by somatic cells (precursors of granulosa cells), continue a series of synchronous, incomplete mitotic divisions resulting in “cysts” joined by cytoplasmic bridges by which mitochondria and other organelles can be exchanged (Pepling and Spradling, 1998). Following several synchronized mitotic divisions, oogonia enter their first meiotic division. During this division, the cytoplasmic bridges degrade, and the somatic cells surrounding the cyst or “syncytium” begin to encapsulate individual oocytes. These primary oocytes enter a period of developmental arrest at the diplotene

stage of Prophase I (Cooper, 2000). The flattened somatic cells (granulosa cells) complete their encapsulation of individual primary oocytes and are separated from the ovarian stroma by a basal lamina which is deposited on their outer surface, completing the formation of the primordial follicles (Merchant-Larios and Chimal-Monroy, 1989).

This process of primary oocyte formation occurs at varying time points during embryonic development, depending on the species. In the domestic cat, the process begins at approximately 40-50 days of fetal development and reaches completion at 8 days after birth (Bristol-Gould and Woodruff, 2006). In cattle, fully formed primordial follicles can be found at 90 days of gestation (Aerts and Bols, 2010). It has long been accepted that female mammals are endowed with a finite reserve of these primary oocytes at the time of birth; however, the presence of germ stem cells in mammals after birth into adulthood is still hotly contested and under investigation (Fortune, 2003). It has been shown that in mice, germ stem cells persist after birth, but currently it is unknown as to whether other mammals, in particular the domestic cat, are born with or without germ stem cells (Johnson *et al.*, 2004).

At the shift from mitosis to meiosis, mammals have their highest number of germ cells, most of which will go through apoptosis prior to the animal's birth. The perinatal reduction in germ cell numbers has previously been associated with the breakdown of cysts and the degradation of their cytoplasmic bridges (Ratts *et al.*, 1995). The total number of primordial follicles present at this transition, and the degree of reduction, appears to be species dependent. In humans, a maximum of roughly seven million primordial germ cells are present at this transition, with only about 28.6% surviving until birth (Pepling and Spradling, 2001). In cows, the reduction is even more drastic, with about 2.1 million

primordial germ cells existing at the transition, dropping by about 94% to roughly 130,000 at birth (Erickson, 1966a,b).

The ovaries at the time of birth are complex organs containing several differentiated cell types, all of which work together to achieve healthy organ function (Bristol-Gould and Woodruff, 2006). The gross anatomy of the ovary consists of an outer cortex surrounding a central medulla. The cortex is encapsulated within collagenous connective tissue, the tunica albuginea, which has a single layer of cuboidal epithelial cells on its perimeter. Lymphatic and cardiovascular vessels, as well as nerve fibers, reside within the medullary region of the ovary. The cortical region houses the primordial and primary follicles, which are tightly embedded in elastin fibers, fibroblasts, and collagen (Aerts and Bols, 2010).

1.4. Follicular Classification and Cell Types in Domestic Cats

The mammalian follicle consists of several differentiating cell types, and holds at its core a single oocyte encapsulated within granulosa cells. The follicle is fundamentally responsible for facilitating the development of a viable oocyte, as well as producing hormones and steroids essential to normal female reproduction. Follicle classifications have been established to describe developmental stages in order to understand follicle progression and to allow for systematic study. These classifications ultimately describe the follicles based on cell types present and their morphology, and they also indicate the approximate size of the follicle. The most common terminology used to denote mammalian follicle stages describes four major classes: primordial, primary, secondary, and tertiary follicles. More specific terminology and subclasses exist and are species-specific (Aerts and Bols, 2010).

1.4.1. Primordial Follicles

Primordial follicles are the earliest developmental stage, and consist of a quiescent oocyte, arrested in Prophase I, surrounded by a singular layer of granulosa cells. In cats, there are three subclasses of primordial follicles: B Class, B/C Class, and C Class (also called Primary Follicles which will be discussed below). B Class primordial follicles consist of an oocyte which is roughly 20-30 μm in diameter, surrounded by a single layer of squamous granulosa cells. Anywhere from one to eight granulosa cells can be present at this stage and directly surrounds the oocyte. B/C primordial follicles, or transitory primordial follicles, have entered the first growth phase and contain both squamous and cuboidal granulosa cells in a singular layer surrounding the oocyte (Bristol-Gould and Woodruff, 2006; Gougeon and Chainy, 1987; Meredith *et al.*, 2000).

1.4.2. Primary Follicles

Primary follicles, also called Class C Primordial follicles, continue to grow and develop beyond their predecessor primordial follicles. Their growth is accompanied by an increase in size of the enclosed oocyte, which now ranges from 30 to 50 μm in diameter. These follicles are distinguished by a single layer of uniformly cuboidal granulosa cells surrounding the oocyte. This class of follicle is completely isolated from the ovarian stroma by a basement membrane (Bristol-Gould and Woodruff, 2006).

1.4.3. Secondary Follicles

Secondary follicles have entered a secondary growth phase, and are identified by the presence of two or more layers of cuboidal granulosa cells surrounding the oocyte. Their size varies depending upon the number of layers of granulosa cells present, but typically ranges from 100 to 400 μm in diameter. The multiple layers of granulosa cells surround the oocyte, which at this point is between 40 and 75 μm in diameter. In addition to granulosa cell layers, these follicles also contain a theca cell layer which is distributed opposite the basement membrane to the granulosa cells (Bristol-Gould and Woodruff, 2006). At this point in follicular development the zona pellucida has already begun formation and is easily detected around the oocyte (**Figure 1.1**) (Fair, 2003).

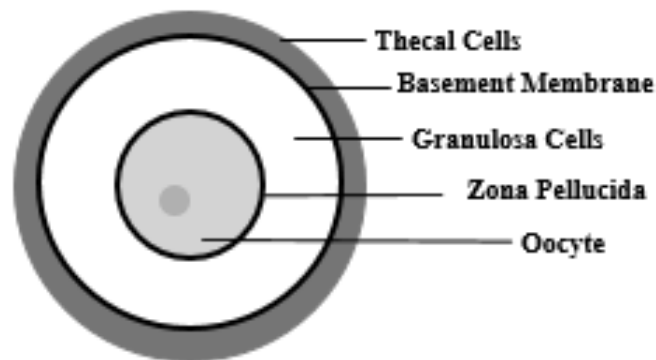


Figure 1.1: Morphology of a Secondary Follicle (Schematic).

1.4.4. Tertiary Follicles

Tertiary follicles are distinguishable from other developmental stages by the formation of fluid-filled cavities. Early antral formation begins as several isolated pools developing within the granulosa layers, which eventually increase in size and unite into a single antrum (Smitz and Cortvrindt, 2002). Additional distinguishing characteristics of early antral follicles include the presence of two or three layers of thecal cells bordering the basement membrane. Late antral follicles, however, contain many layers of thecal cells, divided into two categories, the interna and externa, distinct mural and cumulus granulosa cell layers, as well as a single, large antrum (**Figure 1.2**). These late antral follicles are aptly located at the perimeter of the ovarian cortex, poised for ovulation (Bristol-Gould and Woodruff, 2006). These follicles vary greatly in size depending on the stage of development of the antrum. Smaller, early antral follicles can be between 300 and 1000 μm in diameter, surrounding an oocyte 75 to 90 μm in diameter, while late antral follicles or Graafian follicles can range from 2000 to 3000 μm in diameter, housing an oocyte 85 to 100 μm in diameter.

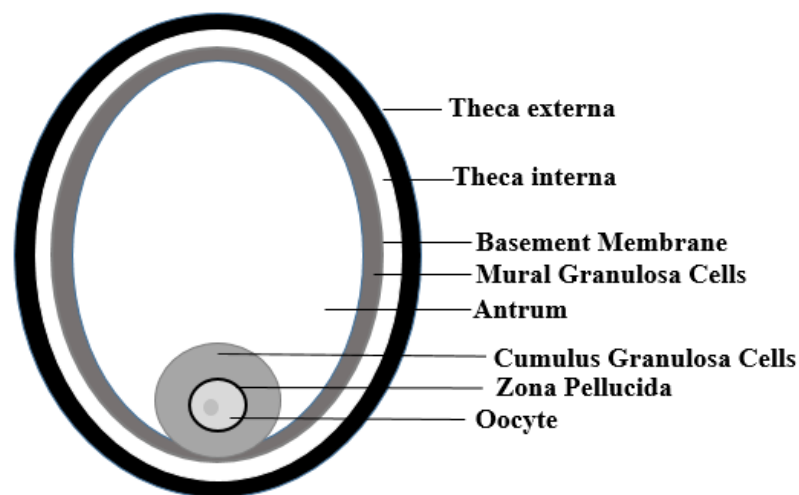


Figure 1.2: Morphology of a Graafian Follicle (Schematic). Adapted from Aerts and Bols, 2010.

1.5. Folliculogenesis and Oocyte Growth and Development

1.5.1. General Patterns of Folliculogenesis and Oocyte Growth

At birth, most mammals are born with a finite ovarian reserve of primordial follicles. In many livestock species and in humans, upon attainment of sexual maturity, groups of quiescent primordial follicles begin to mature in waves, during a highly coordinated process known as folliculogenesis. While it is known that a vast number of these dormant primordial follicles are activated to begin growing and maturing, the mechanisms by which this occurs, and by which follicles are selected for dominance, are largely unknown and still being explored (Jewgenow and Goritz, 1995; Aerts and Bols, 2010). Conversely, the pattern of follicle development in cats is not as well understood, and is complicated by the fact that they are induced ovulators.

In cattle, follicles are initiated to develop in two or three waves. The first wave is initiated on the day of ovulation of the previous cycle, the second 9-10 days later (two wave) or 8-9 days later (in cows with three waves), and on day 15-16 (if three waves). In cattle, only the dominant follicle of the second wave (if two waves develop) or the third wave (if three waves are present) is ovulated.

The ovarian reserve of primordial follicles is dormant prior to puberty, and is marked by relatively quiescent transcription and translation. The oocytes enveloped in these primordial follicles are arrested at the diplotene stage of Prophase I. The activation of folliculogenesis is gonadotropin independent, that is, primordial follicles develop to the primary follicle stage free from the control of FSH and LH. Evidence suggests that this initial stage of activation requires KIT ligand (KL) from granulosa cells to bind to KIT tyrosine kinase receptors on the oocyte. This prompts oocyte survival and growth, which

in turn stimulates granulosa cell proliferation (Parrott and Skinner, 1999; Kidder and Vanderhyden, 2010). At this transition, follicles are considered to be committed to continued development; however, atresia is the fate of most of these follicles rather than survival.

These primary follicles continue to develop through to the late preantral or early antral stage independent of the control of FSH. In cattle, many growth factors are involved during this process (Lucy, 2007). Bone morphogenic proteins (BMPs) and receptors, as well as epidermal growth factors (EGFs) are among the members of the transforming growth factor- β superfamily (TGF- β) which contribute (McNatty *et al.*, 2005; Knight and Glistler, 2006). Insulin-like growth factors also contribute during this period of development (Lucy, 2000). Throughout this time course, the oocyte begins to grow and accumulate mass, which is only achievable because it does not divide. Once the early antral phase is achieved by the maturing follicles, the recruitment process occurs. Due to increasing levels of circulating FSH, which acts as a “survival factor” for these follicles, several are recruited to continue development, escaping the atretic fate of the other follicles in the cohort.

Of the recruited early antral follicles, one or more are selected to continue development, depending on the ovulatory pattern of the species, while the others become atretic. It has been suggested that during this process, growing follicles secrete inhibin and estradiol, decreasing FSH release, and aiding in the selection process (Aerts and Bols, 2010). Throughout this process of selection, all selected antral follicles retain their ability to become dominant follicle(s).

The number of follicles which attain dominance and survive in each wave is dependent upon the species (Kidder and Vanderhyden, 2010). In monovular species, such as bovids and equids, generally only a single dominant follicle will be present; conversely, in polyovular species, such as felids and canids, multiple dominant follicles will be present. When the largest follicles of the cohort attains their maximal size, a differentiation occurs between those follicles which achieve dominance, and the subordinate follicles. All selected follicles had the capacity to become the dominant follicle(s); however, post-differentiation, only those that have achieved dominance have the potential to ovulate, while the subordinates simply regress in size. Vascularization of the thecal layer is of utmost importance during the process of achieving dominance. Factors which promote vascularization in cattle include vascular endothelial growth factor, angioproteins, and basic fibroblast growth factor (Tamanini and DeAmbrogi, 2004; Berisha and Schams, 2005). Of those follicles which obtain dominance, only those follicles belonging to the second wave, in a cow with a two-wave pattern, or those belonging to the third wave, in the case of a three-wave pattern, are actually ovulated, while the dominant follicles of the first and second (in the case of a three wave pattern) become atretic.

Due to the wave-like nature of activation, recruitment, selection, and dominance, at any point in time there are follicles at almost every stage of development in the ovary (Bristol-Gould and Woodruff, 2006).

1.5.2. Dominance in the Domestic Cat

Malandain *et al.* (2011) found that on the first day of estrus in domestic cats, roughly four to five follicles were healthy dominant follicles, with a range of two to seven

per female cat. Their mean diameter was 2.3 ± 0.01 mm on the initial day of estrus, and they continued to grow $0.2 (\pm 0.04)$ mm per day, with at least one follicle in the cohort measuring 3.0 mm by the end of behavioral estrus. The maximum size of the dominant, preovulatory follicles was $3.5 (\pm 0.04)$ mm, reached approximately 3.8 days after the onset of estrus. If ovulation was not achieved, the dominant follicles became atretic and decreased in size, largely due to the collapse of the formed antrum. It is important to note, however, that during estrus, the growth of dominant follicles is not wholly synchronous. The ultimate size of the dominant follicles, as well as number of days from the onset of estrus it takes them to reach maximum diameter, varies between follicles and cohorts. The size can easily be monitored using transabdominal ultrasonography techniques, which are a more reliable indicator of follicular size than behavioral observation, vaginal smears, or estradiol assays from serum (Malandain, 2011).

1.5.3. Additional Proposed Coordination Strategies

Coordination of this highly complicated process is extremely dependent on cell to cell communication within the follicle – including communication between somatic cells and between somatic cells and the oocyte. While paracrine factors and direct communication via gap junctions are well documented, many methods of communication have been proposed.

In addition to being involved in the initial activation of primordial follicle growth, KL and the receptor c-kit are also involved in the coordination of thecal cell growth, steroid (androstenedione) production, and differentiation in bovine follicles. Granulosa cells produce kit-ligand in increasing amounts as follicles increase in size; however, c-kit

receptor abundance does not increase in the same size-dependent manner (determined by total RNA measured via reverse transcription PCR). Still, it suggests that KL/c-kit interactions play an increasing role in supporting growth and steroid production for dominant follicles (Parrott and Skinner, 1995).

Fibroblast growth factors (FGFs) have been associated with the coordination of folliculogenic events as well. In several species, including the rat and cow, FGF-2 from the oocyte has been implicated in the stimulation of primordial follicle growth, in their transition to primary follicles, and in recruitment (van den Hurk and Zhao, 2005). A similar pattern is observed in canids. For dogs not in a period of anestrus, FGF-2 is localized in the oocyte and granulosa cells of primordial, primary, and secondary follicles. FGF-7 localization was dependent upon follicular stage: being found in granulosa cells in primary follicles, granulosa and theca cells in secondary follicles, and only in the thecal cells of antral follicles during the proestrus and estrus reproductive phases (Songsasen *et al.*, 2009).

In mares, membrane enclosed vesicles, “microvesicles”, and exosomes have been proposed as a mode of communication within the follicle. Microvesicles and exosomes located in the follicular fluid of equine antral follicles are taken up by proximal granulosa cells. The exosomes contain known exosomal proteins, while both the microvesicles and the exosomes contain micro-RNA (miRNA). The miRNAs found within these structures were also isolated from surrounding mural and cumulus cells, suggesting the exosomes and microvesicles were taken up from the follicular fluid. Interestingly, the amount and types of miRNA isolated varied between in mares of different ages, which could suggest a reason for altered fertility during aging (da Silveira *et al.*, 2011).

1.6. Historical Understanding of Follicle and Oocyte Metabolism

The process of follicular growth and development is a very energy-dependent process; however, the metabolic processes by which follicles and oocytes obtain this energy are not very well understood (Sutton *et al.*, 2003). Metabolic studies have historically focused on a limited number of exogenous substrates thought to be required by oocytes and follicles, and are hindered by the fact that substrate utilization is generally not measured directly, but rather through analysis of spent media (Biggers *et al.*, 1967; Brinster, 1971; Rieger and Loskutoff, 1994; Songsasen *et al.*, 2007; Spindler *et al.*, 2000; Gardner *et al.*, 2001; Sakkas *et al.*, 2008).

1.6.1. Follicle and Cumulus-Oocyte Complex Metabolism

Commercially available kits and photometric assays have been employed to study relationships between the concentrations of metabolites found in follicular fluid to their concentrations in serum. Leroy *et al.* (2004b) examined the levels of glucose, urea, total protein, non-esterified fatty acids, triglycerides, β -hydroxybutyrate (β -OHB), and total cholesterol in the serum and follicular fluid of high-producing dairy cows. It was found that in follicular fluid as compared to serum, glucose levels were much higher. Conversely, with the exception of urea and β -hydroxybutyrate, all other compounds were found at significantly lower concentrations in follicular fluid. A poignant finding was that metabolite concentration changes in follicular fluid mirrored the changes in serum throughout the study, cementing the importance of the follicular environment, whether *in vivo* or *in vitro*, to the metabolism of the follicle.

1.6.1.1. Glucose Metabolism

The pattern of glucose uptake and presence in follicular fluid is consistent across species: as follicle size increases, glucose concentrations in the fluid increase. Commercially available clinical analyzer kits have been used to determine the levels of glucose in follicular fluid of buffalo, heifer, and sheep follicles. In buffalo, follicular fluid concentrations of glucose in small follicles (<3mm) was 2.04 (\pm 0.25) mM, whereas significantly higher concentrations (2.74 \pm 0.21 mM) were observed in large follicles (>8mm). This trend was mirrored in sheep, which exhibited a glucose concentration of 1.18 (\pm 0.13) mM in small follicles (<2mm) and 1.64 mM in large follicles (>4mm) (Nandi *et al.*, 2008). In dairy cows, concentrations of glucose are also higher (3.75 \pm 0.18 mM) in larger follicles compared to smaller follicles (2.01 \pm 0.10 mM) (Leroy *et al.*, 2004a). In heifers, growing follicles (<8.5mm) exhibited glucose concentrations of 2.37 (\pm 0.95) mM in follicular fluid, while concentrations in preovulatory follicles (>8.5mm) were much higher (4.04 \pm 0.33 mM) (Nishimoto *et al.*, 2009).

This finding is supported through the monitoring of incorporation of fluorescent glucose analogs from culture media. It has been shown that granulosa cells facilitate glucose transport into the follicle, but limited quantities are delivered to the oocyte, due to the oocyte's reduced capacity for glucose uptake (Sutton-McDowall *et al.*, 2010). As follicle size increases, especially through early stages of development, the number of granulosa cells greatly increase, which allows for higher levels of glucose to be taken up from the surrounding environment.

The glycolytic pathway in the cumulus-oocyte complex (COC) – particularly in the cumulus cells – is a highly active pathway. In the granulosa cells, glycolytic activity

accounts for the majority of glucose utilization for ATP production as well as for the synthesis of substrates used by the oocyte. Due to the limited ability of oocytes to uptake glucose, granulosa cells preferentially metabolize glucose to pyruvate and lactate which the oocyte metabolizes for energy. It has been observed that glucose uptake increases during *in vitro* oocyte maturation; however, glycolytic activity (approximated by the disappearance of glucose, and appearance of lactate in spent media) does not reflect that increase (Sutton-McDowall *et al.*, 2010).

While the pentose phosphate pathway (PPP) only constitutes a small proportion of glucose metabolized by granulosa cells of the COC, it has been suggested that the oocyte has a much higher capacity for PPP activity (Sutton-McDowall *et al.*, 2010).

1.6.1.2. Lactate Metabolism

Follicular fluid concentrations of lactate appear to be inversely related to the concentration of glucose. Follicular fluid concentrations of lactate in small follicles from buffalo were 10.18 (\pm 1.04) mM, decreasing to 5.16 (\pm 1.02) mM in large follicles. In sheep, lactate concentrations of 14.12 (\pm 1.42) mM were observed in small follicles while 6.47 (\pm 0.84) mM was observed in larger follicles (Nandi *et al.*, 2008). In dairy cows, lactate in follicular fluid is also lower in large (5.6 \pm 0.37 mM) follicles compared to smaller follicles where concentrations were greater than two fold higher (14.4 \pm 0.35 mM) (Leroy *et al.*, 2004a). By contrast, in heifers, lactate concentrations in follicular fluid of growing follicles (5.43 \pm 0.82 mM) is higher than in preovulatory follicles (3.37 \pm 1.16 mM) (Nishimoto *et al.*, 2009).

1.6.1.3. Pyruvate Metabolism

Pyruvate concentrations do not appear to be dependent upon follicular development. Follicular fluid concentrations remain relatively constant across the range follicular sizes in buffalo and sheep, varying from 0.01 (\pm 0.01) mM to 0.04 (\pm 0.01) mM and from 0.001 (\pm 0.01) mM to 0.003 (\pm 0.00) mM in buffalo and sheep, respectively (Nandi *et al.*, 2008).

1.6.1.4. Amino Acid Metabolism

Recently, Guérin *et al.* (2012) reported one of the most comprehensive studies in cats, and the concentrations of amino acids in fallopian tube and follicular fluid aspirations. These authors found that the most abundant amino acids in feline follicular fluid were alanine (359 μ M), glutamine (351 μ M), and taurine (258 μ M); however, the most abundant amino acids in tubal fluid were glycine (840 μ M), glutamate (808 μ M), and taurine (596 μ M). Whole fluid samples were analyzed by high-performance liquid chromatography (HPLC).

1.6.1.5. Fatty Acids, Triglycerides, and Lipids

Fatty acid and lipid profiles vary among species and developmental stages of mammalian follicles. In dairy cows, concentrations of triglycerides significantly differed between follicle sizes, with the highest levels found in small follicles (21.8 ± 0.60 mg/dl) and the lowest in larger follicles (12.4 ± 0.45 mg/dl). Non-esterified fatty acids have also been measured in dairy cow follicles; however, concentrations were not observed to differ with follicle size, ranging from 0.47 (\pm 0.04) mM to 0.44 (\pm 0.08) mM (Leroy *et al.*, 2004a).

In studies considering murine, bovine, and porcine COCs, murine COCs had the lowest lipid concentrations, while porcine COCs exhibited the highest concentrations. Of all fatty acids, palmitic and oleic acids were the most abundant in immature bovine and porcine COCs. Paczkowski *et al.* (2013) evaluated the role of fatty acid beta-oxidation (FAO) in *in vitro* COC metabolism and viability when in the presence or absence of the FAO inhibitor etomoxir (carnitine palmitoyltransferase 1 inhibitor). Oocyte nuclear maturation was inhibited in all three species when FAO was inhibited, demonstrating that FAO is essential for oocyte nuclear maturation. In mice and cows, when etomoxir was added at concentrations which did not wholly prevent oocyte nuclear maturation, glucose consumption increased, suggesting that when FAO is compromised, glucose metabolism increases to fulfill the metabolic demands of the COC.

1.6.1.6. Additional Metabolic Markers

Determination of fractional oxygen concentration in aspirated follicular fluid from preovulatory follicles has been performed using fluorometric fiber-optic oxygen sensors. In Holstein cows, typical oxygen concentrations in the follicular fluid of preovulatory follicles is 6.9%. While it is known that heat stress can negatively affect fertility in dairy cows, oxygen consumption is not significantly affected (concentrations increased to 7.3%) (de Castro e Paula *et al.*, 2007).

Follicular steroid synthesis has been evaluated by determining the concentration of estradiol-17 β and progesterone in the preovulatory follicular fluid of Holsetin cows by radioimmunoassay. In cows with a preovulatory follicle, follicular fluid concentrations of estradiol-17 β were 1,264.5 (\pm 84.3) ng/mL while those of progesterone were 142.6 (\pm 12.7)

ng/mL. While heat stress is known to decrease fertility in cows, these authors did not observe differences in steroid concentrations in preovulatory follicular fluid from cows exposed to thermo-neutral conditions compared to those under heat stress conditions (de Castro e Paula *et al.*, 2007).

Several commercially available kits and photometric assays have been employed in the study of bovine follicular fluid and serum. Leroy *et al.* (2004a) examined the levels of urea, total protein, β -OHB, total cholesterol, and the electrolytes chloride, potassium, and sodium in follicular fluid of high-producing dairy cows. In large follicles, concentrations of β -OHB and total cholesterol were significantly higher, while those of urea, chloride and potassium were significantly lower compared to smaller follicles (Leroy *et al.*, 2004a).

1.6.2. Oocyte Metabolism

Radioactive isotope tracers of pyruvate, glucose, and glutamine have been used as probes to interrogate the metabolism of oocytes derived from cattle and dogs (Steeves and Gardner, 1999; Songsasen, 2012). Oocytes were cultured in maturation media, then transferred to a “hanging drop” on the lid of an Eppendorf tube containing a sodium bicarbonate trap to determine oocyte oxidation of the above substrates. For oocytes from adult cows, peak pyruvate metabolism was reached at 12 hrs of maturation, peak glutamine metabolism was achieved at 24 hrs (increasing linearly throughout maturation), while glucose metabolism increased throughout the 24 hr maturation period. A similar temporal pattern of substrate oxidation was also observed for bovine oocytes collected from prepubertal animals (Steeves and Gardner, 1999). Similarly, in dogs, oocytes achieving

nuclear maturation by 48 hrs had higher glycolytic rates than oocytes which arrested. In addition, metaphase II stage oocytes from larger follicles had higher rates of glutamine oxidation than same stage oocytes derived from smaller follicles (Songsasen, 2012).

1.7. Assisted Reproductive Technologies

In vitro culture (IVC) of gametes, follicles, and embryos, *in vitro* fertilization (IVF) of oocytes with sperm followed by embryo transfer (ET) to recipients, and artificial insemination (AI) of females are all ARTs that are currently employed in humans, livestock, and wild species (Yamamoto et al., 1999).

1.7.1. Techniques Available

To date, the only species that the entire processes of folliculogenesis (from primordial to late antral), oocyte maturation, fertilization and subsequent ET have been successfully achieved *in vitro* is the mouse. The success of this process is dependent upon many endocrine and paracrine factors, communication between the oocyte and follicular cells, as well as the culture media and conditions.

Preantral follicles can be isolated from ovaries enzymatically or mechanically. While enzymatic digestion of the ovarian cortex allows for greater numbers of recovered preantral follicles, their structural integrity is compromised. Mechanical isolation allows for lower recovery, but better preserves the follicle's three dimensional structure (Eppig and Schroeder, 1989; Demeestere *et al.*, 2002). Isolated follicles can be cultured under varying conditions, but typically, they are cultured under non-adherent conditions, attached to the culture dish, embedded within a collagen matrix, or cultured on collagen-

impregnated membranes (Torrance *et al.*, 1989; Eppig *et al.*, 1996; Cortvrintd *et al.*, 1996, Nayudu and Osborn, 1992).

To increase survival, it is critical that the three-dimensional structure of isolated follicles (whether preantral stage or later) is preserved during whole follicle incubation; however, the method of preservation presents a challenge – how to encase the follicle, yet allow for adequate substrate availability. Several methods have been employed to achieve these two goals, including follicle encapsulation in alginate hydrogel. Alginate hydrogels (0.5%) have been used successfully in several species for *in vitro* follicle culture, including human follicles. However, culture in alginate hydrogel can present unique challenges. For example, a high concentration of alginate (1-1.5% w/v) leads to a selective reduction in steroidogenesis and prevents follicular growth due to the encapsulation restricting the follicle during expansion. This issue tends to arise when culture is carried out for long periods of time (West *et al.*, 2007; Telfer and McLaughlin, 2011). Shikanov *et al.* (2011) proposed a method using fibrin-alginate interpenetrating networks. These provide the structural support of alginate hydrogels which the follicle requires, but also allows for normal expansion of the follicle as the fibrin-matrix degrades over time as a result of protease secretions from the follicle.

During *in vitro* culture of murine follicles, low concentrations of LH increase the follicle's capacity to form an antral cavity, as well as increasing oocyte meiotic maturation (Cortvintd *et al.*, 1998). FSH is required at levels of at least 10 mUI/mL (up to 100 mUI/mL) for successful intact preantral follicle culture. Survival rates in the absence of FSH are only 10-17% (Mitchell *et al.*, 2002; Cortvintd *et al.*, 1997; Nayadu and Osborn, 1992). FSH does not appear to be required for successful *in vitro* culture of COCs because

oocyte maturation can be achieved in the absence of FSH (Eppig and Shroeder, 1989). Fetal calf serum or hypogonadal mouse serum are typically added (5%) to intact follicle culture systems as a source of protein (amino acids) as well as to reduce the incidence of apoptosis (Mitchell *et al.*, 2002; Demeestere *et al.*, 2005). Ascorbic acid can also be added to serum-free culture media of intact follicles, or to culture media of COCs, to reduce the incidence of apoptosis (Eppig *et al.*, 2000).

Certain paracrine factors exhibit inhibitory effects on follicular growth *in vitro*. Interleukin-6 and tumor necrosis factor- α induce apoptosis, while administration of leptin suppresses follicular growth (Chun and Hsueh, 1998; Kikuchi *et al.*, 2001). Contradictory effects of anti-müllerian hormone on *in vitro* culture systems have been observed (Durlinger *et al.*, 2001; McGee *et al.*, 2001). Initial follicular recruitment is partially dependent upon growth differentiation factor-9 and BMP-15, both expressed by the oocyte, which stimulate granulosa cell proliferation (Hayashi *et al.*, 1999; Shimasaki *et al.*, 2004). In addition, interaction between c-kit (encoded in the oocyte) and KL (encoded in the granulosa cells) are responsible for initiation of follicular growth. This interaction has continued effects throughout antral follicle growth and differentiation (see review by Demeestere *et al.*, 2005). Addition of KL increases granulosa cell proliferation and oocyte maturation during *in vitro* culture of preantral follicles (Reynaud *et al.*, 2000). Addition of EGF at physiologic concentrations to *in vitro* culture media also increases the number of follicles that reach the antral stage (McGee *et al.*, 1997).

Fouladi-Nashta and Campbell (2006) have demonstrated that insulin has a positive effect on bovine follicular survival during *in vitro* culture at concentrations of 5 $\mu\text{g}/\text{mL}$ in

culture media. However, it was also shown that the addition of insulin can cause oocytes to prematurely achieve cytoplasmic maturation, before nuclear maturation is induced.

In vitro culture of ovarian explants from prepubertal mice with R-spondin2, a paracrine factor, allowed for the development of preantral follicles from the primary stage to secondary follicles (Cheng *et al.*, 2013). R-spondin2 provides a potential future treatment option for infertile females. In mice, *in vivo* administration of R-spondin2 to immature mice or those that were GnRH deficient, induced the development of primary follicles to the antral stage. In addition, subsequent administration of equine chorionic gonadotropic (eCG) allowed for dominant, preovulatory follicle development, and an administration of human chorionic gonadotropin (hCG) induced ovulation. Those oocytes released were competent and upon collection, were able to undergo successful *in vitro* fertilization (Cheng, 2013).

Oocytes ready for fertilization can be obtained either through superovulation and flushing of the oocytes, or via *in vitro* maturation of oocytes after follicle culture. The source of follicles and oocytes for *in vitro* culture, when maturation and eventual fertilization of the oocyte is the goal, is very important. Uchikura *et al.* (2010) has demonstrated that follicle size from which gametes are obtained, as well as the ovarian status from which the follicles are obtained, has a large effect on the maturational ability of feline oocytes. For mature cats, those oocytes which are collected from larger follicles (1200-2000 μm in diameter) have a higher *in vitro* maturation rate than those collected from smaller, earlier stage follicles. However, for oocytes isolated from smaller follicles (800-1200 μm in diameter) and cultured in maturation media *in vitro*, maturation rates were higher for those oocytes obtained from prepubertal cats, than from those obtained from

sexually mature cats. It is now possible in many species, with limited efficiency, to grow preantral follicles up to antral stage (Yamamoto et al., 1999).

Once oocytes have progressed to Metaphase II, fertilization with sperm (either fresh or cryopreserved) can be achieved either through *in vitro* fertilization, or through intracytoplasmic sperm injection, in which sperm are injected directly into the oocyte. This has proven useful to rescue valuable genetics from males with less than ideal sperm, or from those suffering from teratospermia, which is the case with many wild felids (Uchikura et al., 2011). After *in vitro* culture of embryos, they can be transferred to recipient females, where implantation, pregnancy and birth could result. This has been achieved in many species using oocytes from antral follicles; however, live young have only been successfully produced from *in vitro* grown and matured oocytes derived from preantral follicles in mice (Eppig and Schroeder, 1989).

1.7.2. Issues with ART

Some issues with ART arise simply because of stressors placed on donor animals. For example, heat stress has deleterious effects on the gametes of both female and male donors (e.g., DNA damage in epididymal sperm and lowered oocyte competence), as well as on early preimplantation embryos at the cleavage stage (Perez-Crespo et al., 2008; Ealy et al., 1993; Hansen, 2009). In the summer when heat stress is most prevalent, the diameter of dominant follicles, total cholesterol, and concentrations of glucose and insulin like growth factor-1, as measured in the follicular fluid, in cows is significantly lower than in winter. Conversely, concentrations of urea and non-esterified fatty acids are significantly higher in the summer than in winter (Shehab-El-Deen et al., 2010). Age is another stressor

affecting fertility of the donor animal. In mares, oocytes obtained from older donors result in significantly lower pregnancy rates after oocyte transfer and insemination. In addition, embryos produced via ICSI with oocytes from older donors result in decreased pregnancy rates after ET (Carnevale *et al.*, 2010).

Sustaining viability of selected follicles for culture, oocytes for fertilization, and embryos for transfer pose the largest hurdles for ART efficiency. In the case of follicle culture, preantral follicles isolated from feline ovaries experience a drastic drop in viability immediately upon isolation (32.5%). Depending upon the method of culture, follicle viability varies from 9.3% in conditioned medium to 37.5% with granulosa cell co-culture. Other culture methods examined included culture in monolayer (33.3% viability), in collagen gels (30.8%), and on an agarose pad (17.9%); generally, a slight increase in follicle size (10 μ m) was observed in the growing preantral follicles. A decrease in granulosa cells surrounding the oocyte was detected, but this issue could be partially prevented with the addition of epidermal growth factor and insulin-transferrin-selenite to the culture media during *in vitro* culture (Jewgenow and Göritz, 1995). Similar to these results, addition of EGF and FSH significantly increases maturation rate of buffalo oocytes during *in vitro* maturation (Raghu *et al.*, 2002). Finally, cryopreservation of preantral follicles resulted in a reduction of viability to 40% (Jewgenow and Göritz, 1995).

It is likely that the low efficiencies of *in vitro* techniques are due, at least in part, to the inadequate provision of the correct compilation of substrates. This has been a long standing issue that largely results from a lack of knowledge regarding follicle, oocyte, and embryo metabolism and nutrient utilization. There are several commercial media available for incubation; however, standardization of culture practices (e.g., culture media

composition, culture media practices, time in culture, culture temperature and atmospheric conditions) has not yet occurred in ART (Sepulveda *et al.*, 2009; Biggers and Summers, 2008; Nel-Themaat and Nagy, 2011). This prevents comprehensive evaluation of ART efficiencies across species and sample types, but also across laboratories and clinics utilizing the same species and samples

1.7.3. Selection of Viable Follicles, Oocytes, and Embryos for Use in ART

In order to overcome the issues of low efficiency, focus has shifted to finding biomarkers and other benchmarks for development, to determine which structures are of high quality and most likely to result in successful pregnancy and birth. While morphologic assessment of oocytes and embryos are common, it has been asserted that morphologic assessment alone provides more information regarding poor quality oocytes than an indication of a good quality oocyte (Revelli *et al.*, 2009).

1.7.3.1. Oocytes and Follicles

Glucose-6-phosphate dehydrogenase (G6PDH) activity, measured by brilliant cresyl blue (BCB) dye, has been used as a marker for viability of oocytes in mice, buffalo, cattle, goats, and pigs. High G6PDH activity is marked by an oocyte's ability to process the stain, converting it from blue to colorless; low G6PDH activity results in an oocyte's inability to convert the dye. Furthermore, low G6PDH activity is linked to oocytes which have completed their growth phase. Recently, Mohammadi-Sangcheshmeh *et al.* (2011) have demonstrated that those oocytes with low G6PDH activity have higher maturation rates than those with high G6PDH activity. In addition, those oocytes with an expanded

cumulus complex, larger oocyte diameter, and higher oocyte volume have lower G6PDH activity.

Vascular endothelial growth factor (VEGF) has been implicated for use as a biomarker for oocyte maturation. Studies of equine oocyte maturation in young and old mares have shown that, at least in older mares, levels of VEGF are significantly higher in mature oocytes than in immature or intermediate oocytes (Gündüz *et al.*, 2011). Levels of hormones, TGF- β , interleukins, and renin in the follicular fluid have also been proposed as potential biomarkers for follicle and subsequent oocyte viability (Arya, 2012).

1.7.3.2. Embryos

Historically, embryo developmental potential and viability have been determined by morphological assessment and cleavage rates. While these two techniques have improved the efficiency of ARTs, they have proven to be insufficient to bring efficiency rates to an acceptable level, and have not alleviated the issue of multiple pregnancies (Seli *et al.*, 2010).

Oxygen consumption by oocytes and embryos have been proposed as a primary screen for fertilization and developmental potential. While further testing is necessary with respirometers before implementation in a clinical setting, current studies suggest that oocytes and embryos with higher oxygen consumption are correlated with higher fertilization rates, morphological quality, and pregnancy rates (Nel-Themaat and Nagy, 2011).

Metabolic markers of viability, as measured by ultra-micro fluorescence assays, have also been proposed. While some contradictory results have been reported, the general

consensus is that early preimplantation embryos (cleavage stage and pre-compaction) are more reliant on carboxylic acids (i.e., pyruvate and lactate) for energy and carbon sources. Conversely, post-compaction morula and blastocysts switch to glucose utilization for energy and carbon (Seli *et al.*, 2010; Nel-Themaat and Nagy, 2011). This pattern has been observed in a number of species including humans, mice, rats, cattle, sheep, and pigs (reviewed by Ayinder *et al.*, 2010).

More recently, a cross-disciplinary approach has been proposed, uniting DNA microarrays, transcriptomics (via proton nuclear magnetic resonance (^1H NMR) spectroscopy), and metabolomics (via mass spectrometry (MS)) to provide an integrated approach to viability evaluation. Results for individual tests correlated, and transcript profiles corresponded to metabolite accumulation trends over time (Soanes *et al.*, 2011).

Preimplantation genetic screening employs genomic evaluation of embryos for viability. These tests generally rely upon fluorescent *in situ* hybridization (FISH), and are invasive, requiring removal of cells from the preimplantation embryo (Seli *et al.* 2010). Unfortunately, evaluation by this method typically results in lower sustained implantation rates, instead of increasing the efficiency of ARTs. Another analysis technique employs comparative genomic hybridization, which compares test DNA to “normal” control DNA, and can determine any instances of aneuploidy for all chromosomes. Transcriptomic analysis has also been employed to evaluate RNA transcripts located in the embryo as well as in cumulus and granulosa cells from oocytes used for IVF, but is difficult due to the rapid degradation of RNA. Proteomic evaluation has been explored; however, traditional methods are limited because of the amount of material needed for analysis. New techniques utilizing mass spectrometry analysis are promising for identifying proteins in

oocytes, but, protein information in databases is limited for many larger animals like humans and livestock species (Seli *et al.*, 2010).

1.8. Metabolomic Technologies

Metabolomics is the systematic analysis of the metabolic fingerprint of cells, tissues and organs that represents their functional phenotype. It can be more valuable and informative than its “-omics” technology predecessors (e.g., genomics, transcriptomics, and proteomics) because the metabolic information about the cell or tissue occurs downstream of genetic, enzymatic, and environmental controls. Therefore, metabolomics provides a greater understanding of the metabolism of cells, after they have been subjected to both intrinsic and extrinsic control factors. Untargeted metabolomics requires that identification and quantification is achieved in an unbiased manner for all metabolites present. Metabolites are small (<1 kDa), non-proteinaceous compounds present in a biological sample, including ATP, hormones, signaling molecules, metabolic intermediates, and secondary metabolites, which contribute to the maintenance, growth, and normal function of cells. The ultimate goal of metabolomics is to establish the metabolome, a complete profile of metabolites present in a sample or cell that defines the underlying dominance and connectivity of related metabolic pathways. (Botros *et al.*, 2008; Seli *et al.*, 2010; De la Luz-Hdez, 2012; McRae *et al.*, 2013)

1.8.1. Measurement and Identification of Compounds

Metabolites by their nature are very diverse in type, chemical and physical properties, and in relative abundance. The field of metabolomics is highly reliant upon

sample processing and procedure development to extract maximal quantities of metabolites and to yield highly reproducible analysis (Botros *et al.*, 2008; De la Luz-Hdez, 2012; McRae *et al.*, 2013). No one processing procedure and analytical platform (eg., gas versus liquid chromatography) is capable of covering the diverse range of metabolites present in all types of samples (Niwa, 1995). Extensive testing and optimization during development are necessary to determine the most appropriate processing approach and analytical platform suited for the sample type and the goal of the analysis. Additionally, extraction and derivatization (if required by the platform) methods must be tested for suitability across metabolite classes (Sobolevsky *et al.*, 2003; Koek *et al.*, 2006; Madla *et al.*, 2012). Derivatization methods routinely undergo testing and innovation to increase efficiency of derivatization (classes of compounds and completeness of derivatization) as well as the ease of preparation (Paik and Kim, 2004; Kouremenos *et al.*, 2010).

Metabolomics, although still in its infancy, has well established methods across many platforms. Metabolomics platforms include nuclear magnetic resonance (NMR) spectroscopy, mass spectrometry, gas chromatography-mass spectrometry (GC-MS), high pressure liquid chromatography, liquid chromatography-mass spectrometry (LC-MS), near infrared spectroscopy, fourier transformation infrared spectroscopy, and raman spectroscopy for applications across disciplines (Botros *et al.*, 2008; Ferreira *et al.*, 2010; De la Luz-Hdez, 2012). Mass spectrometry is a well-established platform for evaluation of drug-metabolite interactions and pharmacokinetics, and is now playing a larger role in metabolite profiling and characterization. Its ability to accurately monitor normal physiological events (metabolites), makes it a powerful tool to detect even slight deviations that characterize diseased states. Historically, GC-MS has been the preferred platform for

identification and quantification of metabolites. Newer platforms including NMR and LC-MS/MS have recently demonstrated advantages over GC-MS, including ease of sample preparation and expanded abilities to detect high and low molecular weight compounds (Want *et al.*, 2005; Koek *et al.*, 2010). Nevertheless, numerous mass spectral libraries are available for compound identification with GC-MS, which offers a distinct advantage over other platforms.

Generally, large sample volumes (>100 μL) are required for analysis on these platforms to obtain the minimum amount of each metabolite necessary for accurate detection (Koek *et al.*, 2010). However, sample size can be reduced through optimization of analytical platforms and innovative processing and derivatization techniques (Doherty, 2003). Indeed, recent studies report using “ultrasmall” samples with GC-MS and matrix assisted laser desorption ionization-mass spectrometry (Koek *et al.*, 2010; Ferreira *et al.*, 2010).

Many current platforms used for metabolomics offer high-throughput analysis when coupled with supporting software for metabolite identification (e.g., the National Institute of Standards and Technology (NIST), Fiehn, and Wiley libraries) allowing fast and easy analysis (Palazoglu and Fiehn, 2009; DeHaven *et al.*; Dunn *et al.*, 2011). Given the sheer quantity of platforms that can be used for metabolomics, as well as the breadth of compounds that can be analyzed, metabolomics has become a more accessible means to quantify metabolism in a variety of applications.

1.8.2. Metabolomics Applications

Metabolomics has been employed in a number of applications, from basic to biomedical and clinical research.

Untargeted metabolomic analysis has been conducted on a variety of biological samples from blood serum and plasma, to plant material, and fungal and microbial populations to identify both common and uncommon metabolites (Roessner *et al.*, 2000; Koek *et al.*, 2006; Madla *et al.*, 2012; Fiehn *et al.*, 2000ab).

Uses in the biomedical field have included cancer research, as well as the identification of disease biomarkers. For example, mass spectrometry has elucidated basic metabolic pathways of rapidly proliferating cancer cells. In particular, increased glycine uptake and mitochondrial glycine biosynthetic pathway activity is correlated with rapidly proliferating cancer cells. Through this work, new targets for cancer therapies have been proposed (Jain *et al.*, 2012).

GC-MS has previously been used to evaluate serum, plasma, and urine samples. Metabolites in these biofluids are identified by retention time and ion fragmentation patterns of metabolites by comparison to spectral libraries and known standards. Potential biomarker identification for pathologies as well as normal biological differences could be achieved through use of this platform (Pasikanti *et al.*, 2008).

¹H NMR spectroscopy has been utilized to determine metabolic profile differences between induced pluripotent stem cells (iPSCs) and their parental somatic cells (fibroblasts) – iPSCs express a metabolite profile characterized by higher levels of glycolytic end-products that result from their markedly higher rate of glucose uptake and glycolytic activity (Folmes *et al.*, 2011).

1.8.3. Metabolomics Applications in Reproduction

Until recently, the main measure of embryo quality has been examination of morphological characteristics, which fails to yield high efficiency of ARTs. Oxygen consumption, amino acid turnover, and time lapse videos of oocytes and/or embryos following *in vitro* maturation, fertilization, and culture have also been explored as methods of viability assessment. A major shortcoming of many of these proposed methods of evaluation is that they often consider only a single biomarker, without regards to the “complete picture” of metabolism within the cells. The implementation of metabolomic assessment of follicular fluid, oocytes, and embryos will allow for a more comprehensive understanding of potential biomarkers, as well as interactions between metabolites, which could serve as a biomarker(s) of viability (Revelli *et al.*, 2009). Metabolomics has implications in reproductive science to improve ART efficiencies. While some have proposed the use of metabolomics to determine the physiological status and therefore the developmental potential and viability of oocytes and embryos, there is still limited application of this technology (Nel-Themaat and Nagy, 2011; McRae *et al.*, 2013).

1.8.3.1. Follicle and Oocyte Evaluation

It is widely accepted that a contributing factor to the low efficiencies of ARTs is the inability to select oocytes with the highest competence and viability for fertilization. Metabolomics provides an objective, comprehensive method to noninvasively identify substantial quantities of small molecules which could serve as biomarkers for oocyte quality. This concept has been explored in bovine and human oocytes and has been proposed for use in equine oocytes (Dell’ Aquila *et al.*, 2012). An issue to overcome with

metabolomic study is the accurate separation of cell types within the follicle. Recently, a new dissection technique, Laser Capture Microdissection was developed by Bonnet *et al.* (2011). This process was developed using ovine follicles of differing developmental stages, and was able to accurately separate granulosa cells and oocytes, even at the primordial follicle stage. While researchers used this technique to separate cells for transcriptomics, it could easily be used for metabolomics to allow for accurate dissection of oocytes from granulosa cells for separate assessment.

Metabolomic evaluation of oocytes can be achieved non-invasively by evaluating the follicular fluid aspirated from the follicle of origin or by evaluating spent culture media. For basic research and understanding, analysis of the follicular fluid is ideal as it contains secretions from the oocyte of interest, as well as from the granulosa cells enveloping it. However, for widespread clinical applications, isolation of individual follicles and individual aspiration of follicular fluid is impractical, so spent media evaluation provides an adequate alternative (Nel-Themaat and Nagy, 2011).

LC-MS evaluation of amino acid turnover by bovine oocytes has been utilized experimentally to determine differences between those oocytes which were able to cleave following *in vitro* fertilization and those that were not. Competent oocytes depleted lower levels of glutamine from maturation medium, and released lower levels of alanine into the media as compared to incompetent oocytes (Hemmings *et al.*, 2012). Evaluation of glutamine utilization and production via metabolomics technologies is of particular interest. Glutamine is a major carbon source for the TCA cycle (for ATP production and as an anapleurotic substrate), a contributor to glucose metabolism regulation, has protective properties against oxidative stress, and has the ability to contribute to the *de novo* synthesis

of other essential molecules. Thus, glutamine has become a target as a metabolic biomarker of viability (Nel-Themaat and Nagy, 2011).

Metabolomic analysis of human follicular fluid has been achieved using ^1H NMR spectroscopy and high resolution NMR platforms. Intermediates of metabolic pathways including acetate, lactate, pyruvate, and glucose were positively identified in follicular fluid with high resolution NMR (Piñero-Sagredo *et al.*, 2009). Via ^1H NMR analysis, distinct metabolic profiles were determined between uncleaved fertilized oocytes and fertilized oocytes which progressed. In addition, metabolites which were discriminant between embryo stages, whether the corresponding oocyte was able to produce a one or two cell embryo, and between pregnancy outcomes were determined. Fertilized oocytes which progressed to the two-cell stage had higher concentrations of lactate and choline/phosphocholine and lower intensities of glucose and high density lipoproteins than those that arrested as a one-cell zygote. In those that resulted in a positive pregnancy, lactate, proline, and leucine/isoleucine concentrations were higher, while glucose intensities were lower. Therefore, the developmental competence of human oocytes is correlated with the metabolite profile of the follicular fluid within its follicle (Wallace *et al.*, 2012).

Following these findings, application of metabolomics in reproduction was proposed for the analysis of follicular fluid to determine oocyte quality of women with polycystic ovary syndrome (PCOS). It is expected that in patients with PCOS, there is compromised glucose availability which forces follicles to use alternative energy sources to compensate (e.g., amino acid degradation, lipids, lactate, pyruvate). It has been hypothesized that by identifying and quantifying the metabolites present, the level of

compensation can be determined; therefore, oocyte quality can be inferred (Arya *et al.*, 2012).

Fatty acid and lipid profiles, employing a metabolomics approach, have also been suggested as potential biomarkers of viability. GC-MS based metabolomics has been employed in the analysis of bovine follicular fluid to determine differences in fertility between heifers and cows. Follicular fluid has a distinct fatty acid composition between differing reproductive statuses, and a unique fatty acid composition as compared to serum. Cows have higher levels of palmitic and stearic acid (saturated fatty acids) in follicular fluid, while heifers have higher docosahexaenoic acid levels (Bender *et al.*, 2010). Matrix-assisted laser desorption/ionization mass spectrometry has been utilized to analyze macro lipid profiles (triacylglycerols, phosphatidylcholines, and sphingomyelins) in a single human, bovine, ovine, and piscine oocyte, as well as in single bovine and insect embryos (Ferreira *et al.*, 2010). Desorption electrospray ionization-mass spectrometry has also been utilized by this group to monitor several classes of lipids (free fatty acids, phosphatidylserines, phosphatidylcholines, and phosphatidylinositols) in single murine oocytes and embryos, in addition to bovine embryos (Ferreira *et al.*, 2012).

While comprehensive studies have been completed to analyze the nutrient compositions of follicular fluid in several livestock species (e.g., cattle), these have not yet been assessed in the cat (Bender *et al.*, 2010; Campbell *et al.*, 2010; Harris *et al.*, 2009; Sutton-McDowall *et al.*, 2010). A recent study by Apparicio *et al.* (2010) has examined lipid profiles of feline oocytes, identifying phosphatidylcholines, sphingomyelins, and triacylglycerols. As compared to canine oocytes, feline oocytes had higher levels of 52

and 54 carbon triacylglycerols with a higher number of unsaturated bonds, which indicated a high level of linoleic and oleic fatty acid residues.

1.8.3.2. Embryo Evaluation

Metabolomic evaluation of embryos provides two important advantages over existing ART embryo evaluation techniques. First, it is a completely objective method of evaluation, unlike morphological assessment. Secondly, it provides a high throughput method of analysis with Raman and near infrared spectroscopy which could be implemented in clinical settings (Nel-Themaat and Nagy, 2011).

Leese *et al.* (2007, 2008) assert that those embryos which exhibit the “quietest” metabolism are those that have the highest overall developmental potential. However, even with a quiet metabolism, IVC embryos require energy sources and amino acids for growth and development.

Metabolomic analysis of embryos has focused on pyruvate, glucose, and amino acid analysis of spent media, which provides a non-invasive evaluation of embryonic viability (Katz-Jaffe and McReynolds, 2011). Viable embryos at earlier developmental stages (cleavage) rely heavily on TCA cycle activity for generation of ATP, while later developmental stages (compacted morula and early blastocyst) are characterized by a marked increase in glycolytic function (Nel-Themaat and Nagy, 2011). Employing principal component analysis of ¹H NMR spectral data of metabolites in preimplantation embryos, Naib *et al.* (2009) demonstrated that metabolites of 2 to 4 cell and 8 cell stage embryos clustered separately from those that had already undergone genome activation (16 cell stage, morula, and blastocysts). Amino acid uptake and release profiles, as evaluated

through metabolomic techniques, have also been suggested as markers for viability (**Table 1.2**).

Table 1.2: Amino acid uptake and release corresponding to viable embryos in humans (reviewed by Ayinder *et al.*, 2010)

Embryo Stage	Amino Acids	
	Uptake	Release
Zygote ¹	-	Low: Glycine, Leucine High: Asparagine
Zygote to 4-Cell Stage ²	-	High: Glutamate
Zygote to 4-Cell Stage ¹	Low: Arginine, Glutamine, Methionine	Low: Alanine, Asparagine
8-Cell, Morula ³	Low: Serine	Low: Alanine, Glycine

¹ Houghton *et al.*, 2002

² Seli *et al.*, 2008

³ Brison *et al.*, 2004

Metabolomic analysis of spent culture medium from embryos (produced *in vitro* through ICSI) with known implantation results, has recently been used to develop models to predict implantation potential in humans (Cortezzi *et al.*, 2013). When subjected to validation tests, the model was able to predict the embryos that implanted with 100% probability, and was able to predict embryos that failed to implant with 70% probability. This suggests that non-invasive metabolomic analysis could eventually serve as an evaluation tool to increase ART efficiency. Likewise, metabolomic profiling of embryo culture media via rapid near infrared spectroscopy has allowed for the development of a “viability model” (Seli *et al.*, 2008). This model exploits differences in isoleucine/leucine,

lactate, alanine, glutamate, pyruvate, and glucose levels between human embryos which implanted and resulted in live birth, and those embryos which did not result in a birth. When human embryos were scored by this model, varying scores were observed, even in embryos of similar morphological quality. This result is not surprising and provides an explanation for consistently low ART efficiencies when morphologic assessment of embryos is the sole determinant of embryo viability (Sakkas *et al.*, 2008).

Of particular interest to the goal of increasing ART efficiency is developing *direct* methods to evaluate the metabolism of oocytes and embryos. While analysis of spent media has provided a non-invasive evaluation of embryos, this approach only provides an indirect measure of metabolism. D'Alessandro *et al.* (2012) have employed a method utilizing aspirated blastocoele fluid where metabolites were identified and quantified using sample sizes as small as 0.5 nL. While this method is invasive, it has been previously reported that collapsing the blastocoele by aspirating the blastocoele fluid actually improves survival and pregnancy rates after cryopreservation, thawing, and transfer (Mukaida *et al.*, 2006).

1.9. Fluxomic Technologies

Fluxomics, the newest “-omics” technology, builds upon metabolomics analysis through the use of stable isotope enriched compounds (“tracers”), thus allowing for the assessment of the biofunctionality of metabolic pathways. Fluxomics ultimately yields quantitative measures of metabolic turnover or flux through operational pathways in a cell(s) (Zamboni and Sauer, 2009). It has been used successfully to elucidate pathways in

multiple species, but most often it has been employed in microbial systems (Feng *et al.*, 2010; Kromer *et al.*, 2009; Zamboni and Sauer, 2009).

This new technology exhibits several advantages over metabolomic analysis alone. While metabolomics can provide a static snapshot of the metabolic status of a cell, it provides limited information regarding its true physiologic status. Fluxomics provides a dynamic picture of pathway activities in a cell, including specific metabolites which are derived from a tracer. In addition, it allows for a more directed evaluation of metabolites by allowing for the elimination of “noise” compounds and for focus to be applied to downstream metabolites linked to the tracer (Hiller *et al.*, 2010).

1.9.1. Stable Isotope Tracers

Radioisotopes have been extensively used as tracers, but they possess several shortcomings, including their decay, complications with measurement of specific activity, and health and safety concerns. The most common stable isotopes employed in biological systems are ^{13}C , ^{15}N , and ^2H labeled organic compounds and metabolites. Each stable isotope ion is either one or two mass units heavier than the most abundant natural isotope and can be incorporated into many different compounds (e.g., glucose, pyruvate, lactate) that are metabolically important. These features allow for easy measurement via mass spectrometry, which measures the extent to which the stable isotope tracers are introduced into compounds. Upon entry of the compound into the mass spectrometer, the analyte is subjected to an ionizing source which results in the predictable fragmentation such that fragment ions containing the incorporated stable isotope can be selectively monitored and their mass isotopomer distribution (MID) determined. MID is calculated by quantifying

ion fragments containing stable isotopes as a ratio of the ion containing the unlabeled atoms and labeled atoms of interest (**Table 1.3**). One caveat to utilizing stable isotope tracers is that the crude ion abundances calculated with this ratio must be corrected for the natural abundances (appearance) of the stable isotope atoms (giving the atom percent excess (APE)), the correction of which is easily performed utilizing many currently available multiple-linear regression softwares (Bequette *et al.*, 2006).

The ability to integrate stable isotopes into a variety of compounds, as well as to integrate them in a specific manner to produce different isotopomers (e.g., [1,2-¹³C₂] glucose versus [3-¹³C₁] glucose) has produced a robust method to analyzing metabolic pathways. Depending on the tracer selected, various pathways can be targeted for analysis. In mammals, [1,2-¹³C₂] glucose is commonly used to probe the PPP, while [3-¹³C₁] glucose is often used to evaluate pyruvate oxidation. Several tracers are used for evaluation of fluxes through the Krebs Cycle (Metallo *et al.*, 2009).

Table 1.3: Crude mass isotopomer abundances (moles of tracer per 100 moles of tracee) for D-Glucose

Mass Isotopomer	Quantity of each carbon isotope		Moles of Isotopomer
	¹² C	¹³ C	
[M+0]	6	0	100
[M+1]	5	1	([M+1]/[M+0])*100
[M+2]	4	2	([M+2]/[M+0])*100
[M+3]	3	3	([M+3]/[M+0])*100
[M+4]	2	4	([M+4]/[M+0])*100
[M+5]	1	5	([M+5]/[M+0])*100
[M+6]	0	6	([M+6]/[M+0])*100

While many compounds enriched with stable isotopes can be used as probes, the use of uniformly labeled ^{13}C -glucose ($[\text{U-}^{13}\text{C}_6]$ glucose) as a tracer will be the focus of this explanation, as it was the tracer employed in this thesis research. Through the use of $[\text{U-}^{13}\text{C}_6]$ glucose and calculations of the APE for metabolic intermediates, it is possible to probe the fluxes through many pathways in central carbon metabolism. Firstly, incorporation of an intact tracer molecule can be determined. For example, if unlabeled and $[\text{U-}^{13}\text{C}_6]$ glucose are employed, this will lead to synthesis of unlabeled and $[\text{U-}^{13}\text{C}_3]$ labeled pyruvate molecules upon glycolytic metabolism of glucose. Secondly, incorporation of the ^{13}C atoms into metabolites can only occur when these compounds are synthesized *de novo* by the cell or tissue upon metabolism of the labeled tracer. In the case of the liver, if these labeled pyruvate molecules are eventually metabolized and contribute to gluconeogenesis, $[\text{M}+3]$ glucose (i.e., three of the six carbons in glucose are ^{13}C labeled) will result (Lee *et al.*, 1991).

1.9.2. Central Carbon Metabolism

Metabolic pathways are intrinsically connected within a cell, with the intermediates and products of one pathway serving as substrates or intermediates in linked pathways. With cells in culture, cellular intermediates are often released into the media and when their ^{13}C -enrichment is determined, these released metabolites provide a direct measure of the cellular activity of the pathways from which they were derived. Stable isotope tracers are used to exploit these two aspects of metabolism; therefore, providing information regarding the fluxes through linked pathways. Amino acids linked to Krebs Cycle intermediates are summarized in **Table 1.4** (Owen *et al.*, 2002). Pathways of interest in

central carbon metabolism, as well as substrates, intermediates, and products, are depicted in **Figure 1.3**.

Table 1.4: Anapleurotic and Catapleurotic Amino Acids related to Krebs Cycle Intermediates

Krebs Cycle Intermediate	Amino Acids
Pyruvate	Alanine, Cysteine, Glycine, Threonine, Tryptophan, Serine
Acetyl-CoA	Isoleucine, Leucine, Lysine, Phenylalanine, Threonine, Tryptophan, Tyrosine
α -Ketoglutarate	Arginine, Glutamate, Glutamine, Histidine, Proline
Succinyl-CoA	Isoleucine, Methionine, Valine
Fumarate	Phenylalanine, Tyrosine
Oxaloacetate	Aspartate (Asparagine)

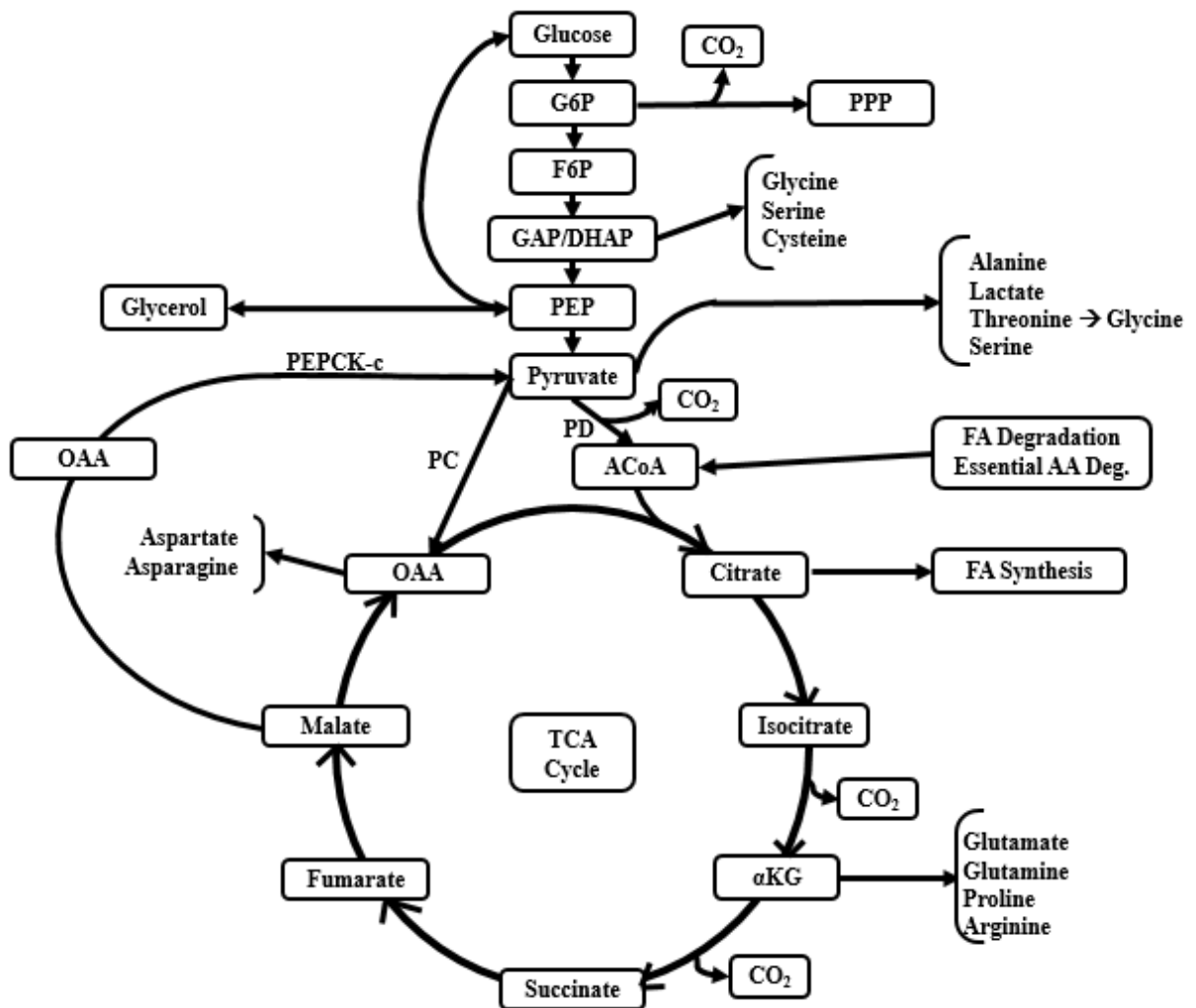


Figure 1.3: Connected pathways of carbon metabolism including Glycolysis, Gluconeogenesis, Pentose Phosphate Cycle (PPP), and the Krebs Cycle (TCA Cycle). Linked pathways of non-essential amino acid synthesis, fatty acid metabolism, and glycerol synthesis and degradation are also included. Other abbreviations: Glucose-6-Phosphate (G6P), Fructose-6-Phosphate (F6P), Glyceraldehyde-3-Phosphate (GAP), Dihydroxyacetone Phosphate (DHAP), Phosphoenol Pyruvate (PEP), Acetyl CoA (ACoA), alpha-Ketoglutarate (α KG), Oxaloacetate (OAA), Pyruvate Carboxylase (PC), Pyruvate Dehydrogenase (PD), Phosphoenolpyruvate carboxykinase – cytosolic (PEPCK-c)

A mixture of an unlabeled compound and a labeled tracer can be introduced to a biological sample through a variety of means, including incorporation into a fed diet, venous infusion, or incorporation into culture media for cells (Bequette *et al.*, 2005). Given a 50:50 mixture of unlabeled and [U-¹³C₆] glucose: upon entry to the cells the two isotopomers of glucose are processed in an unbiased fashion through the pathways of central carbon metabolism. Based on known carbon rearrangements in the pathways, the theoretical enrichment of each intermediate can be determined (Mu *et al.*, 2007). Furthermore, exploiting the fact that intermediates in carbon metabolism quickly achieve isotopic equilibrium with the non-essential amino acids (NEAAs) they synthesize, comparison of the determined MID for NEAAs to their theoretical enrichments allows for crude measures of the actual fluxes through pathways to be calculated (Berthold *et al.*, 2004).

Stable isotope tracer kinetics have been extensively reviewed; however, pertinent calculations related to 50:50 unlabeled and [U-¹³C₆] glucose tracer infusions are summarized below (Bequette *et al.*, 2005; Berthold *et al.*, 1994; Metallo *et al.*, 2009).

1.9.2.1. Pyruvate

Pyruvate synthesized directly from glucose only via glycolysis will result in the production of only [M+0] and [M+3] pyruvate. Pyruvate synthesized *de novo* from alternative carbon sources (e.g., amino acid degradation or glycerol) will result in a [M+0] pyruvate. [M+1] and [M+2] pyruvate can derive from pentose phosphate pathway activity or from pyruvate synthesis via PEPCK (Bequette *et al.*, 2005).

1.9.2.2. α -Ketoglutarate

[M+3] α -Ketoglutarate can only derive from [M+3] oxaloacetate (Carbons 2-4 enriched) formed via pyruvate carboxylase. [M+2] α -Ketoglutarate can be formed from [M+3] oxaloacetate (Carbons 1-3 enriched) in the first turn of the Krebs Cycle, [M+2] oxaloacetate in the second turn of the Krebs Cycle, or from entrance of [M+2] Acetyl CoA, derived from [M+3] or [M+2] pyruvate (Carbons 2 and 3 enriched).

1.9.2.3. Oxaloacetate

[M+3] Oxaloacetate can be derived from [M+3] pyruvate via pyruvate carboxylase. [M+2] Oxaloacetate can be derived from [M+2] Acetyl CoA entrance to the TCA cycle on the first turn, or from [M+3] Oxaloacetate on the first turn. [M+1] Oxaloacetate can originate from [M+3] Oxaloacetate on its second turn through the TCA cycle.

1.9.2.4. Acetyl CoA

Acetyl CoA can derive from alternative carbon sources, such as amino acids or FAO, giving [M+0] Acetyl CoA. It can also derive directly from pyruvate via pyruvate dehydrogenase.

Of particular interest in studies is the amount of Acetyl CoA entering the Krebs Cycle. Following the assumptions for origination of [M+2] and [M+3] α -Ketoglutarate, and that [M+3] oxaloacetate is in positional isotopomer equilibrium, the amount of Acetyl CoA entering the Krebs Cycle can be calculated as:

$$\{1 - ([M+3] \text{ Glutamate} / [M+3] \text{ Aspartate})\} * [M+3] \text{ Aspartate.}$$

1.9.3. Fluxomic Applications

The use of stable isotope tracers to determine flux through metabolic pathways have been employed in several different cell types and disciplines including industry and biomedical research.

The field of bioengineering has seen exponential growth in recent years. Engineering organisms, particularly microorganisms and plant species with well-defined metabolic pathway maps, to utilize unimportant byproducts of industry and to produce compounds of interest has proven to be a very profitable endeavor. In order to maximize production, the flux through biosynthetic pathways must first be monitored, and then in some cases, be altered, rerouting compounds to the pathways of interest. Tracer studies have proven to be an invaluable tool for developing engineering strategies, as well as in evaluating engineered systems for production efficiency (Kajiwara *et al.*, 1994; Iyer *et al.*, 2008).

Enzyme kinetics are under constant scrutiny, whether in pursuit of basic biochemical knowledge, for evaluation of novel reactions, or as a potential biomedical therapy targets. Stable isotope tracers provide an invaluable method for assessment of enzymatic reactions. Questions regarding the reversibility of Isocitrate Dehydrogenase have been explored using [U-¹³C₅] glutamate tracers. After infusion, glutamate, in isotopic equilibrium with α -Ketoglutarate, could only result in [M+4] Citrate if all TCA cycle reactions occurred in the forward direction, whereas [M+5] Citrate could only occur if the reaction converting Isocitrate to α -Ketoglutarate was reversible. Des Rosiers *et al.* (1994) demonstrated through the production of [M+5] Citrate, that the reaction catalyzed by Isocitrate Dehydrogenase is in fact reversible.

Stable isotope tracers have also been utilized to evaluate the altered metabolism of immortalized cells. [1,2-¹³C₂] glucose inclusive media has been utilized to examine the effects of extracellular matrix detachment in immortalized, non-tumorigenic mammary epithelial cells. It was found after analysis with GC-MS that detachment leads to a decrease in flux through glycolysis, the PPP, and through the TCA cycle. Additionally, through examination of the abundances of [M+2] mass isotopomers of pyruvate and TCA cycle intermediates, it was determined that flux through pyruvate dehydrogenase (PDH) is decreased following detachment, which is consistent with findings that lactate synthesis and release increases in those cells. Furthermore, through usage of [U-¹³C₅] glutamate tracer, coupled with monitoring of TCA cycle intermediates, it was found that glutamate was unable to rescue the cells in response to decreased glucose carbon flux through the TCA cycle (Grassian *et al.*, 2011).

Cancer research has increasingly focused on metabolic differences between somatic cells which divide normally, and those cells which become cancerous. In order to achieve this goal, stable isotope tracers have found increased use to assess differences in metabolic pathway flux in cancer cells. ¹³C-labeled glutamine has been used to show that cancer cells undergo reductive carboxylation of α -Ketoglutarate to form the majority of their lipogenic acetyl-CoA (Anastasiou and Cantley, 2012). [U-¹³C₆] glucose has been used to evaluate differences between rhabdomyosarcoma cells and primary myocytes, showing accelerated flux of glucose through glycolysis, as well as higher influx of anapleurotic substrates into the Krebs Cycle in cancerous cells (Fan *et al.*, 2008).

Pathologic conditions including nonalcoholic fatty liver disease (NAFLD) have also been explored using stable isotope tracers and fluxomic technologies. ¹³C and ²H

tracers were employed to evaluate mitochondrial metabolic pathways, lipolysis, and gluconeogenesis in affected and non-affected individuals. Those with NAFLD had 30% higher rates of gluconeogenesis and 50% higher rates of lipolysis (Sunny *et al.*, 2011).

One challenge with fluxomic applications, particularly when positional isotopomer analysis is involved, is the accurate quantification of MID's (therefore, the fluxes through interconnected pathways). The development of software to automatically calculate flux values through pathways directly from platform output (e.g., from [¹³C, ¹H] NMR data) has provided a way to complete high-throughput analysis (Sriram *et al.*, 2004)

1.9.4. Fluxomic Applications in Reproduction

While fluxomic technologies have been extensively applied in industrial, biomedical, and basic research in a variety of organisms, its potential has yet to be realized in mammalian reproductive applications. This technology has yet to be applied to analyze the metabolic networks active in follicles and oocytes, and consequently to potentially identify viable oocytes for fertilization.

1.10. Discussion

Given the need for a more comprehensive metabolic analysis of follicles, metabolomic and fluxomic analysis of these developmental structures is necessary. It is the aim of this research to fill gaps in the understanding of follicle metabolism. In particular, this thesis will focus on the shifts in metabolism through follicle development and environmental conditions that impact their metabolism. Therefore, this investigation should provide novel insight into the changing nutrient needs of feline follicles and the intrinsic metabolic differences which define their specific nutrient requirements.

Chapter 2: Metabolomic Analysis of Feline Follicles

2.1. Introduction

The family *Felidae* encompasses 37 species, of which only the domestic cat is not threatened by extinction. Wild species are under constant onslaught from habitat destruction and poaching. Due to the rapid decline in populations, there have been increased conservation efforts fueled by management programs in zoological parks. An invaluable facet to these programs is the use of ARTs to preserve and easily transport valuable genetics. Unfortunately, ART efficiencies are still very low for many populations and research in felids to improve these methods is very limited (Bristol-Gould and Woodruff, 2006).

Past studies have examined follicle metabolism in several species, most of which are livestock animals. Nevertheless, metabolite composition of follicular fluid has been shown to mirror changes in serum metabolite concentrations in cattle, suggesting that the follicle is highly dependent upon its environment for metabolic substrates (Leroy *et al.*, 2004b). This is a critical observation that further supports the view that in order to improve ART efficiency, culture conditions must be improved to better support the metabolic needs of the follicle (or other reproductive structures). The first step to improving culture conditions is defining the metabolism of developing follicles.

Similar patterns in glucose, lactate, and pyruvate concentrations in follicles of different sizes have been observed in several species. In sheep, buffalo, and dairy cows and heifers, glucose concentrations have been shown to be higher in large compared to small follicles. Conversely, lactate concentrations decrease with stage of follicle growth and development (Leroy *et al.*, 2004; Nandi *et al.*, 2008; Nishimoto *et al.*, 2009). By contrast, pyruvate concentration does not appear to change with follicle size (Nandi *et al.*, 2008). In one of the few studies with feline follicles, alanine, glutamine, and taurine were found in the highest concentrations in follicular fluid amongst the amino acids (Guerin *et al.*, 2012). While lipid abundance in follicles varies among species, palmitic and oleic acids have been shown to be the most predominant fatty acids in bovine and porcine COCs (Paczkowski *et al.*, 2013). Other products of metabolism including β -OHB, (total) cholesterol, and urea also vary according to follicle size, with β -OHB and total cholesterol increasing and urea decreasing with increasing follicle size (Leroy *et al.*, 2004a).

Metabolomics provides a novel approach to analyze the metabolism of follicles by assessing the presence and abundance of a large range of metabolites (the metabolome) simultaneously. Amino acids, energy substrates, and lipid profiles have been assessed for human and cattle follicles, as well as other species (Hemmings *et al.*, 2012; Wallace *et al.*, 2012; Ferreira *et al.*, 2012). In the present study, metabolomics was utilized to characterize the metabolites present in feline follicles across stages of development (size) and developmental environments (*in vitro* culture). By analysis of the composition of metabolites, we were also able to identify patterns of metabolism that characterize different stages of follicle growth.

2.2. Rationale and Hypotheses

A comprehensive understanding of feline follicular metabolism is still lacking in reproduction science. It is essential not only for basic knowledge, but also for eventual improvement of assisted reproductive techniques and advancement of *in vitro* culture procedures. Differences in metabolite profiles will provide insights into fundamental metabolic differences between follicles of different developmental stages and growth environments, beyond the point of transcriptional, translational, and post-translational modification control.

Two comparisons are of interest in this study, (1) the metabolic differences between early and late antral follicles developed *in vivo* and (2) the metabolite differences between early antral follicles derived *in vivo* and those cultured *in vitro*. It was expected that the metabolome would differ between stages of follicle development and between environmental conditions for development. For statistical purposes, the null hypotheses are that there are no differences in the metabolite profiles of early and late antral follicles derived *in vivo*, or between early follicles derived *in vivo* and those cultured *in vitro*.

2.3. Materials and Methods

2.3.1. Study Design: Partial Block Design for Cat Age, Type

Three groups of follicles were identified for study: early antral follicles originating *in vivo*, late antral follicles originating *in vivo*, and early antral follicles which were cultured *in vitro* for 12 d. When possible, samples for each group were obtained from the same cat. Otherwise, cats of similar age (± 0.5 yr) and type (housecat or stray cat) were paired and used to obtain samples for each group.

2.3.2. Follicle Collection and Storage

Feline ovaries were acquired as a byproduct of routine ovariohysterectomies from a local spay clinic, Animal Birth Control, LLC, in central Maryland. The paired ovaries from sexually mature cats (defined as at least one year old) were transported to the University of Maryland, College Park, on ice in phosphate buffered solution (PBS; Cellgro Mediatech, Manassas, VA). Cortical slices were obtained from paired ovaries in warmed (38.5 °C) collection media (**Table 2.1**). Morphologically healthy, early antral (follicles <0.5 mm in diameter with a visible antrum) and late antral follicles (follicles >2 mm in diameter with a visible antrum) were mechanically isolated from ovaries as previously described (Jewgenow and Goritz, 1995). Due to their smaller size, ten early antral follicles from each cat were pooled, washed through PBS, and stored at -80 °C until processing. For late antral follicles, a single follicle from each cat was washed through PBS and stored at -80 °C until processing. An additional ten early antral follicles from each cat were encapsulated as previously described (Songsasen, 2011). Briefly, follicles were encapsulated in 20 µL of 0.5% alginate hydrogel (Novamatrix, Sandvika, Norway), which was hardened in a calcium chloride solution (**Table 2.2**) for 3 min, washed through with maintenance media (**Table 2.3**), and cultured in individual wells of a 48-well plate (0.75 cm² growth area) with 500 µL of culture media (**Table 2.4**) for 12 d in 5% CO₂ at 38.5 °C. Half of the culture media was refreshed every 72 hrs throughout incubation, with spent media being discarded. On the final day of incubation, healthy follicles were mechanically isolated from their alginate drops in PBS, pooled, washed through PBS, and stored at -80 °C until processing.

Table 2.1: Composition and Company Source Information for Follicle Collection Media

Follicle Collection Media: Stored at 4°C, used at 38.5°C		
Medium 199 (TCM with Hepes)	200mL	Sigma Aldrich, St. Louis, MO
L-Glutamine	0.0584g	Sigma Aldrich, St. Louis, MO
Sodium Pyruvate: 100 mM Stock Solution	2mL	Gibco-Life Technologies, Grand Island, NY
Penicillin G-Streptomycin Sulfate: 10,000 U/mL Penicillin; 10,000 µg/mL Stock Solution	1mL	Invitrogen-Life Technologies, Grand Island, NY
Bovine Serum Albumin	0.6g	Rockland, Inc., Gilbertsville, PA

Table 2.2: Composition and Company Source Information for Calcium Chloride Solution

Salt Solution: Stored and used at Room Temperature		
distilled H ₂ O	50mL	
Calcium chloride (anhydrous)	0.277g	Sigma Aldrich, St. Louis, MO
Sodium chloride	0.410g	Sigma Aldrich, St. Louis, MO

Table 2.3: Composition and Company Source Information for Maintenance Media

Maintenance Media: Stored at 4°C, used at 38.5°C		
Dulbecco's Modified Eagle's Medium – low glucose	100mL	Sigma Aldrich, St. Louis, MO
L-Glutamine	0.0292g	Sigma Aldrich, St. Louis, MO
Penicillin G-Streptomycin Sulfate: 10,000 U/mL Penicillin; 10,000 µg/mL Stock Solution	0.5mL	Invitrogen-Life Technologies, Grand Island, NY
Bovine Serum Albumin	0.1g	Rockland, Inc., Gilbertsville, PA

Table 2.4: Composition and Company Source Information for Follicle Culture Media.

Follicle Culture Media: Stored at 4°C, used at 38.5°C		
Dulbecco's Modified Eagle's Medium – low glucose	200mL	Sigma Aldrich, St. Louis, MO
L-Glutamine	0.0584g	Sigma Aldrich, St. Louis, MO
Insulin-Transferrin-Selenium: 25 mg/50 mL Insulin-Transferrin, 25 µg/50 mL Selenium Stock Solution	2mL	Sigma Aldrich, St. Louis, MO
Penicillin G-Streptomycin Sulfate: 10,000 U/mL Penicillin; 10,000 µg/mL Stock Solution	1mL	Gibco-Life Technologies, Grand Island, NY
Bovine Serum Albumin	0.6g	Rockland, Inc., Gilbertsville, PA
Follicle Stimulating Hormone: 0.355 mg/mL Stock Solution	563µL	Sigma Aldrich, St. Louis, MO

2.3.3. Sample Processing

All samples were slowly thawed on ice (n=9 per group). To each sample, 1 mL of ice-cold methanol:chloroform:water (5:2:2 v/v; VWR International, Radnor, PA; SP Mallinckrodt Baker, Phillipsburg, NJ) was added followed by homogenization on ice to disrupt cell membranes. Next, samples were placed on a vortex mixer for an additional 15 min, then incubated overnight at -80 °C for maximum metabolite extraction. Following overnight incubation, samples were vortex mixed for 10 min, then centrifuged at 13,000 xg for 10 min to remove cellular debris. The supernatant was dried in a SpeedVac until completely dry. Using the same tube, extracted metabolites were converted to their oximate-trimethylsilyl (TMS) derivative by addition of 60 µL of methoxylamine-HCl (30 mg/mL in pyridine; Acros Organics, Waltham, MA; Thermo Scientific, Waltham, MA)

plus 60 μL of N,O-bis(trimethylsilyl) trifluoroacetamide (BSTFA) containing 1% trimethylchlorosilane (TCMS) (AlfaAesar, Ward Hill, MA), vortex mixing for 30 sec, and microwave heated for 120 sec at 200 watts. Samples were then rotary mixed overnight to allow for maximum derivatization. After overnight incubation, samples were transferred to glass gas chromatography vials prior to GC-MS analysis (Agilent, Palo Alto, CA).

2.3.4. Gas Chromatography-Mass Spectrometry Analysis

One microliter aliquots of samples were injected in split mode (2:1, inlet temperature of 250 $^{\circ}\text{C}$) into the gas chromatographic system (Agilent 6890 gas chromatography system, Palo Alto, CA.; ZB50 capillary column) and separated on a mid-polarity capillary column (ZB50; Phenomenex, Torrance, CA) under the following conditions: initial temperature of 60 $^{\circ}\text{C}$ held for 5 min, heating 5 $^{\circ}\text{C}$ per min to 310 $^{\circ}\text{C}$, hold for 5 min, cooling 50 $^{\circ}\text{C}$ per min to 60 $^{\circ}\text{C}$ and held for 5 min (70 min total run time). The MS (Agilent 5973 inert EI/CI MSD system, Palo Alto, CA) was operated in electron impact mode and ions monitored in full scan mode (mass range 50-650 m/z).

GC-MS data files were captured via Agilent's GC-MSD ChemStation, while Agilent Data Analysis software was used to view and quantitate the raw data files. Retention times and mass spectra of each entity was compared against the Agilent-Fiehn Mass spectral Library and cross-checked with the 2008 NIST Mass Spectral Library for annotation and identification.

2.3.5. Metabolite Abundance Calculations

The abundance of consistently identified metabolites was calculated as a proportion – the abundance of the given metabolite compared to the total abundance of all metabolites in the sample. This was calculated by obtaining the total ion count for the given metabolite and dividing it by the total ion count for the total ion chromatogram for the entire sample.

2.3.6. Statistical Analysis

Files were analyzed with MetaboAnalyst software (online) for Partial Least Squares Discriminant Analysis (PLS-DA), while SAS was used to perform a mixed model analysis of variance (ANOVA) with Dunnett’s Correction (Xia *et al.*, 2009; Xia and Wishart, 2011; Xia *et al.*, 2012). The following model was used:

$$Y_{ij} = \mu + T_i + C_j + \epsilon_{ij}$$

Y_{ij} = Response Variable (Lactic Acid, Alanine, etc.)

μ = Grand Mean

T_i = Treatment Effect (Early Antral, Late Antral, Early Antral *in vitro*)

C_j = Random Effects (Block: age, type)

ϵ_{ij} = Residual Error

Significance was set at $P < 0.05$ ($\alpha = 5\%$). Data was analyzed with the PROC MIXED procedure of SAS (SAS Ins, Inc., Cary, NC) with age/type as blocking factor. For the analysis, follicle stage/type was considered a fixed effect, while cat age/type was a random effect. Least squares means were obtained for each treatment and linear effects of follicle stage/type on the response variables were tested by constructing orthogonal contrasts. Pairwise mean comparisons were performed using the Dunnett’s Adjustment.

2.4. Results

Over 100 entities were annotated using the NIST and Fiehn libraries. Of those entities, 19 metabolites were positively identified and consistently present across samples in each group. These metabolites (**Table 2.5**) ranged from amino acids, to organic and fatty acids, to sterols and carbohydrates, and were involved in a variety of metabolic pathways. Early antral follicles undergoing *in vitro* culture were between 300 and 500 μm upon collection from the ovary. The largest follicles upon collection after incubation were 625 μm in diameter.

Table 2.5: Metabolites identified in follicles by comparison to established metabolite libraries

Metabolite	Approximate Retention Time
L-Alanine	14.45
Cholesterol	56.08
Citrate	32.97
L-Glutamate	28.69
Glycine	19.94
L-Lactate	13.61
L-Leucine	19.00
Linoleic Acid	41.15
D-Malate	25.77
Myo-Inositol	35.31
Oleic Acid	41.04
Palmitic Acid	37.42
L-Proline	22.18
Pyruvate	15.05
L-Serine	20.59
Stearic Acid	40.88
Succinate	22.44
L-Threonine	21.18
L-Valine	17.48

2.4.1. Metabolomics of *in vivo* derived follicles

In late antral follicles, cholesterol was the most abundant metabolite and its concentration was higher ($P < 0.0001$) than in early antral follicles. Likewise, myo-inositol was in higher ($P < 0.0005$) concentrations in late compared to early antral follicles. Amongst the amino acids, proline varied the most with stage, and its concentration was higher ($P < 0.001$) in late compared to early antral follicles. Pyruvate was the only metabolite that was in lower ($P < 0.0001$) concentrations in late compared to early antral follicles. With the exception of succinate, palmitate, stearate, leucine, serine, and valine, there was a general tendency for the remaining identified metabolites to be more enriched in late compared to early antral follicles (**Table 2.6**). Metabolites differing significantly in concentration between early and late antral follicles are summarized in **Figure 2.1 (A)**.

When subjected to a PLS-DA, metabolites from early and late antral follicles formed two clusters with some overlap (95% confidence interval) in a two dimensional plot (**Figure 2.2**). When three components of variation were considered, early and late antral follicles formed two distinct clusters (**Figure 2.3**).

Table 2.6: Relative proportions of metabolites in early and late antral follicles derived *in vivo* (n=9 per group)¹

Compound	Follicle Stage		<i>P</i> ²
	Early Antral (<i>in vivo</i>)	Late Antral (<i>in vivo</i>)	
Alanine	0.11 ± 0.02	0.11 ± 0.03	0.9997
Cholesterol	5.87 ± 1.11	19.85 ± 2.90	<0.0001*
Citrate	0.26 ± 0.08	0.36 ± 0.08	0.4962
Glutamate	0.33 ± 0.06	0.37 ± 0.07	0.9070
Glycine	0.98 ± 0.23	1.14 ± 0.24	0.7783
Lactate	4.34 ± 0.74	6.32 ± 0.39	0.0859
Leucine	0.14 ± 0.03	0.09 ± 0.03	0.3175
Linoleic Acid	0.26 ± 0.09	0.47 ± 0.08	0.1243
D-Malate	0.10 ± 0.01	0.20 ± 0.04	0.0751
Myo-Inositol	0.15 ± 0.04	0.55 ± 0.06	0.0003*
Oleic Acid	0.14 ± 0.03	0.19 ± 0.02	0.2973
Palmitic Acid	2.65 ± 0.57	2.35 ± 0.18	0.6774
Proline	0.02 ± 0.01	0.35 ± 0.09	0.0009*
Pyruvate	0.50 ± 0.02	0.21 ± 0.06	<0.0001*
Serine	0.11 ± 0.02	0.09 ± 0.04	0.9233
Stearic Acid	2.48 ± 0.80	2.25 ± 0.20	0.9078
Succinate	0.40 ± 0.04	0.33 ± 0.05	0.4872
Threonine	0.00 ± 0.00	0.01 ± 0.00	0.4120
Valine	0.15 ± 0.03	0.12 ± 0.04	0.9117

¹Values reported as least squares means, plus or minus the standard error of the mean

²P-value after Dunnett's adjustment

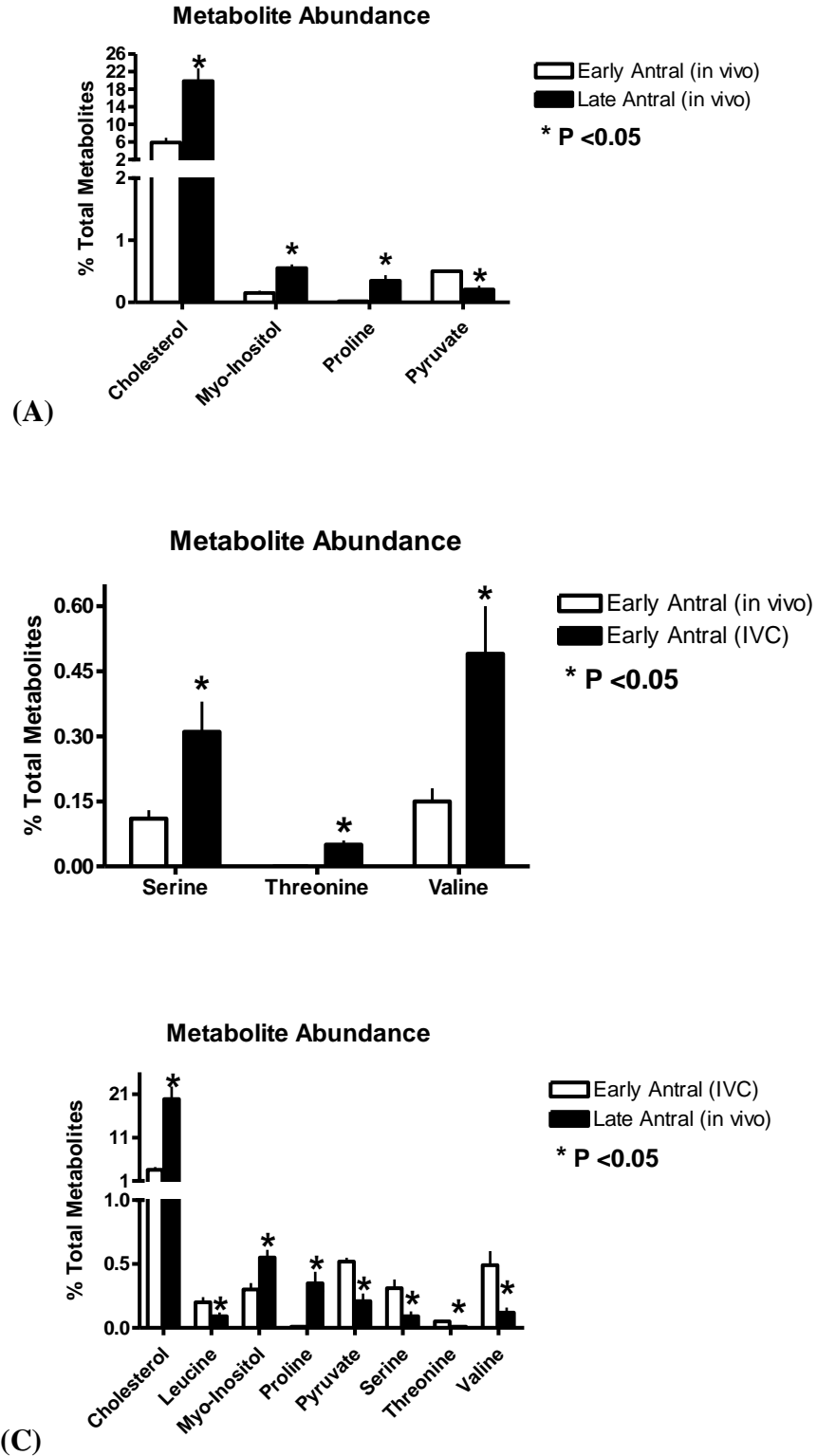


Figure 2.1: Metabolites found in significantly different concentrations between *in vivo* derived early and late antral follicles (A), between *in vivo* derived and *in vitro* cultured (IVC) early antral follicles (B), and between *in vivo* derived late antral follicles and *in vitro* cultured early antral follicles.

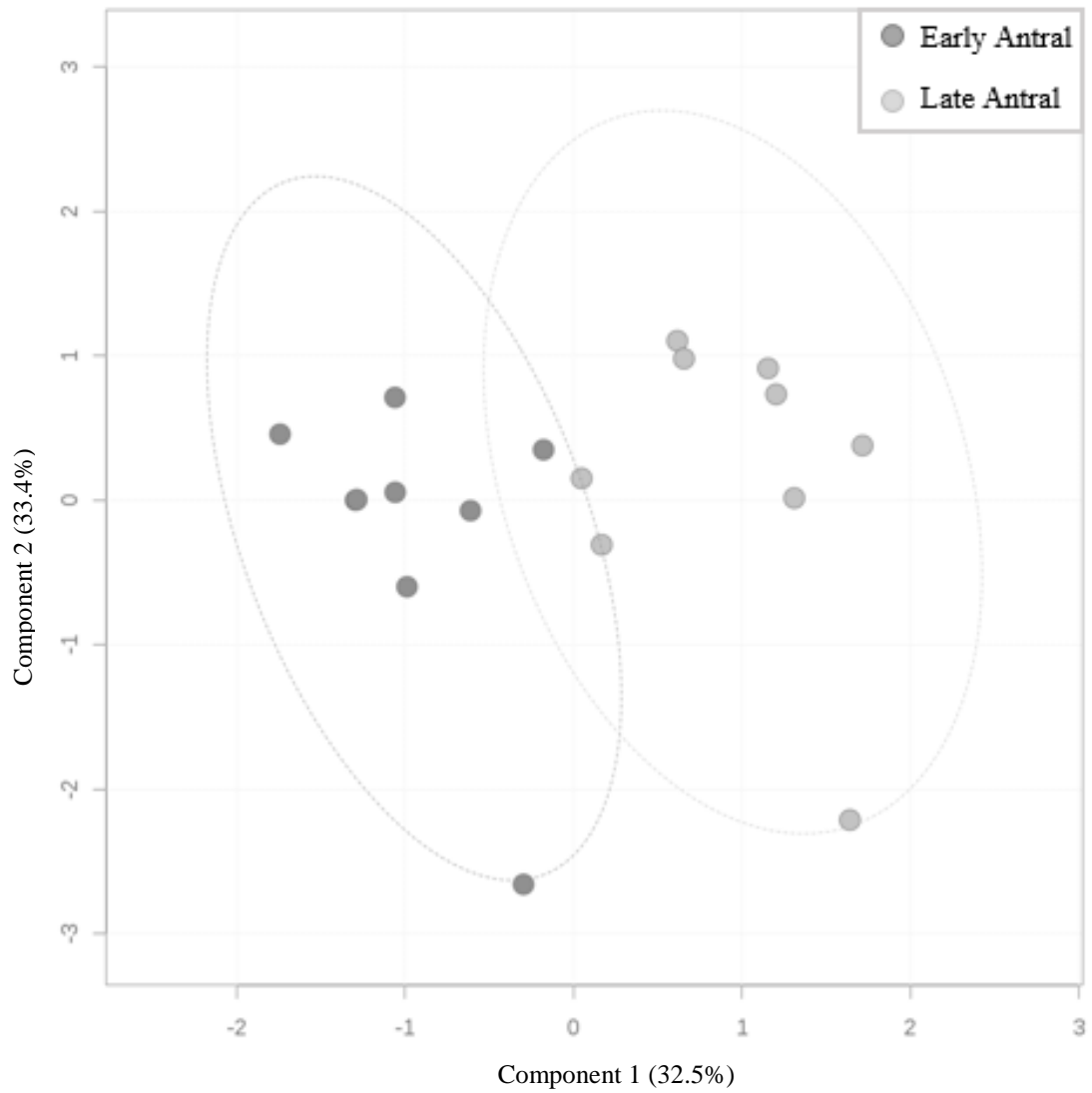


Figure 2.2: Two-dimensional PLS-DA of early (dark gray) and late (light gray) antral follicles, with a 95% confidence interval indicated around each cluster. The variation between samples captured by each component is indicated in parenthesis on each axis.

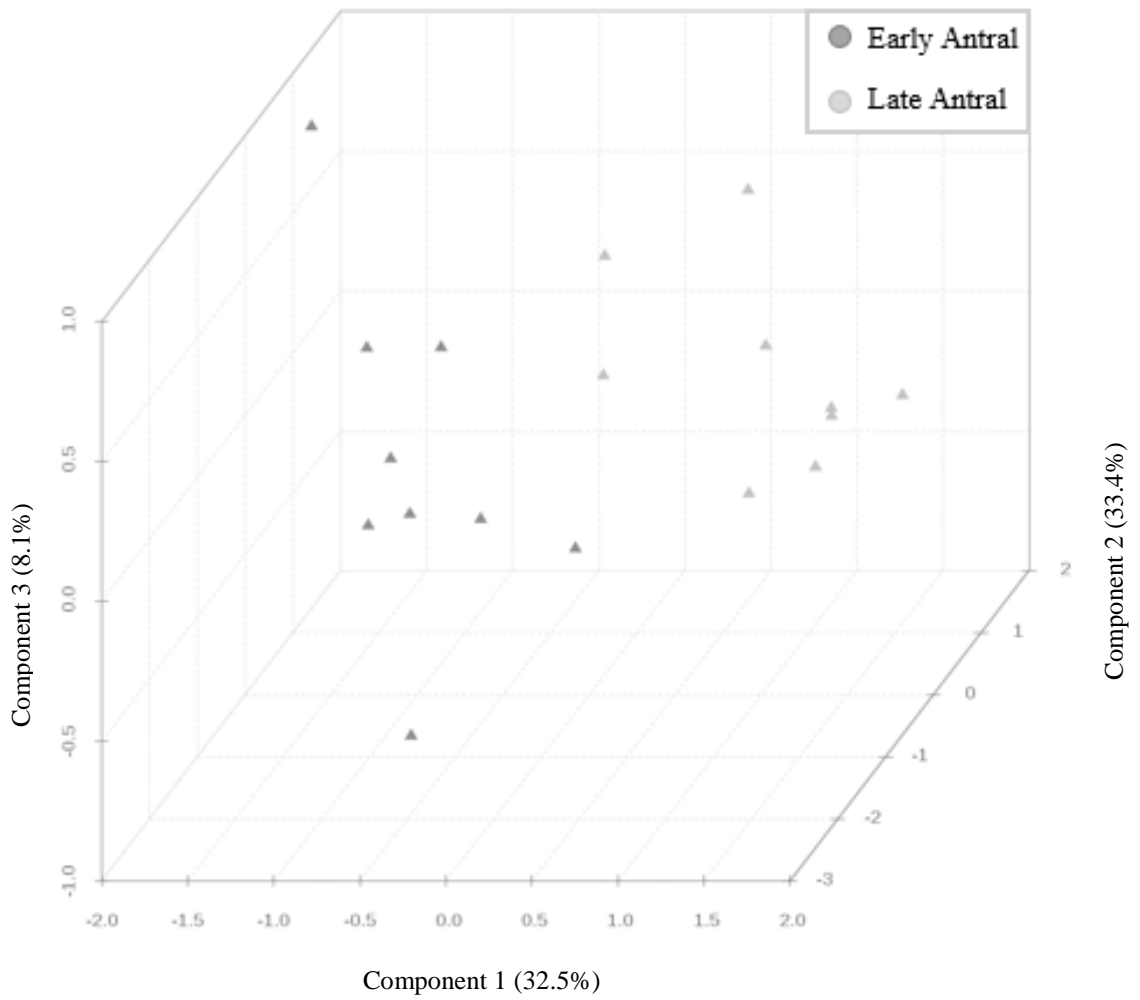


Figure 2.3: Three-dimensional PLS-DA of early (dark gray) and late (light gray) antral follicles. The variation between samples captured by each component is indicated in parenthesis on each axis.

2.4.2. *In vivo* derived versus *in vitro* cultured early antral follicles

Of those metabolites monitored for *in vivo* derived early antral follicles and those cultured *in vitro*, only 3 of 19 metabolites differed. In contrast to the differences observed between *in vivo* derived early and late antral follicles, the differences between *in vivo* and *in vitro* derived follicles were only evident in the proportional abundance of amino acids. Threonine, valine, and serine were all in higher proportions ($P < 0.001$, $P < 0.005$, and $P < 0.01$, respectively) in those follicles cultured *in vitro* compared to *in vivo* derived and analyzed follicles. With the exception of cholesterol, citrate, palmitate, and stearate which were all slightly lower in *in vitro* cultured follicles, there was an overall tendency for the remaining metabolites to be equivalent to or slightly higher in *in vitro* derived follicles (**Table 2.7**). Metabolites differing significantly in concentration between *in vivo* derived early and *in vitro* cultured early antral follicles are summarized in **Figure 2.1 (B)**.

Upon analysis of the samples using PLS-DA, samples from each group clustered together when plotted in two-dimensions; however, given a 95% confidence interval for each group, there is major overlap between the two groups (**Figure 2.4**). When plotted in a three-dimensional space, using the three major components of variation for the data, early antral follicles derived *in vivo* and early antral follicles cultured *in vitro* formed two distinct clusters (**Figure 2.5**).

Table 2.7: Relative proportions of metabolites in *in vivo* derived early antral follicles and *in vitro* culture early antral follicles (n=9 per group)¹

Compound	Follicle Stage		<i>P</i> ²
	Early Antral (<i>in vivo</i>)	Early Antral (<i>in vitro</i>)	
Alanine	0.11 ± 0.02	0.11 ± 0.03	0.9848
Cholesterol	5.87 ± 1.11	3.58 ± 0.61	0.5162
Citrate	0.26 ± 0.08	0.19 ± 0.05	0.7254
Glutamate	0.33 ± 0.06	0.44 ± 0.07	0.4247
Glycine	0.98 ± 0.23	1.39 ± 0.16	0.2384
Lactate	4.34 ± 0.74	6.20 ± 0.88	0.1084
Leucine	0.14 ± 0.03	0.20 ± 0.04	0.2670
Linoleic Acid	0.26 ± 0.09	0.32 ± 0.05	0.8168
D-Malate	0.10 ± 0.01	0.10 ± 0.02	0.9906
Myo-Inositol	0.15 ± 0.04	0.30 ± 0.05	0.1573
Oleic Acid	0.14 ± 0.03	0.14 ± 0.02	0.9994
Palmitic Acid	2.65 ± 0.57	2.32 ± 0.31	0.6171
Proline	0.02 ± 0.01	0.01 ± 0.01	0.9986
Pyruvate	0.50 ± 0.02	0.52 ± 0.03	0.9096
Serine	0.11 ± 0.02	0.31 ± 0.07	0.0085*
Stearic Acid	2.48 ± 0.80	2.15 ± 0.35	0.8209
Succinate	0.40 ± 0.04	0.39 ± 0.08	0.9707
Threonine	0.00 ± 0.00	0.05 ± 0.01	<0.0001*
Valine	0.15 ± 0.03	0.49 ± 0.11	0.0025*

¹Values reported as least squares means, plus or minus the standard error of the mean

²P-value after Dunnett's adjustment

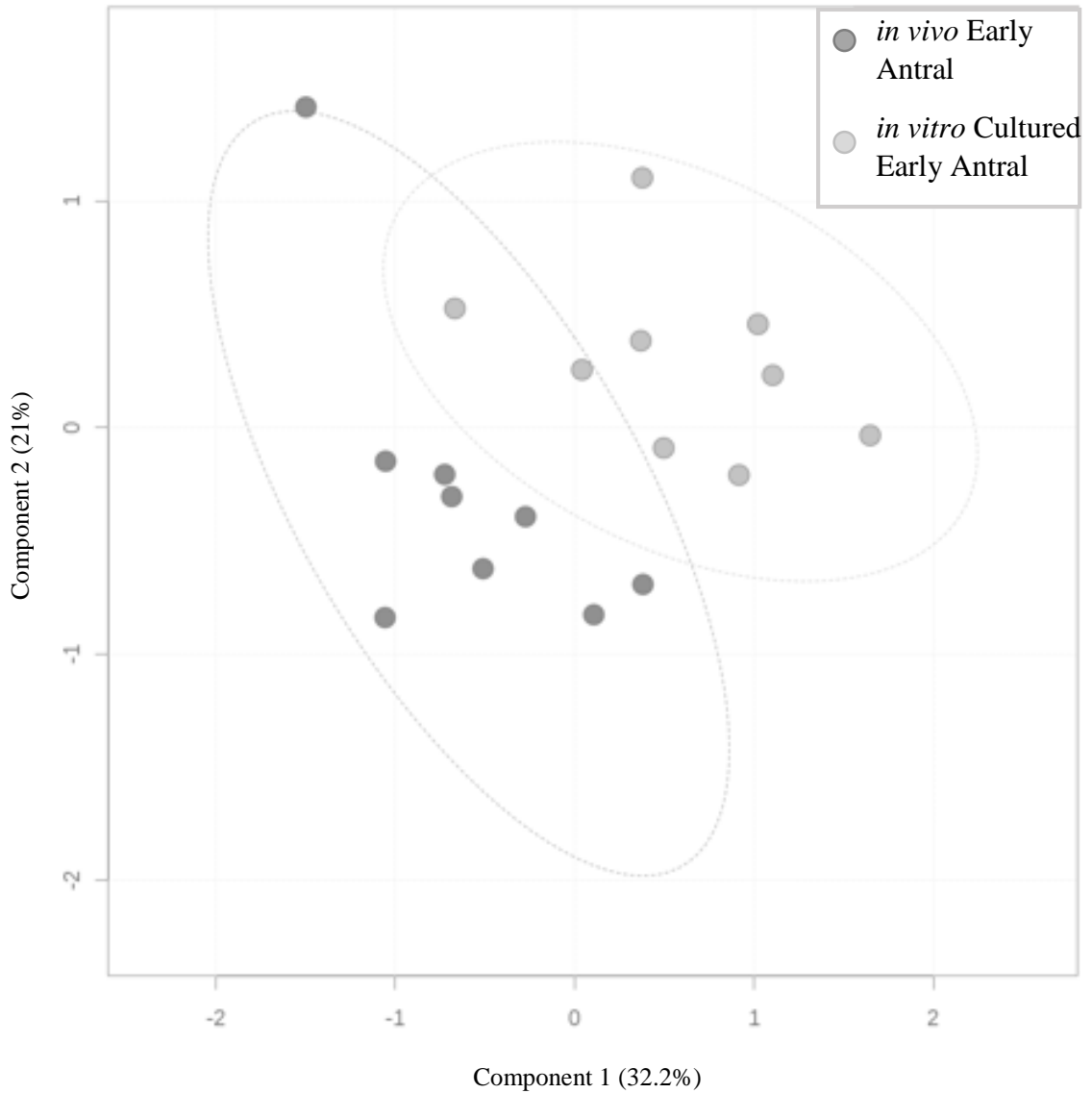


Figure 2.4: Two-dimensional PLS-DA of early antral follicles collected directly from feline ovaries (dark gray) and early antral follicles cultured *in vitro* (light gray), with a 95% confidence interval indicated around each cluster. The variation between samples captured by each component is indicated in parenthesis on each axis.

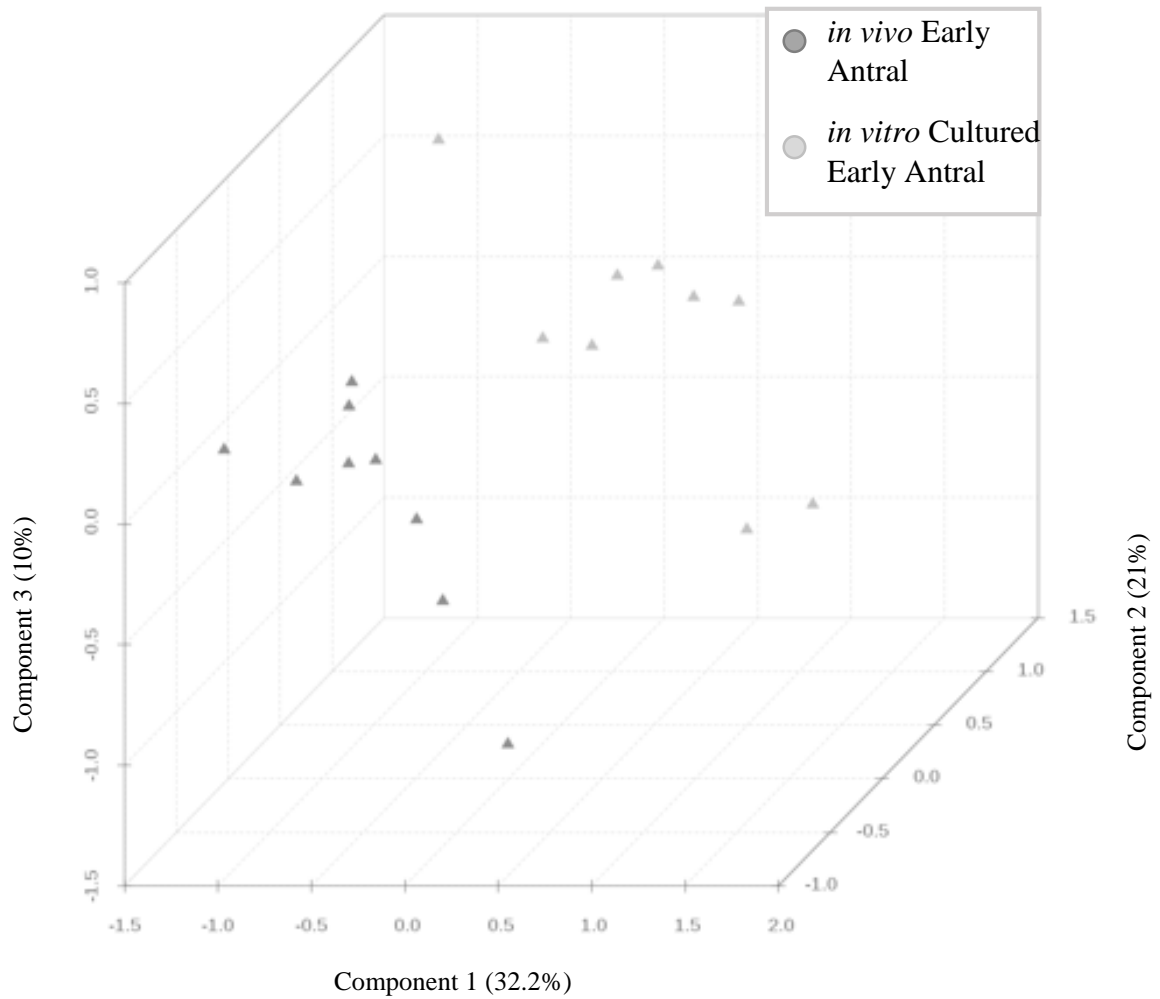


Figure 2.5: Three-dimensional PLS-DA of early antral follicles collected directly from feline ovaries (dark gray) and early antral follicles cultured *in vitro* (light gray). The variation between samples captured by each component is indicated in parenthesis on each axis.

2.4.3. *In vivo* late antral follicles versus *in vitro* cultured early antral follicles

In late antral follicles, cholesterol was the most abundant metabolite and its concentration was higher ($P = 0.0004$) than in *in vitro* cultured early antral follicles. Likewise, myo-inositol was in higher ($P = 0.0315$) concentrations in late antral follicles compared to *in vitro* cultured early antral follicles. Pyruvate was found in lower ($P = 0.0005$) concentrations in late antral follicles compared to *in vitro* cultured early antral follicles. Amongst the amino acids, proline was the only amino acid found in higher concentrations ($P = 0.0052$) in late antral compared to *in vitro* cultured early antral follicles. Leucine, serine, threonine, and valine were all found in lower concentrations ($P = 0.0082$, $P = 0.0198$, $P = 0.0031$, $P = 0.0076$, respectively) in late antral follicles as compared to *in vitro* cultured early antral follicles. There was a general tendency for the identified fatty acids and TCA cycle intermediates, with the exception of succinate, to be more enriched in late antral compared to *in vitro* cultured early antral follicles (**Table 2.8**). Metabolites differing significantly in concentration between *in vivo* derived late antral and *in vitro* cultured early antral follicles are summarized in **Figure 2.1 (C)**.

When subjected to a PLS-DA, metabolites from late antral follicles and *in vitro* cultured early antral follicles allowed for formation of two clusters with some overlap (95% confidence interval) in a two dimensional plot (**Figure 2.6**). When three components of variation were considered, the groups formed two distinct clusters (**Figure 2.7**).

Table 2.8: Relative proportions of metabolites in *in vitro* cultured early antral follicles and late antral follicles derived *in vivo* (n=9 per group)¹

Compound	Follicle Stage		P ²
	Early Antral (<i>in vitro</i> cultured)	Late Antral (<i>in vivo</i>)	
Alanine	0.11 ± 0.03	0.11 ± 0.03	0.8789
Cholesterol	3.58 ± 0.61	19.85 ± 2.90	0.0004*
Citrate	0.19 ± 0.05	0.36 ± 0.08	0.0755
Glutamate	0.44 ± 0.07	0.37 ± 0.07	0.5060
Glycine	1.39 ± 0.16	1.14 ± 0.24	0.4197
Lactate	6.20 ± 0.88	6.32 ± 0.39	0.9149
Leucine	0.20 ± 0.04	0.09 ± 0.03	0.0082*
Linoleic Acid	0.32 ± 0.05	0.47 ± 0.08	0.0695
D-Malate	0.10 ± 0.02	0.20 ± 0.04	0.0764
Myo-Inositol	0.30 ± 0.05	0.55 ± 0.06	0.0315*
Oleic Acid	0.14 ± 0.02	0.19 ± 0.02	0.0878
Palmitic Acid	2.32 ± 0.31	2.35 ± 0.18	0.8448
Proline	0.01 ± 0.01	0.35 ± 0.09	0.0052*
Pyruvate	0.52 ± 0.03	0.21 ± 0.06	0.0005*
Serine	0.31 ± 0.07	0.09 ± 0.04	0.0198*
Stearic Acid	2.15 ± 0.35	2.25 ± 0.20	0.7028
Succinate	0.39 ± 0.08	0.33 ± 0.05	0.3074
Threonine	0.05 ± 0.01	0.01 ± 0.00	0.0031*
Valine	0.49 ± 0.11	0.12 ± 0.04	0.0076*

¹Values reported as least squares means, plus or minus the standard error of the mean

²P-value after Dunnett's adjustment

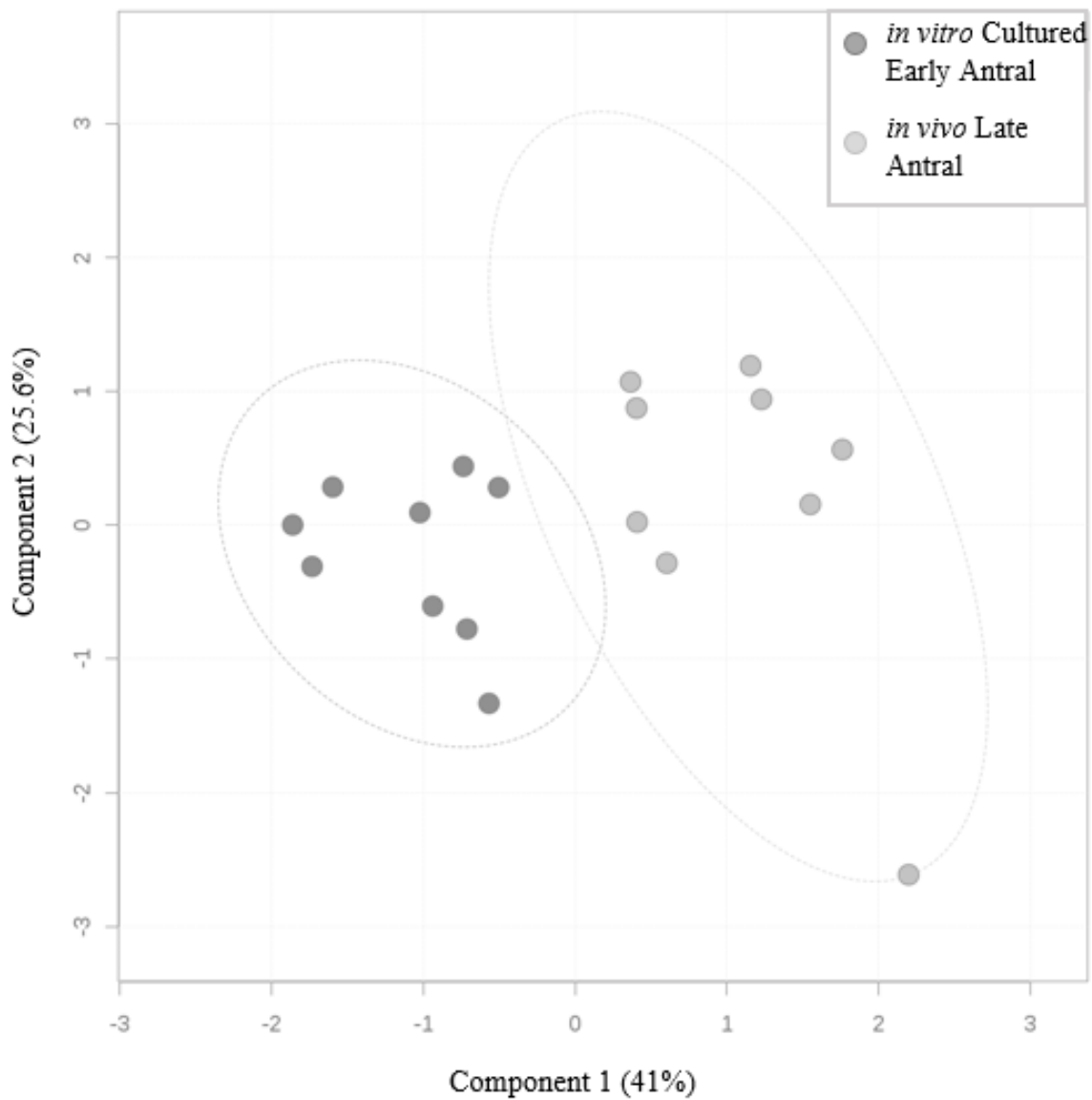


Figure 2.6: Two-dimensional PLS-DA of *in vitro* cultured early antral (dark gray) and *in vivo* derived late (light gray) antral follicles, with a 95% confidence interval indicated around each cluster. The variation between samples captured by each component is indicated in parenthesis on each axis.

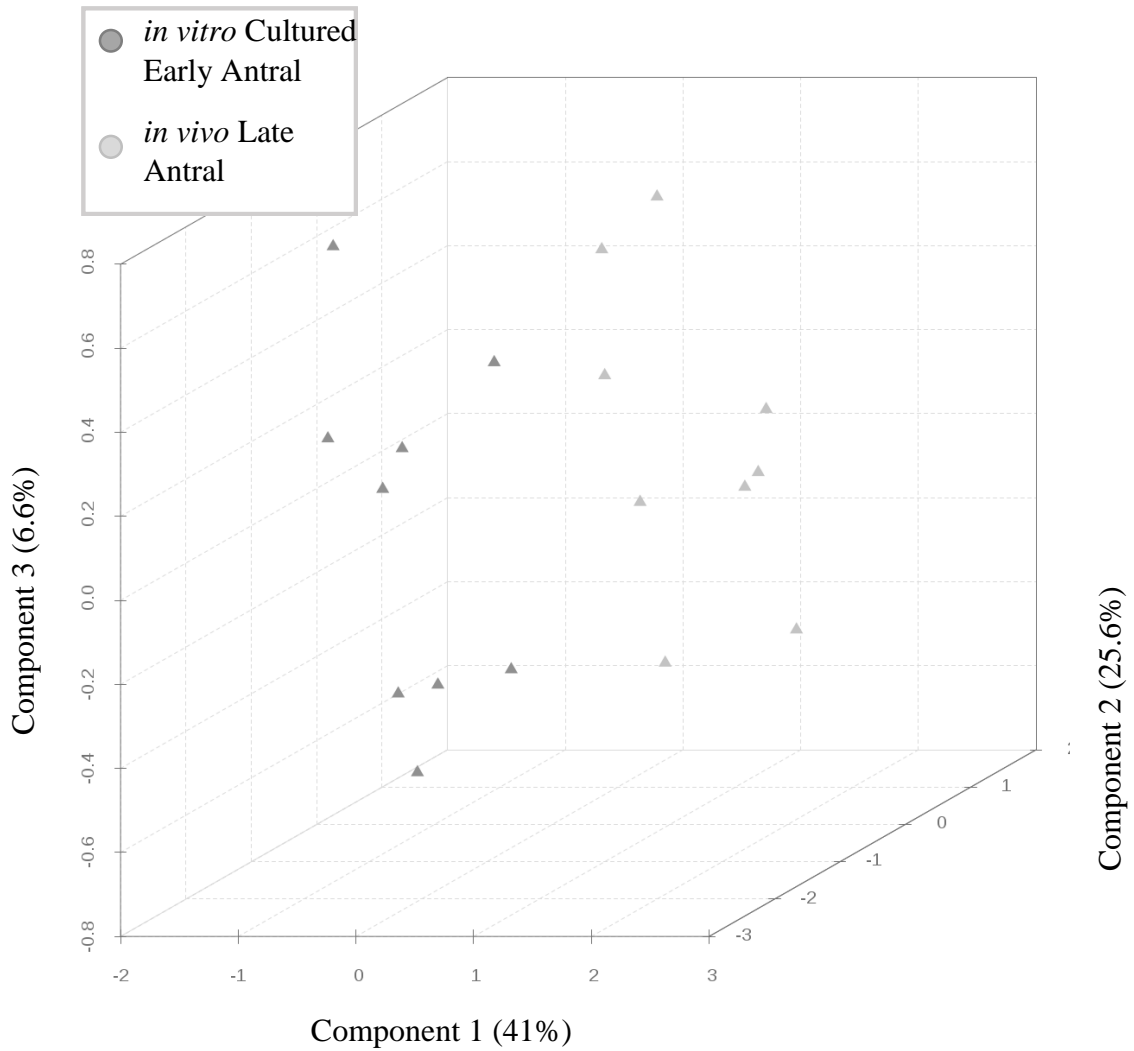


Figure 2.7: Three-dimensional PLS-DA of *in vitro* cultured early antral (dark gray) and *in vivo* derived late (light gray) antral follicles. The variation between samples captured by each component is indicated in parenthesis on each axis.

2.5. Discussion

Folliculogenesis is a highly coordinated and energy-dependent process; however, the means by which follicles and oocytes obtain and process energetic substrates is not well understood. Previous studies exploring follicle metabolism in humans and domestic species have relied upon a limited number of exogenous substrates in spent media. These studies have provided invaluable information regarding the metabolism of follicles, but are hindered by their limited scope and indirect measurement. Recent applications of metabolomic technologies to assess follicle, oocyte, and COC metabolism in human and livestock species have provided a more robust method for metabolic evaluation (Revelli *et al.*, 2009). The objective of this study was to use refined methods of derivatization and evaluation of follicular samples via GC-MS to (1) evaluate intrinsic metabolic differences exhibited by feline follicles of different developmental stages, as well as to (2) assess the influence of *in vitro* culture on the metabolic profile of follicles of the same developmental stage. To address these objectives, early (< 0.5 mm) and late antral follicles (> 2.0 mm) were isolated from reproductively mature females for comparison. In addition, early antral follicles were subjected to long-term (12 d) *in vitro* culture, which should have given the follicles ample time to progress to the late antral stage; however, only minor growth occurred. Previous studies have shown that follicles undergo shifts in substrate utilization and thus metabolism throughout development; understanding the metabolic basis for these shifts, as well as their effect on oocyte maturation and fertilization potential, has been proposed as a major goal towards ART improvement.

2.5.1. Lipids: Fatty Acids, Cholesterol

The lipid and fatty acid profile of follicular fluid has been shown to vary between species (Sturmey *et al.*, 2009). In the current study, the predominant fatty acids detected in feline follicles were palmitic, stearic, oleic, and linoleic acid. Significant changes among fatty acid composition in groups were not observed, however. This is in line with previous reports that non-esterified fatty acid concentrations in the follicular fluid do not vary with bovine follicle size (Leroy *et al.*, 2004b). Stearic and palmitic acid were the most abundant of the four fatty acids in the feline follicles. The most abundant fatty acid observed in cow oocytes was palmitic acid; in sheep, oleic acid; in pigs, palmitic and oleic acids. By contrast, in humans, stearic acid has been reported to be the most abundant fatty acid (Paczkowski *et al.*, 2013). Of the polyunsaturated fatty acids, linoleic and arachidonic acid are the most abundant in cattle, pig, and sheep denuded oocytes (McEvoy *et al.*, 2000). While feline follicle fatty acid profiles have not been examined previously, the findings from the current study reflect fatty acids found in the follicular fluid of other species. In addition, previous reports show that linoleic and oleic acids are present in feline oocytes, which is consistent with the current results (Apparicio *et al.*, 2012). Given the essentiality of fatty acid oxidation for energy production and oocyte nuclear maturation, it is not surprising that saturated fatty acids were found in the highest concentrations (Sturmey *et al.*, 2009).

In bovine follicular fluid, total cholesterol has been reported to increase from 1.45 (± 0.09) to 1.65 (± 0.08) mM between small (< 4 mm) and large (> 10 mm) follicles (Leroy *et al.*, 2004a). In accordance with these findings, cholesterol was most abundant amongst the metabolites in feline follicular fluid, and its relative concentration was higher in late (20%) compared to early (6%) antral follicles and *in vitro* cultured early (4%) antral

follicles. Cholesterol in follicular fluid is primarily bound to high density lipoproteins (HDLs) as other lipoproteins are too large to pass across the blood-follicle barrier. Furthermore, due to the increased permeability of the follicular wall in late compared to early stage follicles, the increase in cholesterol is likely due to an increased uptake of HDL (Leroy *et al.*, 2004a). Cholesterol also plays a key role in steroid hormone biosynthesis; of these hormones, progesterone is produced in high amounts by corpora lutea, formed from the remains of ovulatory follicles and is required to maintain pregnancy. The proportion cholesterol tended to decrease, although not significantly, during *in vitro* culture of early antral follicles.

2.5.2. Lactate and Pyruvate

Most studies have measured follicular fluid concentrations of glucose, lactate, and pyruvate as indicators of follicle metabolic status. Across species, decreased glucose, increased lactate, and no difference in pyruvate concentrations are observed in follicular fluid of large versus small follicles (Nandi *et al.*, 2008). In the present study, lactate tended to comprise an increased proportion of all metabolites in *in vivo* derived late antral follicles and early antral follicles cultured *in vitro* as compared to *in vivo* derived early antral follicles. The proportion of pyruvate did not change significantly between early antral follicles derived *in vivo* and those cultured *in vitro*; however, pyruvate comprised a significantly lower proportion of metabolites in late antral follicles compared to *in vivo* derived and *in vitro* cultured early antral follicles. While these results appear to contradict previous findings in follicular fluid, it is most likely due to the fact that slightly different samples were collected. Granulosa cells are known to metabolize glucose to pyruvate and

lactate, which the oocyte utilizes as an energy substrate. It is possible that pyruvate is released to the follicular fluid in similar concentrations between follicles sizes, but that the oocytes of late antral follicles metabolize pyruvate to other metabolites at higher rates, accounting for the lower detected abundance. In addition, abundances in this study are not absolute concentrations, so it is possible that there are significantly more metabolites present in late antral follicles and that the absolute concentration of pyruvate is not different between follicle sizes.

Alternatively, in previous studies of follicle size, pyruvate concentrations were found to be lower compared to lactate (Nandi *et al.*, 2008). This finding is reflected in the present study where pyruvate contributions to the total metabolite pool were much lower than lactate within a given size of follicle. In *in vivo* derived early antral follicles, lactate accounted for 4.3% of all metabolites, while pyruvate constituted only 0.5% of the same pool. For late antral follicles, lactate constituted 6.3% of all metabolites, while pyruvate contributed only 0.2%. *In vitro* culture of early antral follicles results in 6.2% and 0.5% contributions of lactate and pyruvate, respectively.

2.5.3. Amino Acids

No significant differences in the proportion of amino acids in the metabolite profile were detected between follicles of different developmental stages *in vivo*. However, serine, threonine, and valine were higher in early antral follicles that had been cultured *in vitro* compared to *in vivo* derived early antral follicles. This was mirrored in the comparison of *in vitro* cultured early antral follicles to *in vivo* derived late antral follicles, although leucine was also higher in *in vitro* cultured early antral follicles. It is well documented that

follicles, oocytes, and COCs are very susceptible to changes in their micro-environments. Given that these four amino acids were included in culture media at supraphysiological concentrations (**Table 2.9**), and that leucine, threonine, and valine are essential amino acids that can only be obtained from the environment, it is probable that *in vitro* cultured follicles were simply able to take up higher amounts of these amino acids than their *in vivo* derived counterparts due to their higher availability and were concentrated within the follicle. This pattern was mirrored in glutamate and glycine which tended to be higher in cultured follicles than those derived directly from the cat, while proline and alanine tended to be roughly equivalent. Glycine and glutamine (i.e. a precursor of glutamate) were all included in the culture media, while alanine and proline, which did not vary across treatments, had not been included.

Table 2.9: Physiological and Media concentrations of selected amino acids

Amino Acid	Concentrations (mM)	
	Feline Serum ²	Culture Media ¹
Alanine	0.256	0.000
Glutamate	0.053	0.000
Glutamine	0.190	2.000
Glycine	0.100	0.400
Leucine	0.034	0.802
Proline	0.053	0.000
Serine	0.050	0.400
Threonine	0.054	0.798
Valine	0.064	0.803

¹ Current Study

²Guerin *et al.*, 2002

Previous studies with feline follicles have established the amino acid concentrations in tubal fluid and late antral (2-3 mm) follicular fluid employing HPLC. However, cross-stage developmental comparisons have not been performed. Alanine, taurine, glutamine, and glutamate have been reported to be the most abundant amino acids in follicular fluid, while evaluation of feline tubal fluid revealed that glycine, glutamate, and taurine were the highest (Guerin *et al.*, 2012). Each amino acid detected in this study is represented as a percent of all detected amino acids, for the current and previous data in **Table 2.10**. Amino acid profiles of late antral follicles determined in this manner are quite different for this study compared to Guerin *et al.* (2010). Alanine, glutamate, and glycine were the most abundant in the previous report, while glycine, glutamate, proline were the most abundant in late antral follicles in the present study. Possible sources of differences could be a result of the different sampling methods. Granulosa and theca cells, as well as oocyte contributions to the amino acid profile, in addition to the follicular fluid (exclusively examined in the Guerin study), were examined in the current study. It is possible, for example, that glycine is found in elevated concentrations in the oocyte and follicular cells, compared to the follicular fluid.

Table 2.10: Percent abundance of detected amino acids

Amino Acid	Follicle Developmental Stage and Environment	
	Late Antral (<i>in vivo</i>) ¹	Late Antral (<i>in vivo</i>) ²
Alanine	4.82	29.21
Glutamate	16.23	20.83
Glycine	50.00	18.23
Leucine	3.95	3.99
Proline	15.35	5.70
Serine	3.95	7.24
Threonine	0.44	6.92
Valine	5.26	7.89
TOTAL	100	100

¹ Current Study²Guerin *et al.*, 2002

2.5.4. MyoInositol

No differences in myo-inositol, as a proportion of all metabolites, was detected between *in vivo* derived early antral follicles and those cultured *in vitro*. However, myo-inositol comprised a higher proportion of the metabolite profile in late antral follicles than in *in vivo* derived and *in vitro* cultured early antral follicles.

Inositol is a fundamental structural component of signaling molecules implicated in the process of fertilization. In felids, myo-inositol serves as a substrate for the biosynthesis of inositol-phosphate compounds, including phosphatidylinositol 4,5-bisphosphate (PIP₂). PIP₂ is a phospholipid localized in the plasma membrane of oocytes, which is hydrolyzed upon binding with phospholipase C after fertilization, producing diacylglycerol and inositol trisphosphate (IP₃) (White *et al.*, 2010). The resulting IP₃ serves a secondary messenger, which upon binding to IP₃ receptors, initiates the release of calcium from the endoplasmic reticulum to prevent polyspermy (Runft *et al.*, 1999; Wagner *et al.*,

2004). Decreased expression of type 1 IP₃ receptors has been implicated in the reduced fertility of cryopreserved oocytes (Hirose *et al.*, 2013). Given this information, it is not surprising that throughout growth, the oocyte accumulates myo-inositol for eventual biosynthesis of PIP₂. It is reasonable to assume that late antral follicles, containing oocytes poised for fertilization, would contain higher levels of myo-inositol than early antral follicles.

2.5.5. TCA Cycle Intermediates

No difference between follicle developmental stage or developmental environments (*in vivo* versus *in vitro*) were detected for the Krebs cycle intermediates citrate, malate, and succinate. This finding was somewhat unexpected, given that one would expect elevated Krebs cycle activity (i.e., oxidation, ATP synthesis) to support the increased energy demands of the follicle. However, it does not appear that the proportion of these compounds to the entire metabolite profile is altered. This would be expected given that these compounds are both synthesized and utilized in this circular pathway. The constant need to produce and to use these metabolites would favor regulation over a buildup or deficiency.

2.5.6. Partial Least Squares-Discriminant Analysis

Given that groups cluster together when analyzed via 2-D and 3-D PLS-DA, metabolomics offers a means to classify follicles on a metabolic basis. However, the overlap observed in 2-D PLS-DA plots suggests the need to identify additional metabolites to further discriminate the classes of follicles. A comparative analysis of atretic follicles

or of follicles producing oocytes of known maturational ability, when aided with these additional biomarkers, could be a more definitive approach for identifying healthy follicles and viable oocytes.

Similarity of the early antral follicles cultured *in vitro* to those derived *in vivo* and the marked difference to late antral follicles, in both size (growth throughout *in vitro* culture was minimal) and in metabolite profile after lengthy culture which gave the follicles sufficient time to progress suggests that *in vitro* cultured early antral follicles are not shifting to the metabolism expressed by late antral follicles. It is possible that improvements to follicle culture media formulations are needed in order to allow for this progression of development to the late antral stage to occur.

Chapter 3: Fluxomic Analysis of Feline Follicles

3.1. Introduction

The family *Felidae* encompasses 37 species, of which only the domestic cat is not endangered or threatened by extinction. A rapid decline in wild populations has been experienced, mainly due to constant onslaught from poaching and habitat destruction. Recently, conservation management programs in zoological parks have sparked exploration into expanding the use of ARTs to preserve and easily transport valuable genetics. Unfortunately, ART efficiencies are still very low for many populations and research in felids to improve these methods are very limited (Bristol-Gould and Woodruff, 2006).

Past studies have examined follicle metabolism in livestock species. In these studies, the metabolite composition of follicular fluid has been shown to mirror changes in serum metabolite concentrations in cattle, suggesting that the follicle is highly dependent upon its environment for metabolic substrates (Leroy *et al.*, 2004b). This justifies the assertion that in order to improve ART efficiencies, culture conditions must be improved to better serve the metabolic needs of the follicle (or other reproductive structure). The

first step to improving culture conditions is achieving a better understanding of the metabolic status of the follicles to be cultured.

Static snapshots of follicular metabolism have been gleaned from photometric assays and metabolomic analysis as in Chapter 2. Similar patterns in concentrations of glucose and lactate in follicles across sizes have been observed in several species including sheep, buffalo, and dairy cows and heifers, and in the case of lactate, with cats. Glucose concentrations are higher in large compared to smaller follicles, while lactate concentrations are lower, or tend to be lower, as was shown in cats (Leroy *et al.*, 2004; Nandi *et al.*, 2008; Nishimoto *et al.*, 2009). Pyruvate, unlike glucose and lactate, does not appear to change in concentration across follicle sizes (Nandi *et al.*, 2008). While lipid profiles and abundances vary in follicles from different species, palmitic and oleic acids have been shown to be some of the most prevalent fatty acids in bovine and porcine COCs (Paczkowski *et al.*, 2013). Other products of metabolism including (total) cholesterol and urea also vary according to follicle size, with total cholesterol increasing and urea decreasing as follicle size increases (Leroy *et al.*, 2004a). Unfortunately, examining the presence or absence of metabolites in a sample does very little to provide a dynamic picture of a cell's physiologic state.

Enhanced glycolytic activity is an essential aspect of many rapidly growing and developing cells, including the oocyte and follicle. However, although glucose uptake increases during *in vitro* oocyte maturation, glycolytic rates of COCs as assessed by lactate production does not increase (Sutton-McDowall *et al.*, 2010). In this respect, at best, lactate production provides a crude measure of glycolytic flux. It is clear, therefore, a more

targeted approach is needed to directly assess follicle metabolism and the substrates it requires to fulfill its metabolic requirements.

Fluxomics employs stable isotope tracers to interrogate metabolic pathways, to determine the essential substrates of those pathways, and to assess the various connections between pathways which allow the cell to meet its energetic and biosynthetic needs (Berthold *et al.*, 1994; Bequette *et al.*, 2006). The advantage of ^{13}C -based fluxomics (i.e. ^{13}C -labelled substrates (“tracers”) and intermediates) lies in the fact that many metabolic pathways are interconnected, thus the ^{13}C -labelling of downstream products of the metabolism of the tracer yield dynamic and quantifiable information regarding the operative pathways. Patterns of incorporation of the tracer are predictable, utilizing known interconnections between pathways and established carbon fate maps (Mu *et al.*, 2007, Metallo *et al.*, 2009). While these methods have been extensively employed in several disciplines including biomedical research and bioengineering, its potential has yet to be realized in the field of reproduction. In the following work, ^{13}C -fluxomics was employed to explore and interrogate metabolic pathways and their fluxes in feline follicles of different sizes (developmental stages) and *in vivo* and *in vitro* environments.

3.2. Rationale and Hypotheses

A comprehensive understanding of feline follicular metabolism is still lacking in reproduction science. While strides have been made to determine the profiles of important metabolites, fluxes through essential metabolic pathways (e.g, glycolysis (GLYC), pentose phosphate pathway (PPP), Krebs cycle (TCA cycle)) and the substrates utilized in these pathways have yet to be determined. While the metabolites present within a sample or cell

gives some clues to the function of pathways, they only provide a static, incomplete picture of the underlying metabolism and flux. A more robust understanding of the ebb and flow of metabolites is essential not only for basic knowledge, but also for eventual improvement of ARTs and advancement of IVC procedures. Metabolite fluxes through central pathways of carbon metabolism will provide insights into the altered metabolic demands and fundamental functions of follicles at different developmental stages and from different growth environments.

Two comparisons are of interest in this study, (1) the differences in carbon substrate flux between early and late antral follicles developed *in vivo* and (2) how these metabolic fluxes may be altered in *in vitro* cultured early antral follicles, as opposed to their *in vivo* derived counterparts. In accordance with earlier studies, it was expected that the fluxes through glycolysis would be similar, while PPP and Krebs cycle activities would differ.

3.3. Materials and Methods

3.3.1. Study Design: Partial Block Design for Cat, Age

Three groups of follicles were identified for study: early antral follicles originating *in vivo*, late antral follicles originating *in vivo*, and early antral follicles which underwent *in vitro* culture for 12 d. When possible, samples for each group were obtained from a single cat. Otherwise, cats of similar age (± 0.5 yr) and type (house or stray cat) were paired and used to obtain samples for each group.

3.3.2. Follicle Collection and Storage

Feline ovaries were acquired as a byproduct of routine ovariohysterectomies from a local spay clinic, Animal Birth Control, LLC, in central Maryland. The paired ovaries from sexually mature cats (defined as at least one year old) were transported to the University of Maryland, College Park on ice in phosphate buffered solution (PBS; Cellgro Mediatech, Manassas, VA). Cortical slices were obtained from paired ovaries in warmed (38.5 °C) collection media (**Table 3.1**). Morphologically healthy, early antral (defined as a follicle less than 0.5 mm in diameter with a visible antrum) and late antral follicles (defined as a follicle greater than 2 mm in diameter with a visible antrum) were mechanically isolated from ovaries as previously described (Jewgenow and Goritz, 1995). Ten early antral follicles and singular late antral follicles from each cat were washed through PBS, placed into individual wells with 500 µL of tracer culture media (containing a 50:50 mixture of unlabeled and [U-¹³C]-labeled glucose; **Table 3.2**), and incubated for 24 hrs in a 5% CO₂ incubator at 38.5 °C. Following incubation, the early antral follicles were pooled, washed through PBS, and stored at -80 °C until processing. The spent media from these incubation wells were also pooled and stored at -80 °C. The late antral follicle and its spent media were collected individually and stored in the same fashion. An additional ten early antral follicles from each cat were encapsulated in 20 µL of 0.5% alginate hydrogel (Novamatrix, Sandvika, Norway), which was hardened in a salt solution (**Table 3.3**) for three minutes, washed through maintenance media (**Table 3.4**), and cultured in individual wells of a 48-well incubation plate (0.75 cm² growth area) with 500 µL of culture media (**Table 3.5**). Incubations ran for 12 days in a 5% CO₂ incubator at 38.5 °C. Half of the culture media was refreshed every 72 hours throughout incubation.

On the final day, follicles were washed through warmed PBS, transferred individually to 500 μ L of tracer culture media, and incubated for an additional 24 hrs. Spent media was pooled and frozen; healthy follicles were mechanically isolated from their alginate drops in PBS, washed and pooled, and stored at -80 °C until processing.

Table 3.1: Composition and Company Source Information for Follicle Collection Media.

Follicle Collection Media: Stored at 4°C, used at 38.5°C		
Medium 199 (TCM with Hepes)	200 mL	Sigma Aldrich, St. Louis, MO
L-Glutamine	0.0584 g	Sigma Aldrich, St. Louis, MO
Sodium Pyruvate: 100mM Stock	2 mL	Gibco-Life Technologies, Grand Island, NY
Penicillin G-Streptomycin Sulfate: 10,000 U/mL Penicillin; 10,000 µg/mL Stock	1 mL	Invitrogen-Life Technologies, Grand Island, NY
Bovine Serum Albumin	0.6 g	Rockland, Inc., Gilbertsville, PA

Table 3.2: Composition and Company Source Information for Follicle Tracer Culture Media.

Follicle Tracer Culture Media: Stored at 4°C, used at 38.5°C		
Dulbecco's Modified Eagle's Medium – without Glucose, Glutamine, Pyruvate, and Phenol Red	200 mL	Gibco-Life Technologies, Grand Island, NY
L-Glutamine	0.0584 g	Sigma Aldrich, St. Louis, MO
D-Glucose	0.0991 g	Sigma Aldrich, St. Louis, MO
Universally Labeled Carbon-13 Glucose	0.1024 g	Cambridge Isotope Laboratories, Tewksbury, MA
Insulin-Transferrin-Selenium: 25 mg/50mL Insulin-Transferrin, 25 ug/50mL Selenium Stock	2 mL	Sigma Aldrich, St. Louis, MO
Penicillin G-Streptomycin Sulfate: 10,000 U/mL Penicillin; 10,000 µg/mL Stock	1 mL	Gibco-Life Technologies, Grand Island, NY
Sodium Pyruvate: 100 mM Stock	2 mL	Gibco-Life Technologies, Grand Island, NY
Bovine Serum Albumin	0.6 g	Rockland, Inc., Gilbertsville, PA
Follicle Stimulating Hormone: 0.355 mg/mL Stock	563 µL	Sigma Aldrich, St. Louis, MO

Table 3.3: Composition and Company Source Information for Calcium Chloride Solution

Salt Solution: Stored and used at Room Temperature		
distilled H ₂ O	50 mL	
Calcium chloride (anhydrous)	0.277 g	Sigma Aldrich, St. Louis, MO
Sodium chloride	0.410 g	Sigma Aldrich, St. Louis, MO

Table 3.4: Composition and Company Source Information for Maintenance Media

Maintenance Media: Stored at 4°C, used at 38.5°C		
Dulbecco's Modified Eagle's Medium – low glucose	100 mL	Sigma Aldrich, St. Louis, MO
L-Glutamine	0.0292 g	Sigma Aldrich, St. Louis, MO
Penicillin G-Streptomycin Sulfate: 10,000 U/mL Penicillin; 10,000 µg/mL Stock Solution	0.5 mL	Invitrogen-Life Technologies, Grand Island, NY
Bovine Serum Albumin	0.1 g	Rockland, Inc., Gilbertsville, PA

Table 3.5: Composition and Company Source Information for Follicle Culture Media.

Follicle Culture Media: Stored at 4°C, used at 38.5°C		
Dulbecco's Modified Eagle's Medium – low glucose	200 mL	Sigma Aldrich, St. Louis, MO
L-Glutamine	0.0584 g	Sigma Aldrich, St. Louis, MO
Insulin-Transferrin-Selenium: 25 mg/50mL Insulin-Transferrin, 25 µg/50mL Selenium Stock	2 mL	Sigma Aldrich, St. Louis, MO
Penicillin G-Streptomycin Sulfate: 10,000 U/mL Penicillin; 10,000µg/mL Stock Solution	1 mL	Gibco-Life Technologies, Grand Island, NY
Bovine Serum Albumin	0.6 g	Rockland, Inc., Gilbertsville, PA
Follicle Stimulating Hormone: 0.355 mg/mL Stock Solution	563 µL	Sigma Aldrich, St. Louis, MO

3.3.3. Sample Processing

All samples were slowly thawed on ice. To each follicle sample, 1000 μL of 10% hydrochloric acid (HCl) in dH_2O (JT Baker, Phillipsburg, NJ) was added followed by homogenization on ice to disrupt cell membranes. 200 μL of spent media samples were aliquoted into 2 mL Eppendorf Tubes and 800 μL of 0.625M HCl (JT Baker, Phillipsburg, NJ) was added. All samples were placed on a vortex mixer for 15 mins, then centrifuged at 13,000 rpm for 10 mins to remove proteins and cellular debris. Supernatants were desalted via application to an ion exchange column with 0.5 g of cation exchange resin (AG 50-X8, BioRad, Hercules, CA) to separate positively charged ions from the remaining fraction. The initial flow through of the supernatant, as well as an additional 0.5 mL dH_2O wash, was captured for each sample and stored at $-80\text{ }^\circ\text{C}$. The remaining fraction was liberated with 2 mL of 2 M ammonium hydroxide and 1 mL of distilled water, and stored at $-80\text{ }^\circ\text{C}$. All fractions were lyophilized (Labconco, Kansas City, MO) to dryness.

Cationic Fraction (“Amino Acid Fraction”)

Amino acid fractions were converted to their tert-Butyldimethylsilyl derivatives. To fractions originating from a follicle sample, 30 μL of N-(tert-butyldimethylsilyl)-N-methyltrifluoroacetamide plus 1% t-butyldimethylchlorosilane (MTBSTFA + 1% TBDMCS; UCT Selectra-Sil, Bristol, PA) and 30 μL dimethylformamide (DMF; Thermo Scientific, Waltham, MA) were added. To fractions originating from spent media, 60 μL of MTBSTFA + 1% TBDMCS and 60 μL DMF were added. All samples were vortexed well, transferred to 0.6 mL V-Vials, and microwaved for 120 secs at 200 W.

Samples were transferred to glass gas chromatography vials with inserts (Agilent, Palo Alto, CA).

Anionic Fraction (“Glucose Fraction”)

Glucose was converted to the di-O-isopropylidene acetate derivative (Hachey *et al.*, 1999). The lyophilized glucose fraction was acidified with 1 mL of 0.38 M sulfuric acid in acetone and incubated at room temperature for 60 min. The solution was then neutralized with 2 mL of 0.44 M sodium carbonate, vortexed, and 2 mL of a saturated sodium chloride solution (Sigma Aldrich, St. Louis, MO) added. Next, the O-isopropylidene derivative of glucose was extracted by the addition of 3 mL of ethyl acetate (JT Baker, Phillipsburg, NJ) followed by vortex mixing for 15 min on an orbital shaker. Organic and aqueous phases were allowed to separate for 10 min, and the organic layer removed and reduced to dryness under a gentle stream of nitrogen (2 psi). The O-isopropylidene derivative of glucoses was acetylated with 100 μ L of a 50:50 mixture of ethyl acetate and acetic anhydride (JT Baker, Phillipsburg, NJ) and heated for 30 min at 60 °C.

3.3.4. Gas Chromatography-Mass Spectrometry Analysis of Media and Follicle Samples

One microliter of media and two microliters of follicle sample preparations were injected at 10:1 and 2:1 split modes, respectively, into the gas chromatographic system (Agilent 6890 gas chromatography system, Palo Alto, CA) where metabolites were separated on a mid-polarity capillary column (Zebron ZB-50 capillary column, Phenomenex, Torrance, CA). The column was subjected to the following conditions: initial temperature of 100 °C, ramped at 10 °C per min to temperature of 280 °C, then

heated at 50 °C per min to a final temperature of 300 °C, held for 3 mins (21.4 min elapsed run time). Electron impact quadrupole mass spectrometry (Agilent 5973 inert EI/CI MSD system, Palo Alto, CA) followed, and was operated in selected ion monitoring mode to detect ¹³C-labeled carbon skeletons (**Table 3.6**).

GC-MS data files were captured via Agilent’s GC-MSD ChemStation, while Agilent Data Analysis software was used to convert the raw data files and to determine mass isotopomer abundances for metabolites pertinent to central carbon metabolism.

Table 3.6: Ions monitored for given metabolites in media and follicle samples
Selected Ion Monitoring (SIM) Settings

Amino Acids	Pertinent Ions Monitored*
Alanine	[M+0]:260.2 – [M+3]: 263.2
Aspartate	[M+0]:418.4 – [M+4]: 422.4
Glutamate	[M+0]:432.4 – [M+5]: 437.4
Glutamine	[M+0]:431.4 – [M+5]: 436.4
Glycine	[M+0]:246.2 – [M+2]: 248.2
Proline	[M+0]:286.3 – [M+5]: 291.3
Serine	[M+0]:390.3 – [M+3]: 393.3
Carboxylic Acid	Pertinent Ions Monitored*
Lactate	[M+0]:261.2 – [M+3]: 264.2

*[M+0], unlabeled metabolite; [M+n], [U¹³C]-labeled metabolite

3.3.5 Flux Calculations

Kinetic calculations were adapted from previously described reports (Bequette *et al.*, 2006; Berthold *et al.*, 1994). In brief, actual tracer levels of glucose were obtained by determining the atom percent excess (APE) for the mass isotopomers of glucose (corrected for natural abundances; **Figure 3.1**). APE was also calculated for non-essential amino acids (NEAAs) for use in calculations (**Figure 3.2A, 3.2B**), following the assumption that these metabolites are in isotopic equilibrium with intermediates of carbon metabolism (**Table 3.7**).

The following is a summary of the calculations for Glucose carbon:

Enrichment of Acetyl CoA	$[M+2]Glu - 2*[M+3]Glu$
Flux through PPP and PEPCCK, as compared to GLYC	$\frac{[M+1]Ala + [M+2]Ala}{[M+3]Ala}$
Ratio of flux through Pyruvate Dehydrogenase versus Pyruvate Carboxylase	$\frac{[M+2]Glu - 2*[M+3]Glu}{[M+3]Glu}$

Calculations for the percent of glucose carbon contributing to the pools of:

Acetyl CoA	$\{[M+2]Glu - 2*[M+3]Glu\}/[M+6]Glc$
Pyruvate (mitochondrial pool)	$[M+3]Ala/[M+6]Glc$
Pyruvate (cytosolic pool)	$[M+3]Lac/[M+6]Glc$
3-Phosphoglycerate	$[M+3]Ser/[M+6]Glc$

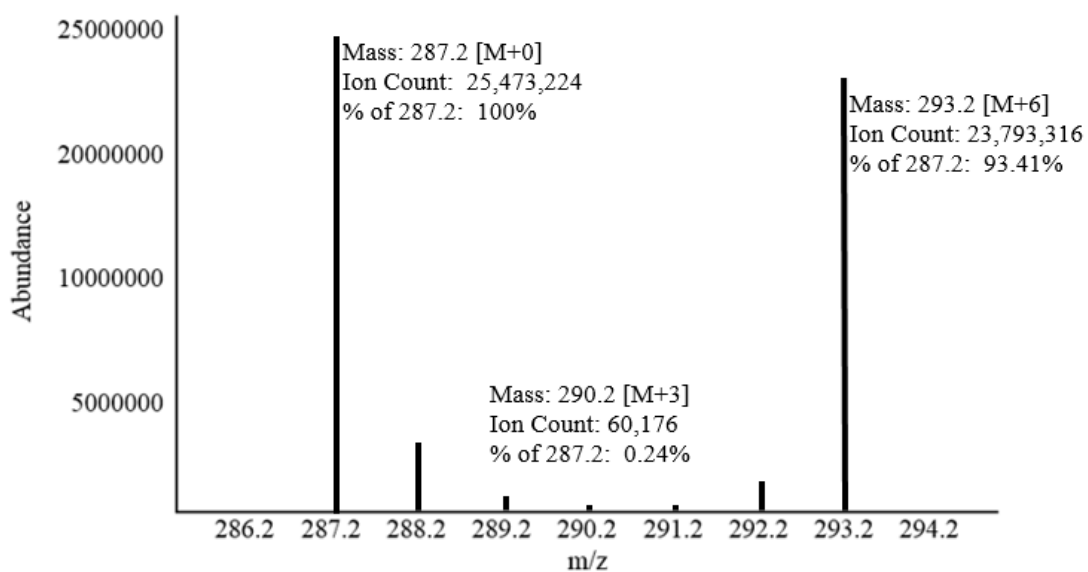


Figure 3.1: Ion spectra of a sample of stock Tracer Culture Media with uncorrected APE's calculated. 287.2, [M+0], is the unlabeled ion; 290.2, [M+3], is a triply labeled ion; 293.2 [M+6], is a labeled ion resulting from [U-¹³C]-labeled glucose fragmentation. The ratio of [M+6] to [M+0] gives the ratio of labeled to unlabeled glucose in the sample. There is 1 mole of tracer for every 1.08 moles of unlabeled glucose, as opposed to the theoretical ratio of 1:1.

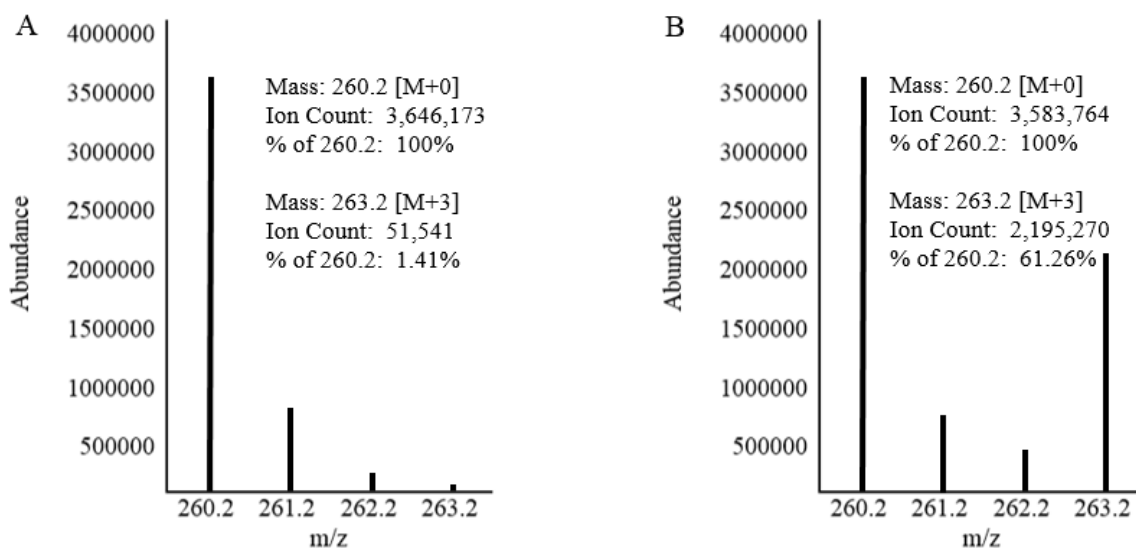


Figure 3.2: Ion spectra of a sample containing unlabeled (A) and a mixture of labeled and unlabeled (B) alanine with uncorrected APE's calculated. The ion spectra of alanine, from a commercially obtained amino acid standard mixture, compared to the ion spectra of alanine resulting from a sample incubated with 50:50 unlabeled and [U-¹³C]-labeled glucose tracer. 260.2, [M+0], is the unlabeled ion; 263.2, [M+3], is a triply labeled ion, resulting from the metabolism of [U-¹³C₆] glucose tracer

Table 3.7: Amino & Carboxylic Acids monitored via SIM and those compounds with which they are in equilibrium with.

Selected Ion Monitoring (SIM) Settings	
Amino Acids	Carbon Metabolism Intermediate Approximated
Alanine	Pyruvate – mitochondrial pool
Aspartate	Oxaloacetate
Glutamate	α -Ketoglutarate
Glutamine	α -Ketoglutarate
Glycine	3-Phosphoglycerate
Lactate	Pyruvate – cytoplasmic pool
Proline	α -Ketoglutarate
Serine	3-Phosphoglycerate

3.3.6. Statistical Analysis

Files were analyzed with MetaboAnalyst software (online) for Partial Least Squares Discriminant Analysis (PLS-DA), while SAS was used to perform a mixed model analysis of variance (ANOVA) with Dunnett's Correction (Xia *et al.*, 2009; Xia and Wishart, 2011; Xia *et al.*, 2012). The following model was used:

$$Y_{ij} = \mu + T_i + C_j + \epsilon_{ij}$$

Y_{ij} = Response Variable (% Alanine from Glucose, % Lactate from Glucose, etc.)

μ = Grand Mean

T_i = Treatment Effect (Early Antral, Late Antral, Early Antral *in vitro*)

C_j = Random Effects (Block: age, type)

ϵ_{ij} = Residual Error

Significance was tested at $P < 0.05$ ($\alpha = 5\%$). Data was analyzed with the PROC MIXED procedure of SAS (SAS Ins, Inc., Cary, NC) with cat age/type blocking factor. For the analysis, follicle stage/type was considered a fixed effect, while the block was a random effect. Least squares means were obtained for each treatment and linear effects of follicle stage/type on the response variables were tested by constructing orthogonal contrasts. Pairwise mean comparisons were done using the Dunnett's Adjustment.

3.4. Results

Ion fragments containing the entire carbon skeleton of alanine, aspartate, glutamate, glutamine, glycine, proline, serine and lactate were monitored by GC-MS. Ion abundances for each ion monitored were obtained, and corrected MIDs were calculated for each compound (**Appendix 1**).

Calculations were performed to determine the contribution of glucose to the acetyl CoA, pyruvate (both the mitochondrial and cytosolic pools), and 3-phosphoglycerate carbon pools. The relative flux through PEPCK-c and the PPP versus glycolysis were calculated, as well as a crude ratio of the flux through pyruvate dehydrogenase as compared to pyruvate carboxylase.

3.4.1. Differences across developmental stages of follicles derived *in vivo*, assessed via Spent Media

As follicles increased in size (development), glucose metabolism made a greater ($P < 0.0001$) contribution to mitochondrial pyruvate pool (i.e. synthesis) (**Table 3.8, Figure 3.3**). By contrast, the contribution of glucose to acetyl CoA and the cytosolic pool of pyruvate did not change. In addition, throughout development, the fluxes through PEPCK-c and PPP compared to glycolytic flux also did not change. In addition, the ratio of pyruvate dehydrogenase to pyruvate carboxylase activity did not change.

When subjected to a PLS-DA to observe clustering patterns, late antral follicles formed a tight cluster based on carbon flux and glucose carbon incorporation data. This allowed for distinct clustering of the two groups, even with the large variation in early antral follicles, without major overlap between groups in a two dimensional plot (**Figure 3.4**). When three components of variation were considered, late antral follicles retained their tight in-group clustering, while the high variation between early antral follicles became more apparent (**Figure 3.5**).

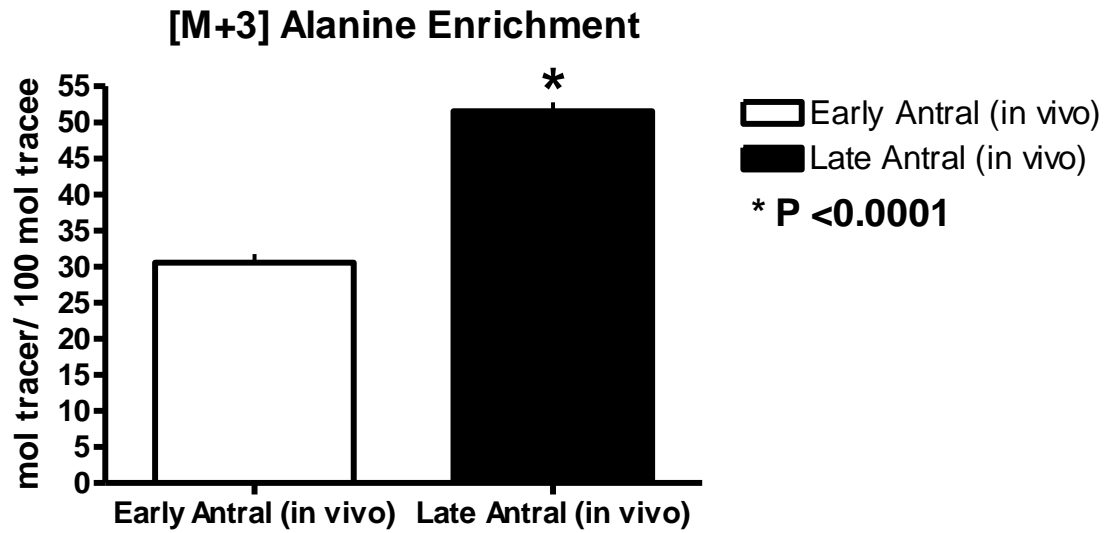
Table 3.8: Calculated flux through pathways of central carbon metabolism and glucose carbon contributions to selected intermediate pools, as calculated from Spent Media (n=9 per group)¹

Flux/Intermediate	Follicle Stage		P ²
	Early Antral (<i>in vivo</i>)	Late Antral (<i>in vivo</i>)	
Acetyl CoA from Glucose	0.49 ± 0.06	0.42 ± 0.06	0.5847
Pyruvate (mitochondrial pool) from Glucose	33.00 ± 1.28	55.55 ± 1.38	<0.0001*
Pyruvate (cytoplasmic pool) from Glucose	0.43 ± 0.14	0.41 ± 0.15	0.9926
3-Phosphoglycerate from Glucose	19.54 ± 5.16	1.56 ± 2.92	0.0367*
PPP and PEPCK flux: Glycolysis Flux	0.09 ± 0.004	0.08 ± 0.004	0.2924
Pyruvate Dehydrogenase: Pyruvate Carboxylase	0.49 ± 0.11	0.49 ± 0.11	1.000

¹Values reported as the least squares means, plus or minus the standard error, expressed as moles per 100 moles of tracee for metabolites from glucose

²P-value after Dunnett's adjustment. Starred values indicate a significant difference between groups based on P < 0.05 significance level.

(A)



(B)

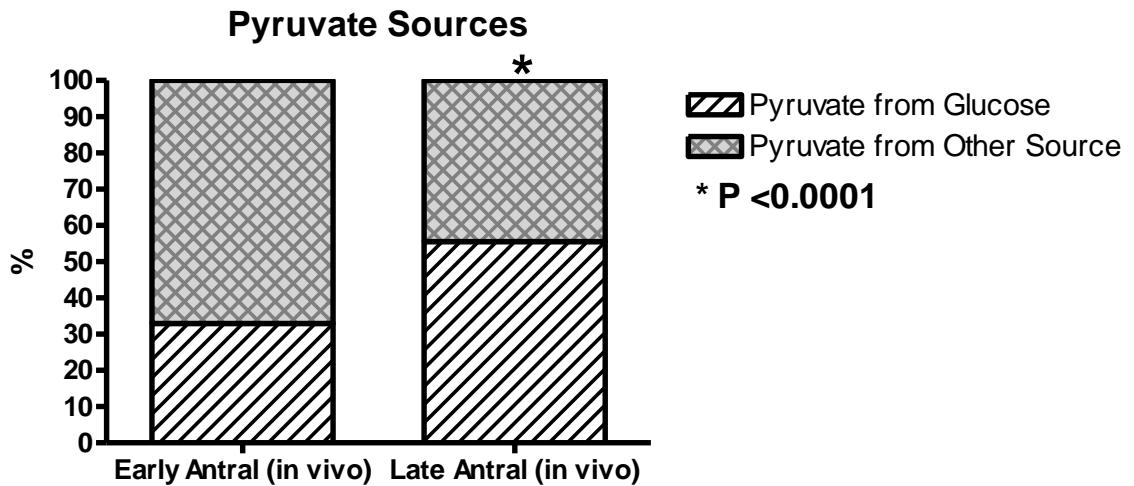


Figure 3.3: [M+3] Alanine enrichment in early antral versus late antral follicles derived *in vivo* (A). Glucose contribution to the pyruvate pool in early versus late antral follicles derived *in vivo* (B).

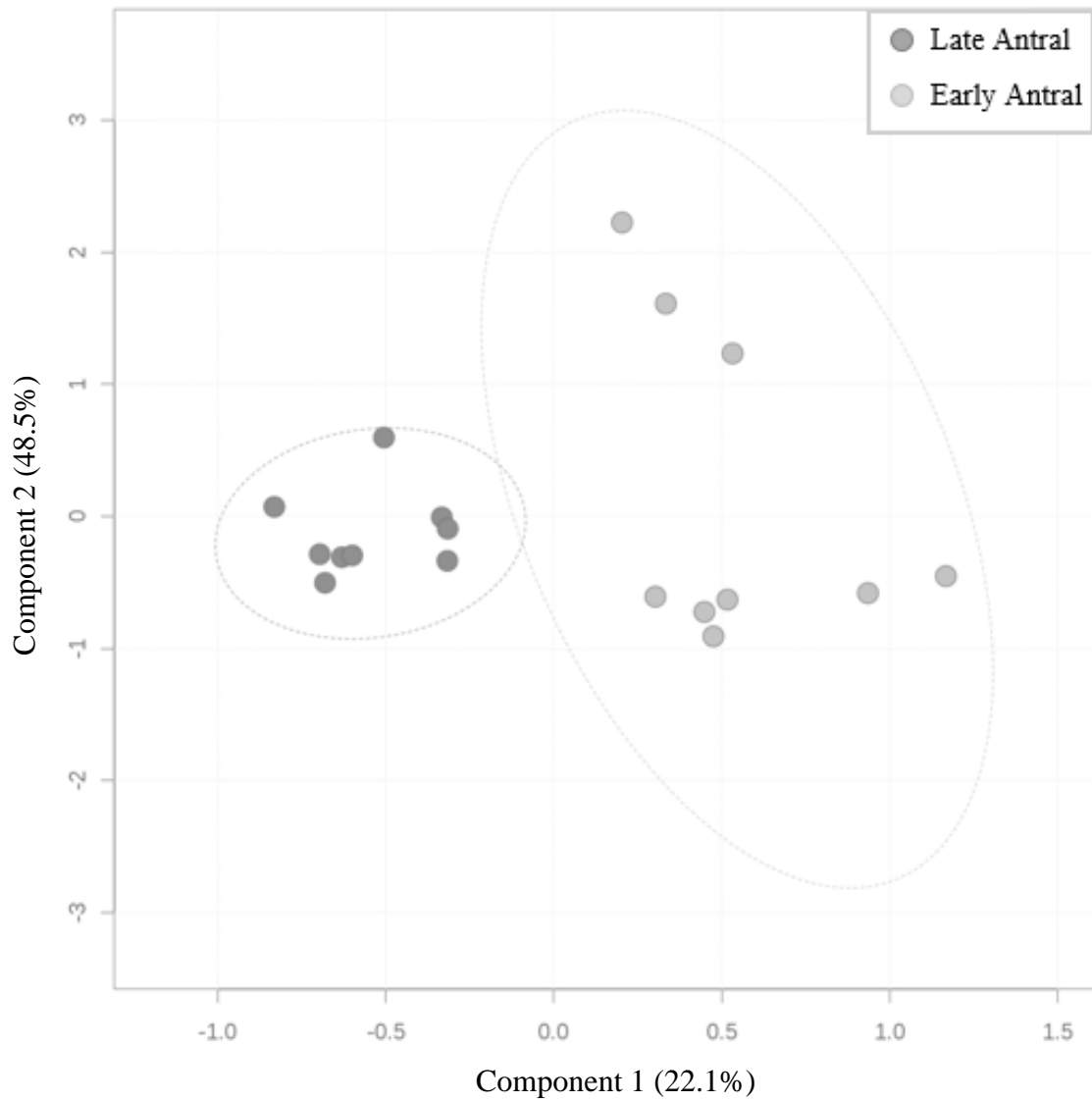


Figure 3.4: Two-dimensional PLS-DA of spent tracer media from early (light gray) and late (dark gray) antral follicles, with a 95% confidence interval indicated around each cluster. The amount of variation between samples captured by each component is indicated in parenthesis.

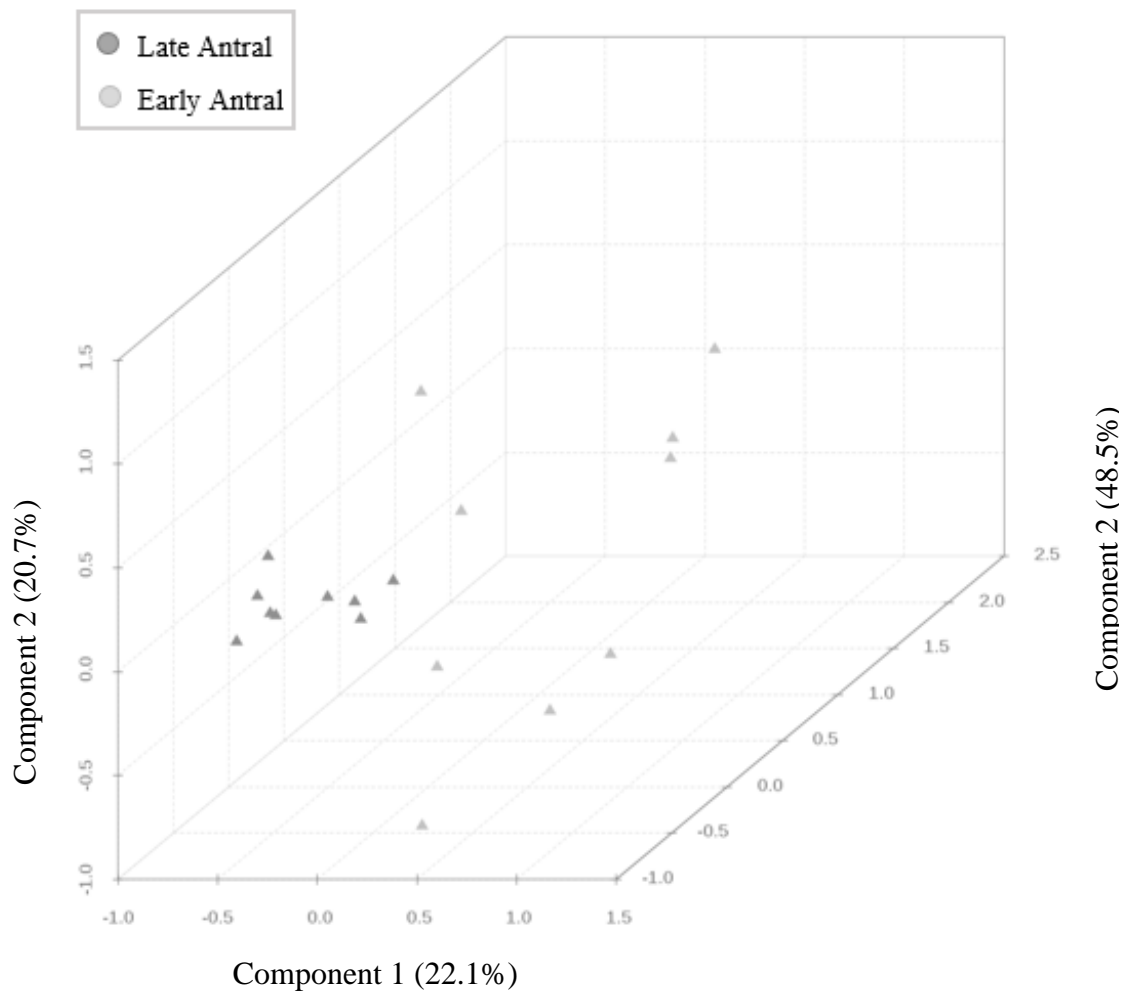


Figure 3.5: Three-dimensional PLS-DA of spent tracer media from early (light gray) and late (dark gray) antral follicles. The amount of variation between samples captured by each component is indicated in parenthesis.

3.4.2. Differences between early antral follicles derived *in vivo* and those cultured *in vitro*, assessed via Spent Media

No significant differences between glucose carbon contribution to intermediate pools or differences in fluxes through central carbon metabolism were detected between *in vivo* derived early antral follicles and those follicles recovered after *in vitro* incubation, when indirectly assessed through spent media (**Table 3.9, Figure 3.6**). However, glucose contribution to the Acetyl CoA pool was at the cusp of being significantly lower ($P = 0.0513$) in *in vitro* cultured early antral follicles. These findings are supported by the seemingly random distribution of *in vivo* derived and *in vitro* cultured early antral follicles in both the two dimensional and three-dimensional PLS-DAs (**Figure 3.7, 3.8**). The cluster formed for *in vitro* cultured follicles nearly encompasses the “cluster” formed for *in vivo* derived follicles, signifying more variation within groups than between the groups.

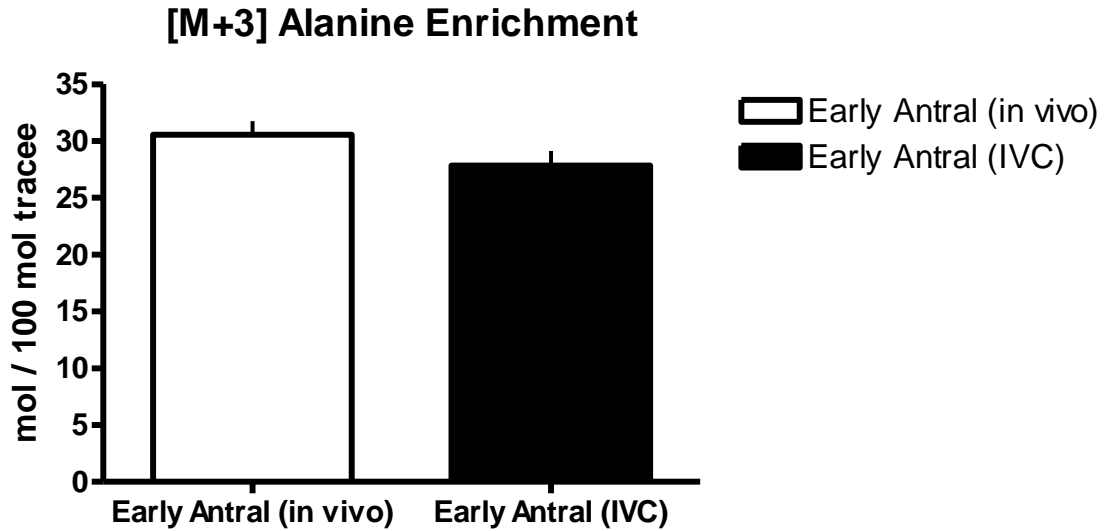
Table 3.9: Calculated flux through pathways of central carbon metabolism and glucose carbon contributions to selected intermediate pools, as calculated from Spent Media (n=9 per group)¹

Flux/Intermediate	Follicle Stage		P ²
	Early Antral (<i>in vivo</i>)	Early Antral (<i>in vitro</i>)	
Acetyl CoA from Glucose	0.49 ± 0.06	0.30 ± 0.06	0.0513†
Pyruvate (mitochondrial pool) from Glucose	33.00 ± 1.28	30.01 ± 1.38	0.2354
Pyruvate (cytoplasmic pool) from Glucose	0.43 ± 0.14	0.50 ± 0.15	0.9223
3-Phosphoglycerate from Glucose	19.54 ± 5.16	13.87 ± 4.05	0.5553
PPP and PEPCK flux:Glycolysis Flux	0.09 ± 0.004	0.10 ± 0.004	0.0843
Pyruvate Dehydrogenase: Pyruvate Carboxylase	0.49 ± 0.11	0.73 ± 0.11	0.2603

¹Values reported as the least squares means, plus or minus the standard error, expressed as moles per 100 moles of tracee for glucose carbon contributions to metabolite pools

²P-value after Dunnett's adjustment. Crossed (†) values indicate P-values at the boundary of P < 0.05 significance level

(A)



(B)

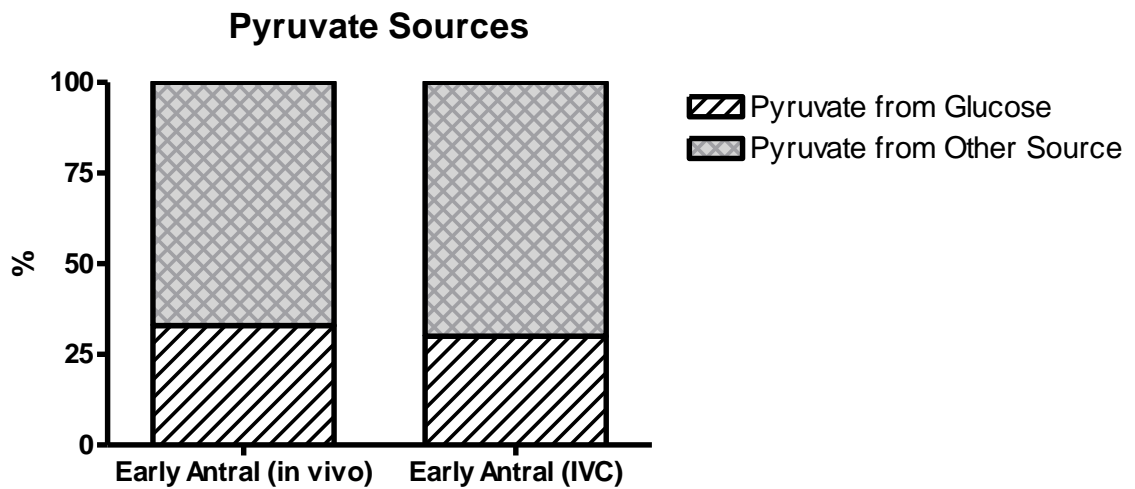


Figure 3.6: [M+3] Alanine enrichment in *in vivo* derived early antral follicles versus *in vitro* cultured early antral follicles (A). Glucose contribution to the pyruvate pool in *in vivo* derived early antral follicles versus *in vitro* cultured early antral follicles (B).

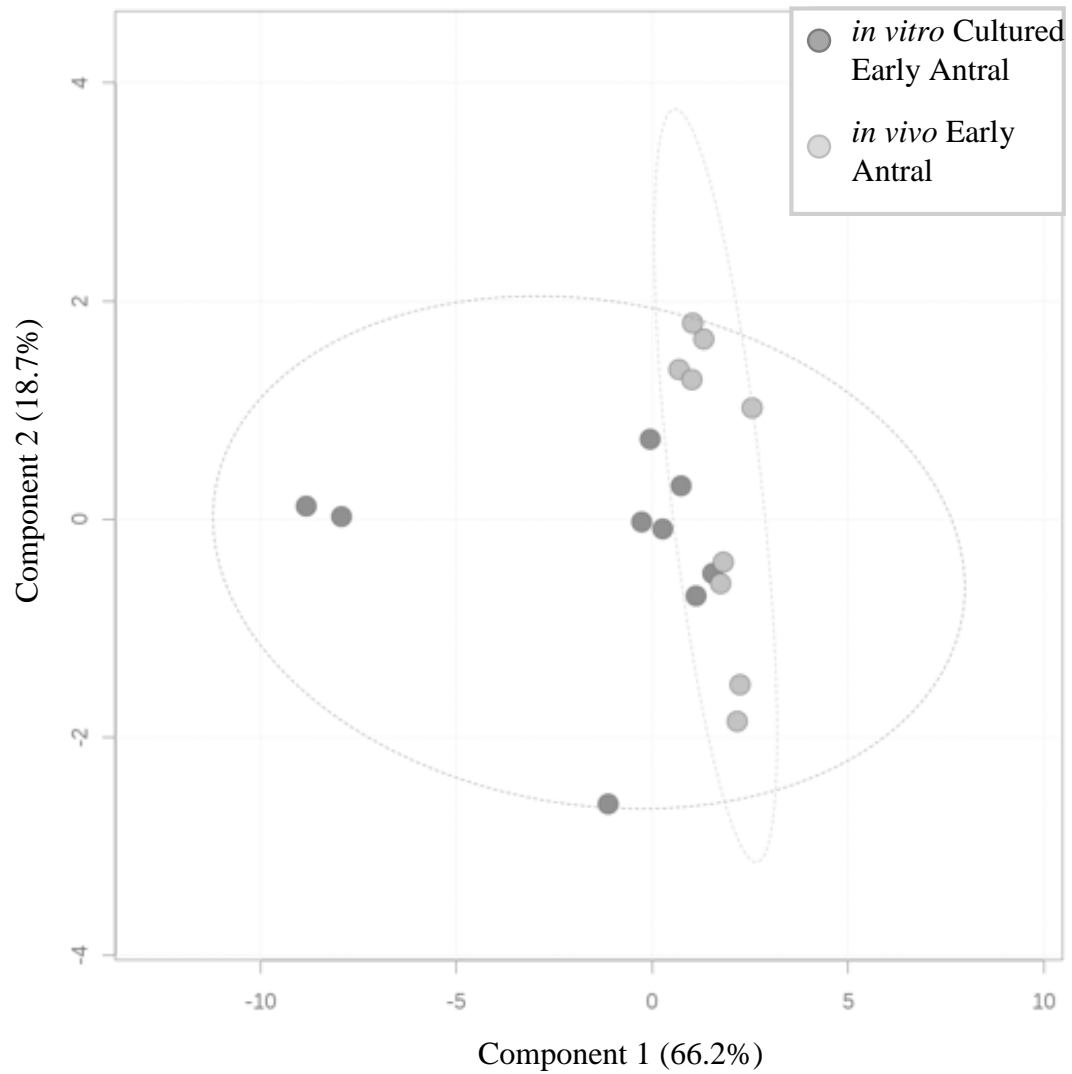


Figure 3.7: Two-dimensional PLS-DA of spent tracer media from early antral follicles collected directly from feline ovaries (light gray) and those subjected to *in vitro* culture (dark gray), with a 95% confidence interval indicated for each cluster. The amount of variation between samples captured by each component is indicated in parenthesis.

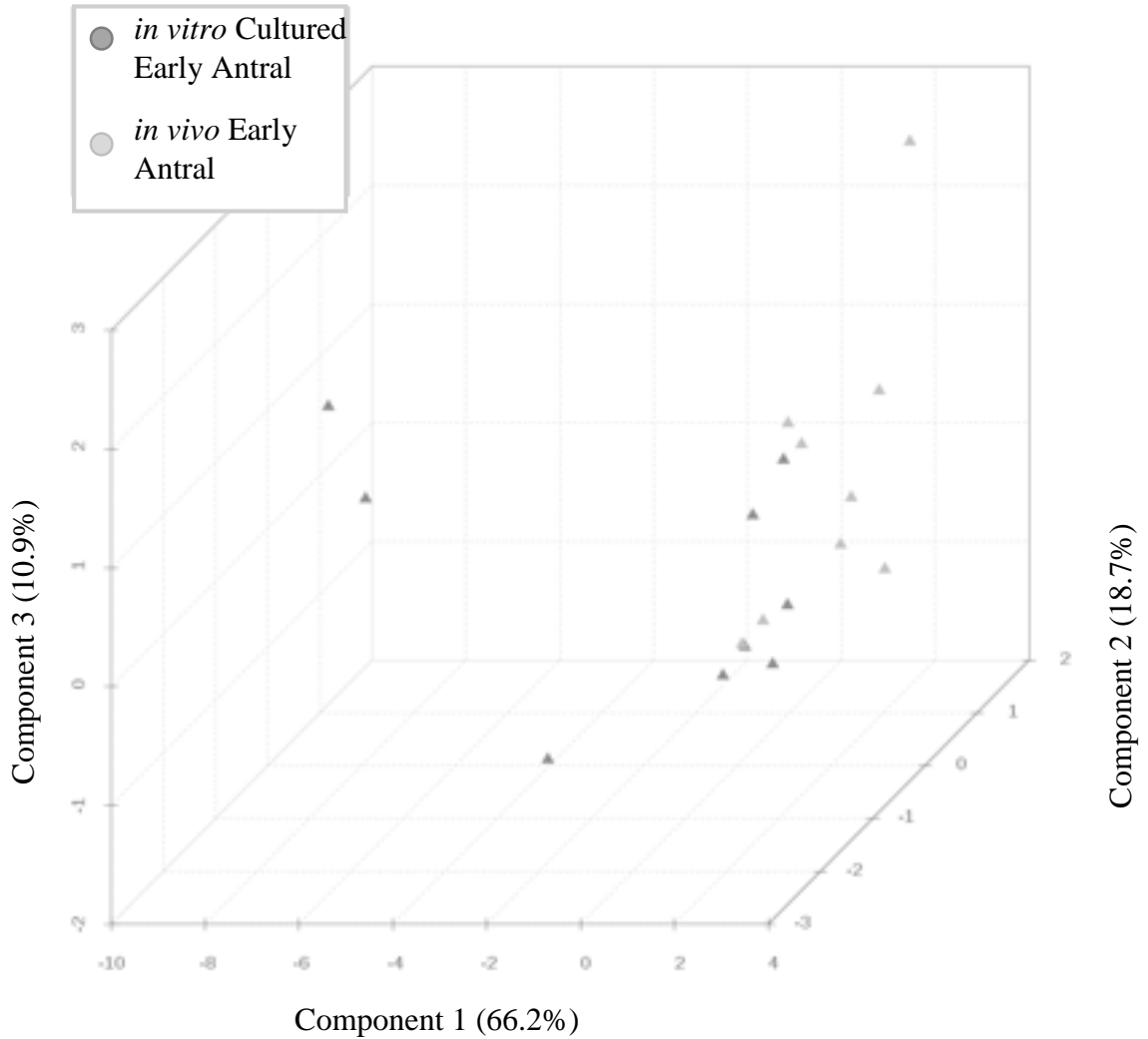


Figure 3.8: Three-dimensional PLS-DA of spent tracer media from early antral follicles collected directly from feline ovaries (light gray) and those subjected to *in vitro* culture (dark gray). The amount of variation between samples captured by each component is indicated in parenthesis.

3.4.3. Differences between late antral follicles derived *in vivo* and *in vitro* cultured early antral follicles, assessed via Spent Media

Glucose metabolism made a greater ($P < 0.0001$) contribution to mitochondrial pyruvate pool (i.e. synthesis) in late antral follicles, as opposed to *in vitro* cultured early antral follicles (**Table 3.10, Figure 3.9**). By contrast, the contribution of glucose to the fluxes of acetyl CoA and to the cytosolic pool of pyruvate did not change. In addition, the ratio of pyruvate dehydrogenase to pyruvate carboxylase activity did not change. There was an observed difference between the ratios of the flux through PPP and PEPCK-c as compared to glycolysis ($P = 0.0166$).

When subjected to a PLS-DA to observe clustering patterns, late antral follicles formed a tight cluster based on carbon flux and glucose carbon incorporation data. This allowed for fairly distinct clustering of the two groups, even with the large variation in *in vitro* cultured early antral follicles in a two dimensional plot (**Figure 3.10**). When three components of variation were considered, clustering became more definitive. In addition, late antral follicles retained their tight in-group clustering, while the high variation between *in vitro* cultured early antral follicles became more apparent (**Figure 3.11**).

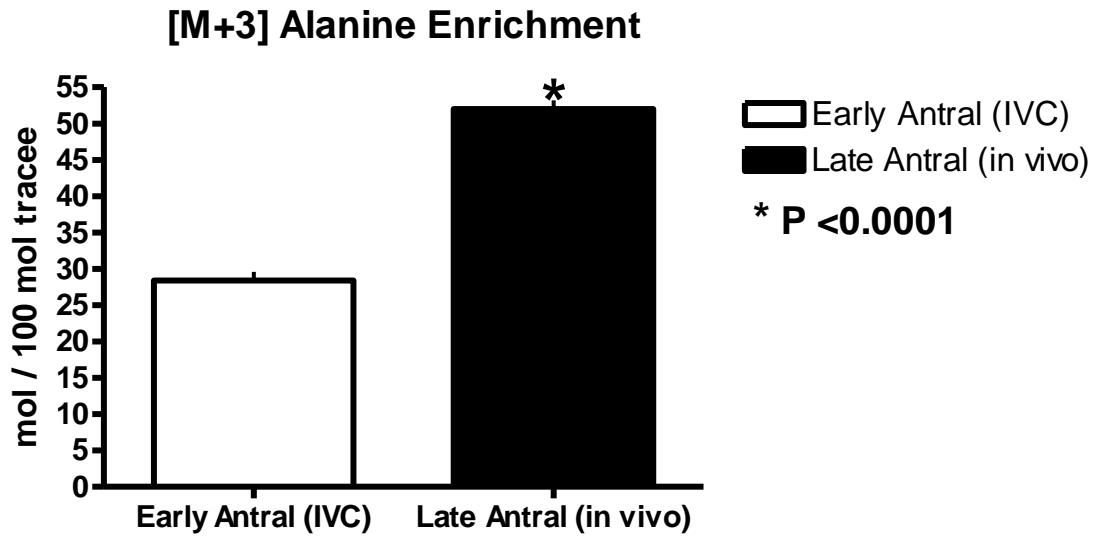
Table 3.10: Calculated flux through pathways of central carbon metabolism and glucose carbon contributions to selected intermediate pools, as calculated from Spent Media (n=8 per group)¹

Flux/Intermediate	Follicle Stage		P ²
	Early Antral (<i>in vitro</i> cultured)	Late Antral (<i>in vivo</i>)	
Acetyl CoA from Glucose	0.31 ± 0.07	0.43 ± 0.07	0.2647
Pyruvate (mitochondrial pool) from Glucose	30.63 ± 1.26	56.07 ± 1.26	<0.0001*
Pyruvate (cytoplasmic pool) from Glucose	0.50 ± 0.12	0.43 ± 0.12	0.6666
3-Phosphoglycerate from Glucose	12.92 ± 4.47	2.76 ± 3.01	0.1324
PPP and PEPCK flux: Glycolysis Flux	0.10 ± 0.004	0.08 ± 0.004	0.0166*
Pyruvate Dehydrogenase: Pyruvate Carboxylase	0.73 ± 0.15	0.48 ± 0.15	0.2794

¹Values reported as the least squares means, plus or minus the standard error, expressed as moles per 100 moles of tracee for metabolites from glucose

²P-value after Dunnett's adjustment. Starred values indicate a significant difference between groups based on P < 0.05 significance level.

(A)



(B)

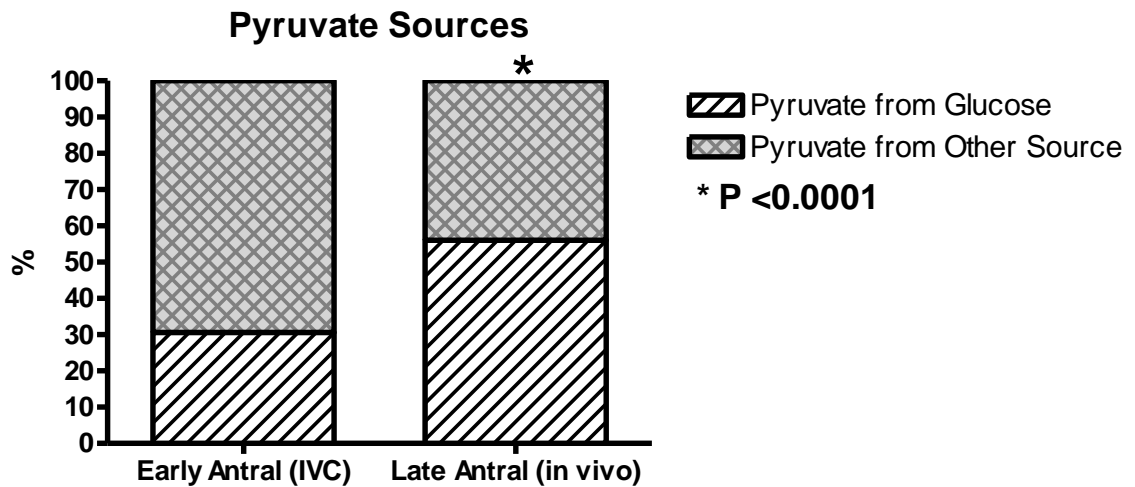


Figure 3.9: [M+3] Alanine enrichment in *in vitro* cultured early antral follicles versus *in vivo* derived late antral follicles (A). Glucose contribution to the pyruvate pool in *in vitro* cultured early antral follicles versus *in vivo* derived late antral follicles (B).

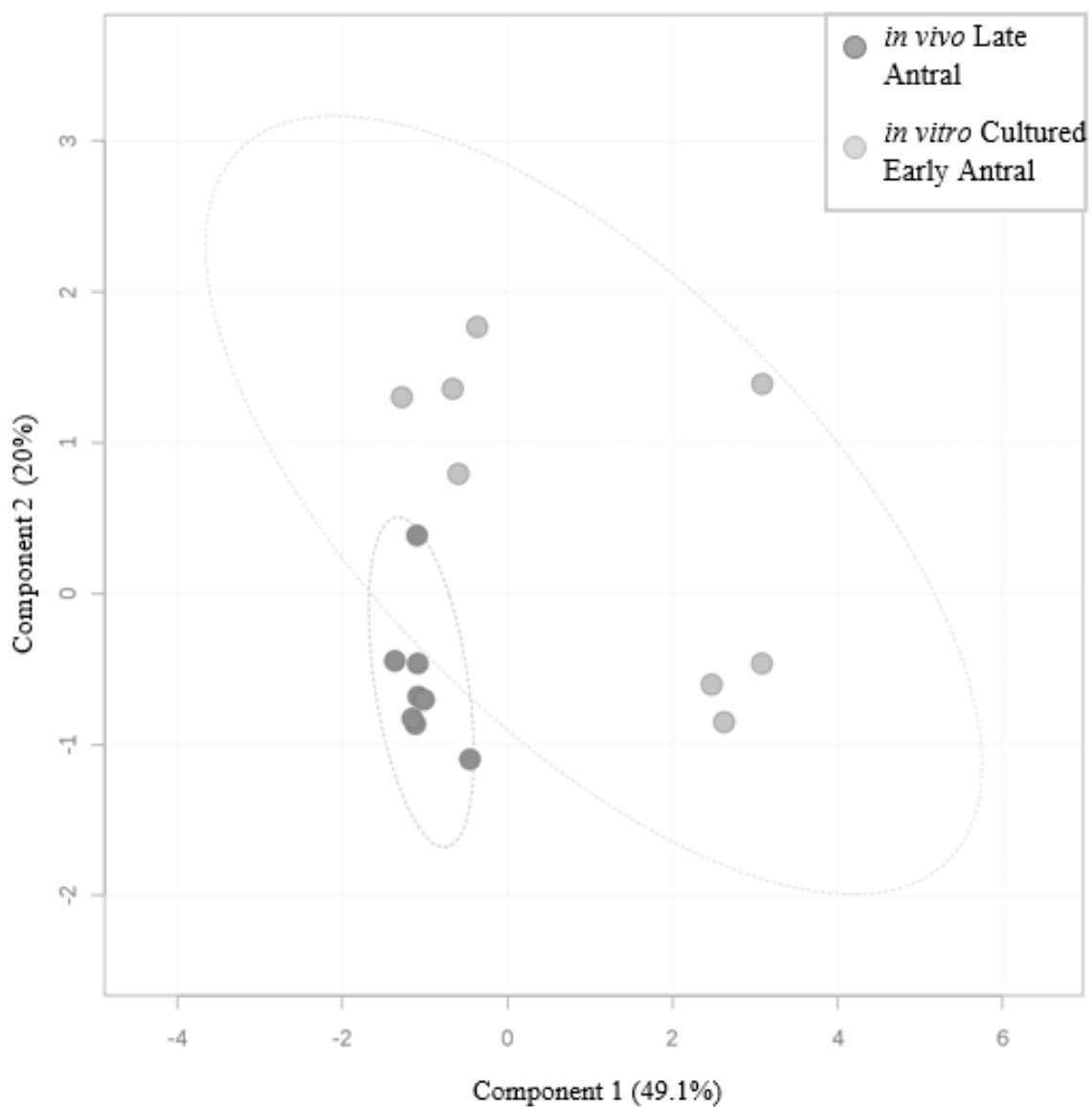


Figure 3.10: Two-dimensional PLS-DA of spent tracer media from late antral follicles collected directly from feline ovaries (dark gray) and *in vitro* cultured early antral follicles (dark gray), with a 95% confidence interval indicated for each cluster. The amount of variation between samples captured by each component is indicated in parenthesis.

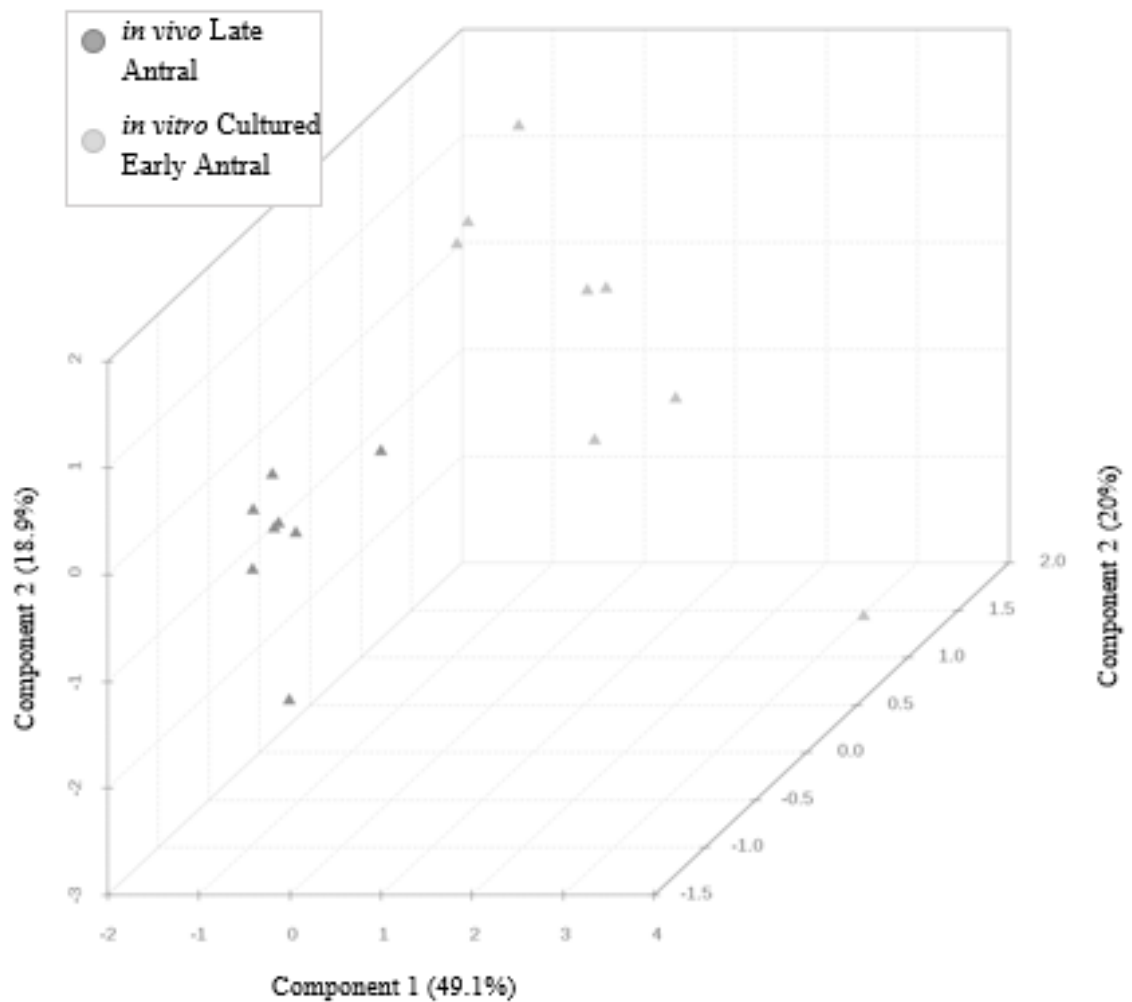


Figure 3.11: Three-dimensional PLS-DA of spent tracer media from late antral follicles collected directly from feline ovaries (dark gray) and *in vitro* cultured early antral follicles (dark gray). The amount of variation between samples captured by each component is indicated in parenthesis.

3.4.4. Differences among follicle stages and environmental conditions, through direct assessment of follicles

Significant differences were not detected between *in vivo* derived early antral follicles and late antral follicles or between *in vivo* derived early antral follicles and *in vitro* cultured early antral follicles when direct analysis of follicles was completed (**Tables 3.11, 3.12**). However, there was a significantly higher contribution of glucose carbon to the mitochondrial pool of pyruvate ($P = 0.0332$) and a significantly lower contribution of glucose carbon to the acetyl CoA pool ($P = 0.0128$) in late antral follicles derived *in vivo* as compared to *in vitro* cultured early antral follicles (**Table 3.13**). Upon analysis with PLS-DA, no distinct clustering patterns were able to be observed in either two-dimensional or three-dimensional analysis for the comparisons between *in vivo* early antral follicles and late antral follicles or between *in vivo* derived early antral follicles and *in vitro* cultured early antral follicles; rather, it appears that individuals from all experimental groups were dispersed randomly (**Figures 3.12, 3.13, 3.14, 3.15**). While there is overlap between *in vitro* cultured early antral follicles and *in vivo* derived late antral follicles in two-dimensional analysis, they do appear to segregate in three-dimensional analysis (**Figure 3.16, 3.17**).

Table 3.11: Calculated flux through pathways of central carbon metabolism and glucose carbon contributions to selected intermediate pools, as calculated from Follicles (n=9 per group)¹

Flux/Intermediate	Follicle Stage		P
	Early Antral (<i>in vivo</i>)	Late Antral (<i>in vivo</i>)	
Acetyl CoA from Glucose	2.04 ± 0.67	1.65 ± 0.38	0.8258
Pyruvate (mitochondrial pool) from Glucose	22.41 ± 5.3	37.99 ± 2.98	0.0726
Pyruvate (cytoplasmic pool) from Glucose	0.50 ± 0.29	0.89 ± 0.33	0.5855
PPP and PEPCK flux:Glycolysis Flux	0.03 ± 0.04	0.08 ± 0.02	0.5631
Pyruvate Dehydrogenase: Pyruvate Carboxylase	0.53 ± 0.23	0.91 ± 0.13	0.2940

¹Values reported as the least squares means, plus or minus the standard error. Contributions of glucose carbon to metabolite pools is expressed in moles per 100 moles of tracee

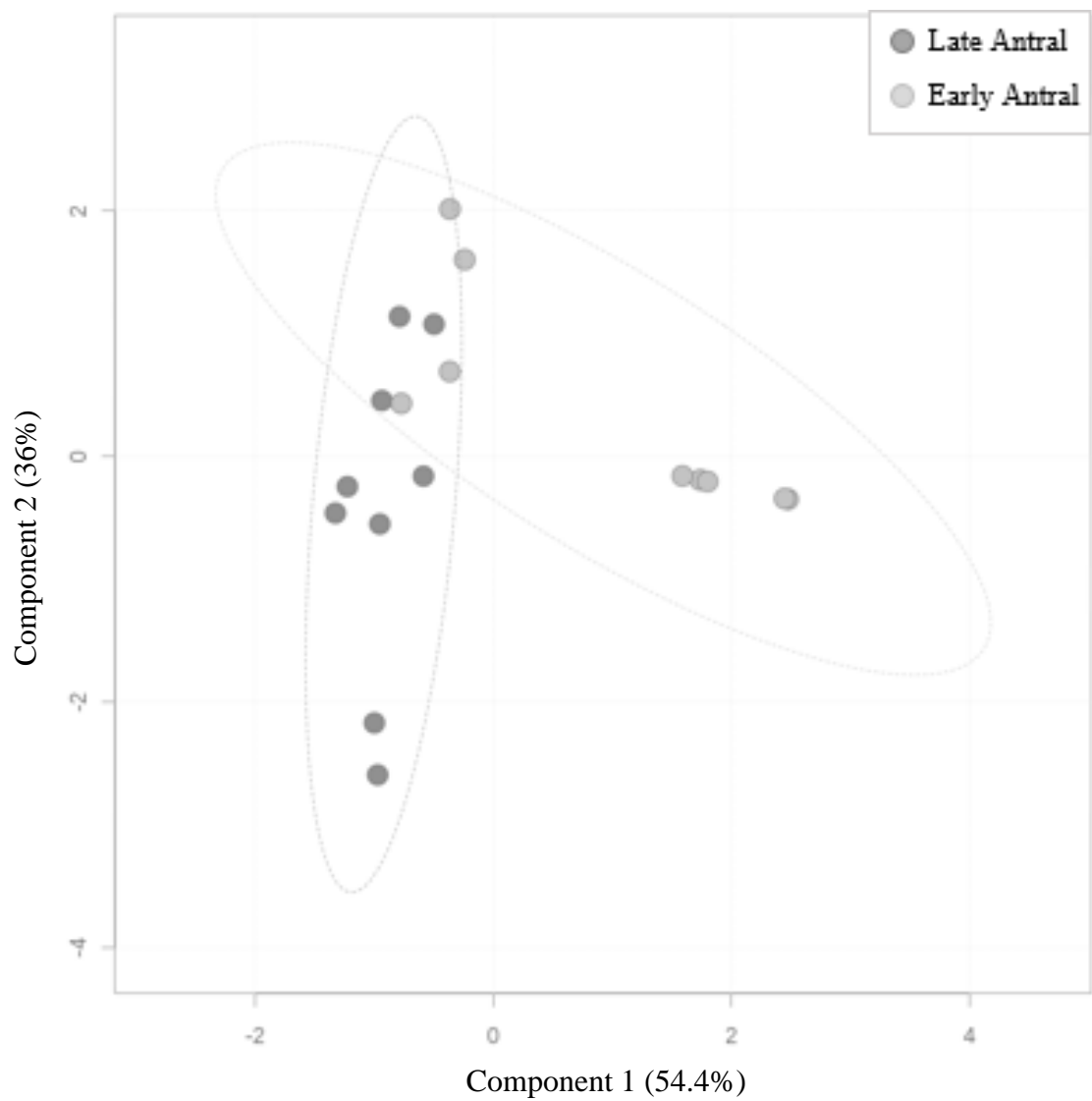


Figure 3.12: Two-dimensional PLS-DA of early (light gray) and late (dark gray) antral follicles after incubation in tracer media, with a 95% confidence interval indicated around each cluster. The amount of variation between samples captured by each component is indicated in parenthesis.

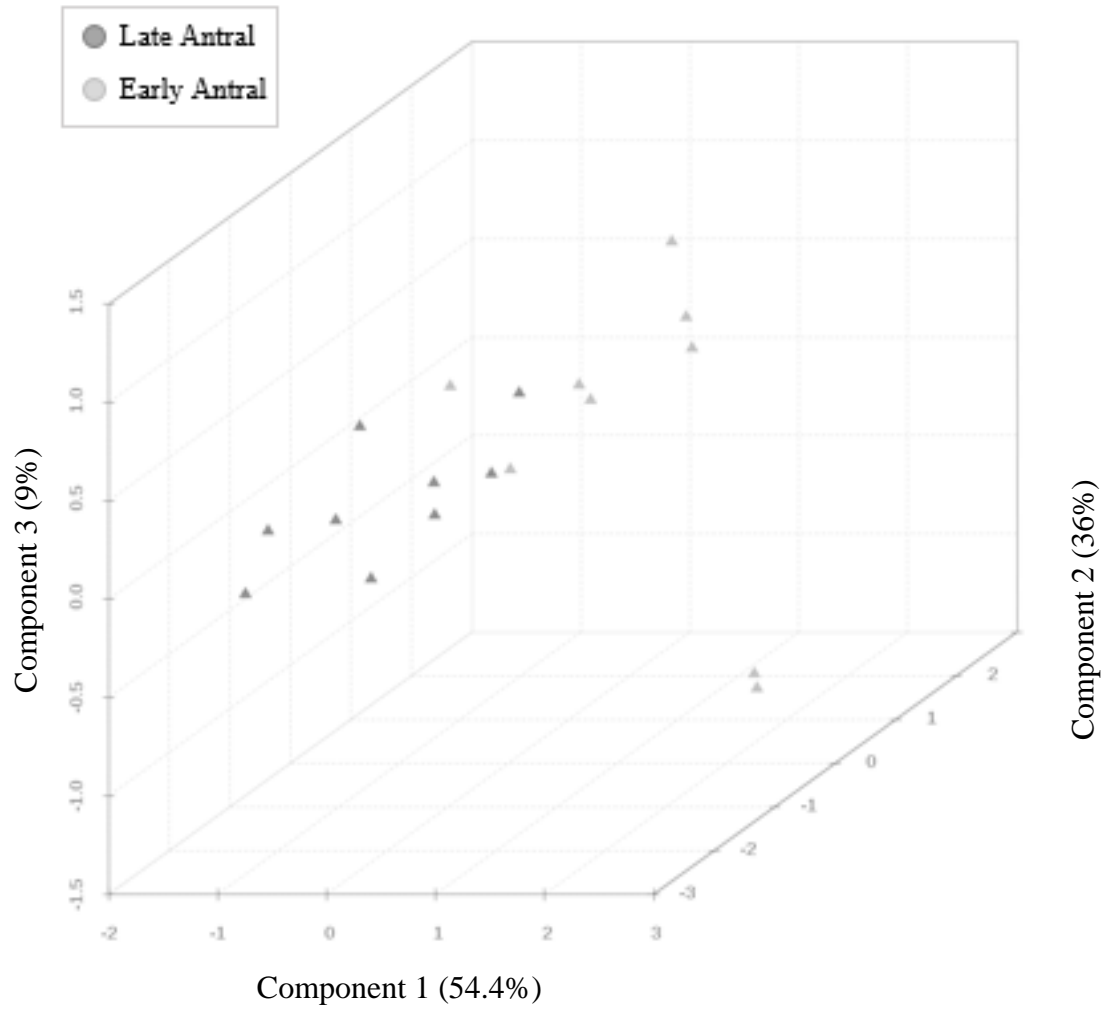


Figure 3.13: Three-dimensional PLS-DA of early (light gray) and late (dark gray) antral follicles after incubation in tracer media. The amount of variation between samples captured by each component is indicated in parenthesis.

Table 3.12: Calculated flux through pathways of central carbon metabolism and glucose carbon contributions to selected intermediate pools, as calculated from Follicles (n=11 per group)¹

Flux/Intermediate	Follicle Stage		<i>P</i>
	Early Antral (<i>in vivo</i>)	Early Antral (<i>in vitro</i>)	
Acetyl CoA from Glucose	2.04 ± 0.67	3.98 ± 0.60	0.0892
Pyruvate (mitochondrial pool) from Glucose	22.41 ± 5.3	26.23 ± 5.33	0.8175
Pyruvate (cytoplasmic pool) from Glucose	0.50 ± 0.29	1.16 ± 0.29	0.2131
PPP and PEPCK flux:Glycolysis Flux	0.03 ± 0.04	0.15 ± 0.04	0.1813
Pyruvate Dehydrogenase: Pyruvate Carboxylase	0.53 ± 0.23	0.83 ± 0.20	0.4807

¹Values reported as the least squares means, plus or minus the standard error. Contributions of glucose carbon to metabolite pools is expressed in moles per 100 moles of tracee

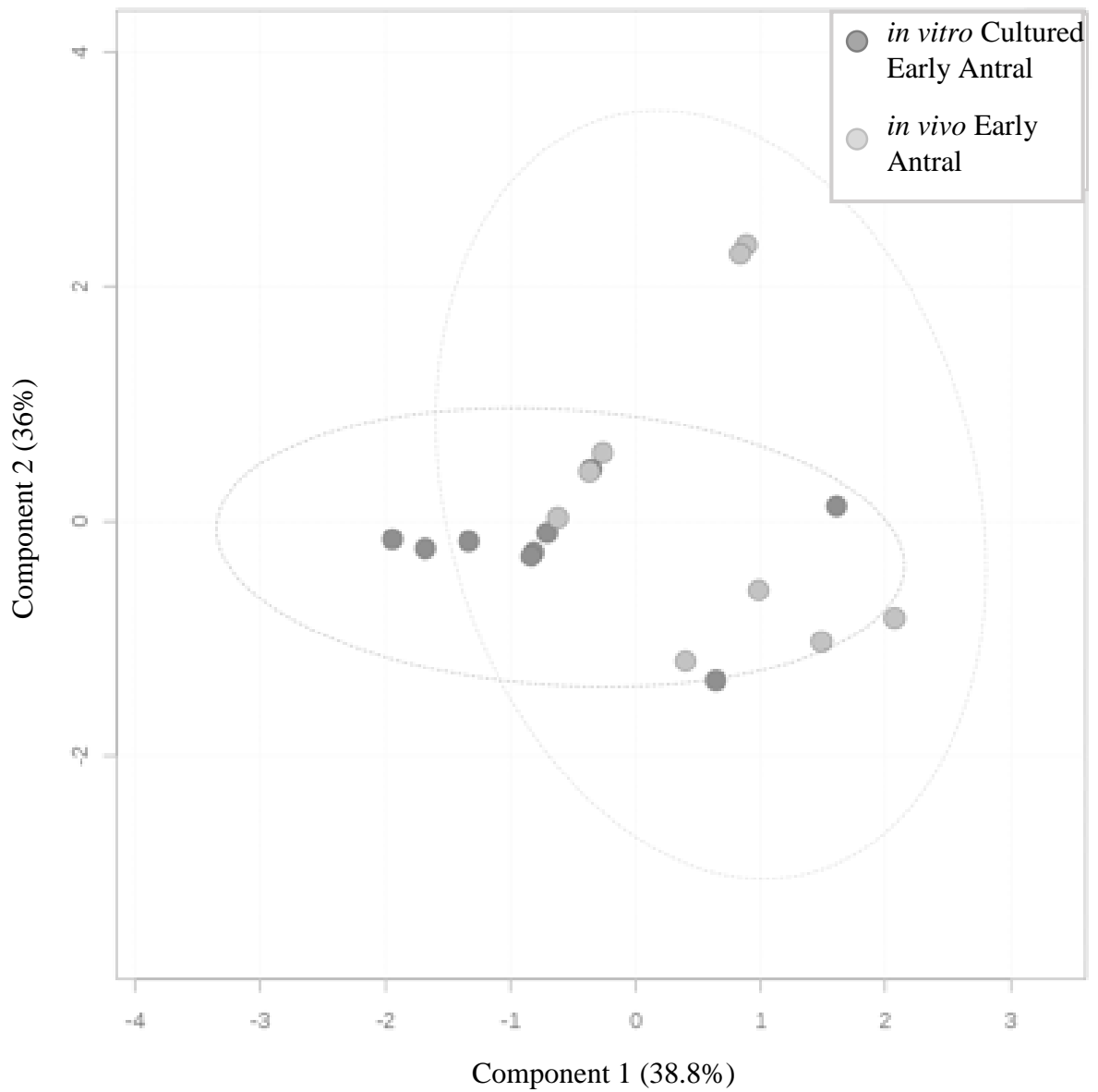


Figure 3.14: Two-dimensional PLS-DA of early antral follicles derived *in vivo* (light gray) and those subjected to IVC (dark gray) after incubation with tracer media, with a 95% confidence interval indicated around each cluster. The amount of variation between samples captured by each component is indicated in parenthesis.

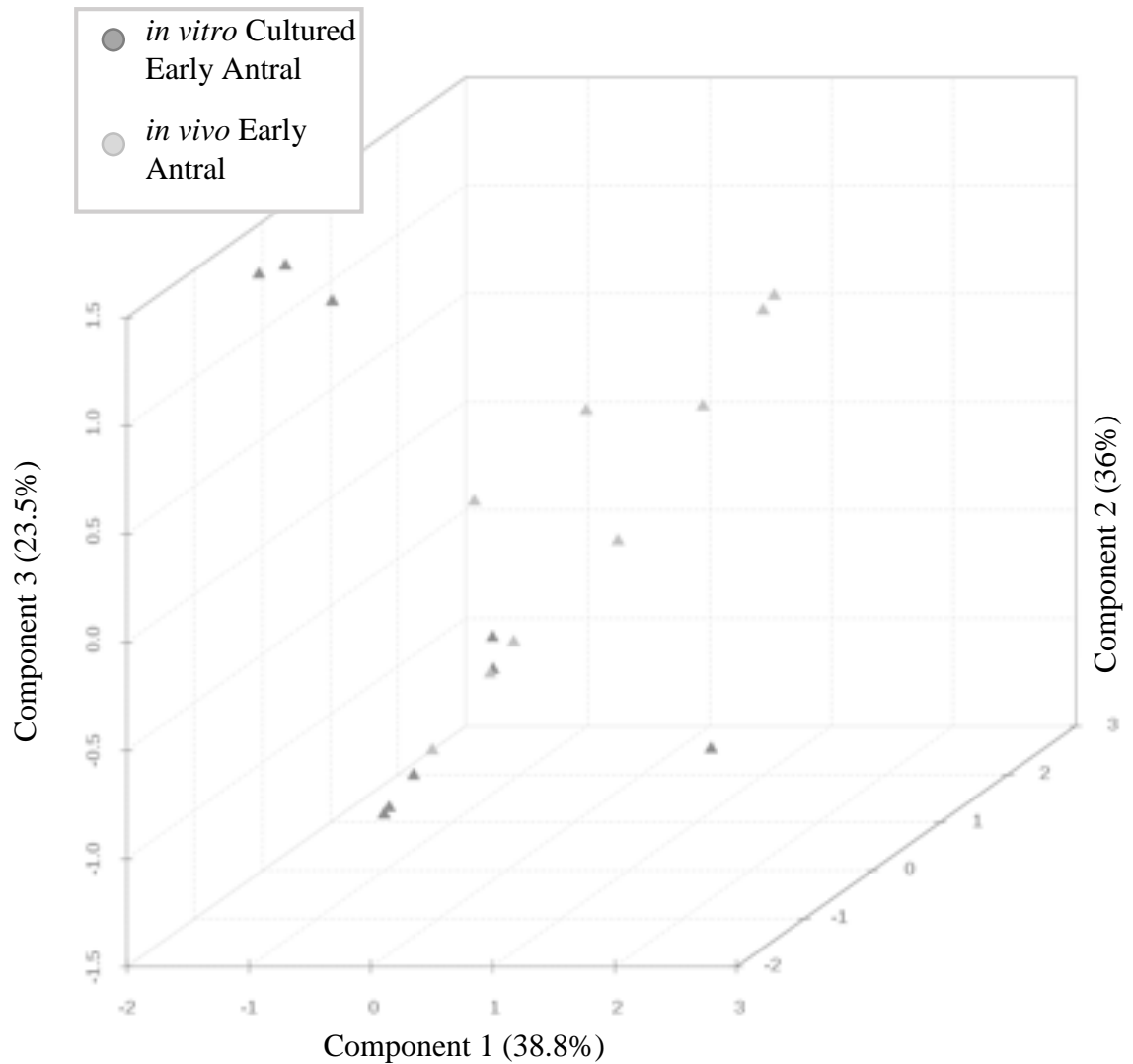


Figure 3.15: Three- dimensional PLS-DA of early antral follicles derived *in vivo* (light gray) and those subjected to IVC (dark gray) after incubation with tracer media. The amount of variation between samples captured by each component is indicated in parenthesis.

Table 3.13: Calculated flux through pathways of central carbon metabolism and glucose carbon contributions to selected intermediate pools, as calculated from Follicles (n=9 per group)¹

Flux/Intermediate	Follicle Stage		P ²
	Early Antral (<i>in vitro</i> cultured)	Late Antral (<i>in vivo</i>)	
Acetyl CoA from Glucose	3.86 ± 0.44	1.65 ± 0.27	0.0128*
Pyruvate (mitochondrial pool) from Glucose	27.95 ± 2.36	37.99 ± 1.26	0.0332*
Pyruvate (cytoplasmic pool) from Glucose	1.35 ± 0.21	0.90 ± 0.21	0.1708
PPP and PEPCK flux:Glycolysis Flux	0.15 ± 0.06	0.08 ± 0.03	0.4170
Pyruvate Dehydrogenase: Pyruvate Carboxylase	0.81 ± 0.19	0.91 ± 0.12	0.6836

¹Values reported as the least squares means, plus or minus the standard error.

Contributions of glucose carbon to metabolite pools is expressed in moles per 100 moles of tracee

²P-value after Dunnett's adjustment. Starred (*) values indicate a significant difference between groups based on P <0.05 significance level.

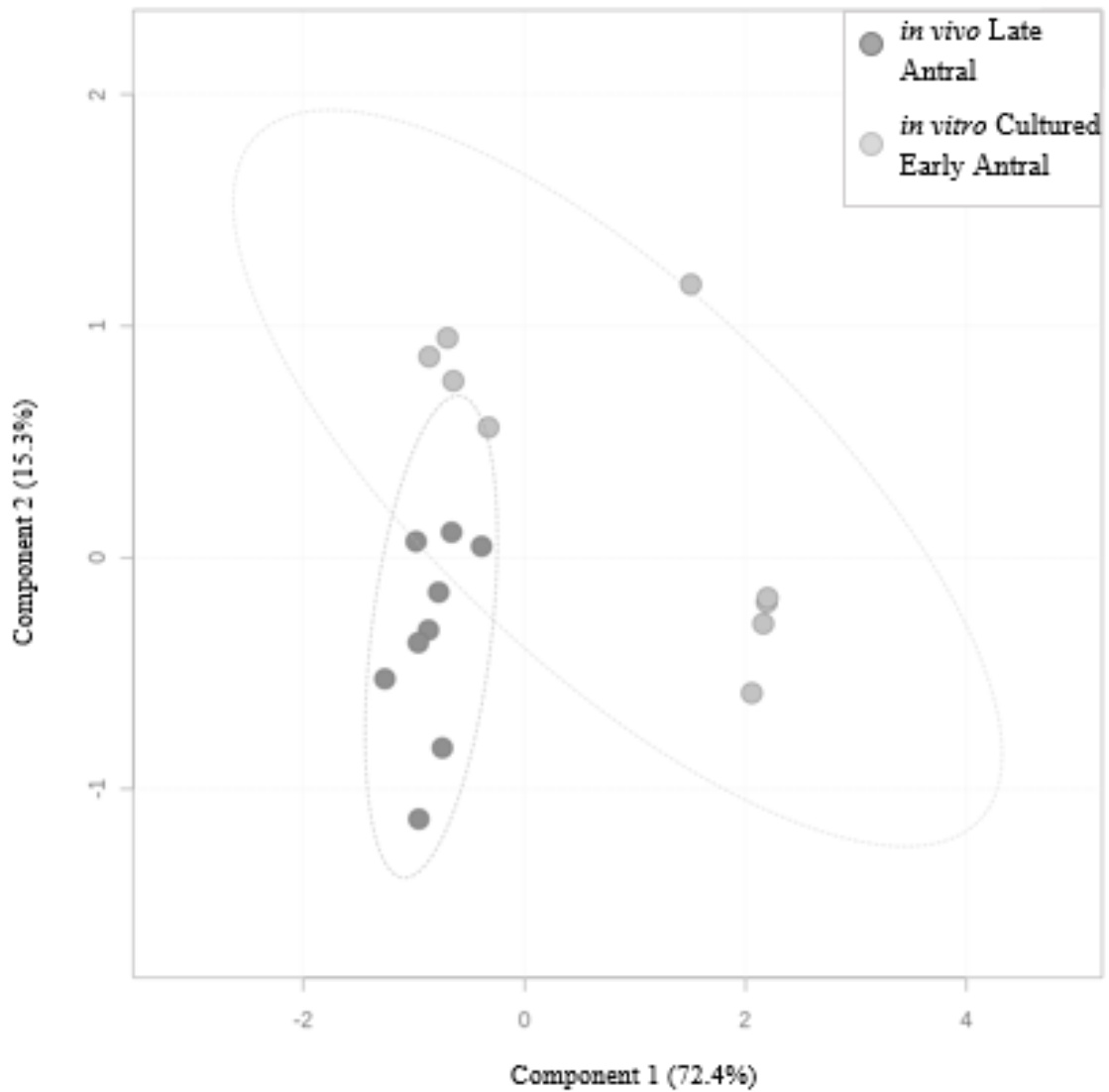


Figure 3.16: Two-dimensional PLS-DA of *in vitro* cultured (light gray) and *in vivo* derived late antral follicles (dark gray) after incubation with tracer media, with a 95% confidence interval indicated around each cluster. The amount of variation between samples captured by each component is indicated in parenthesis.

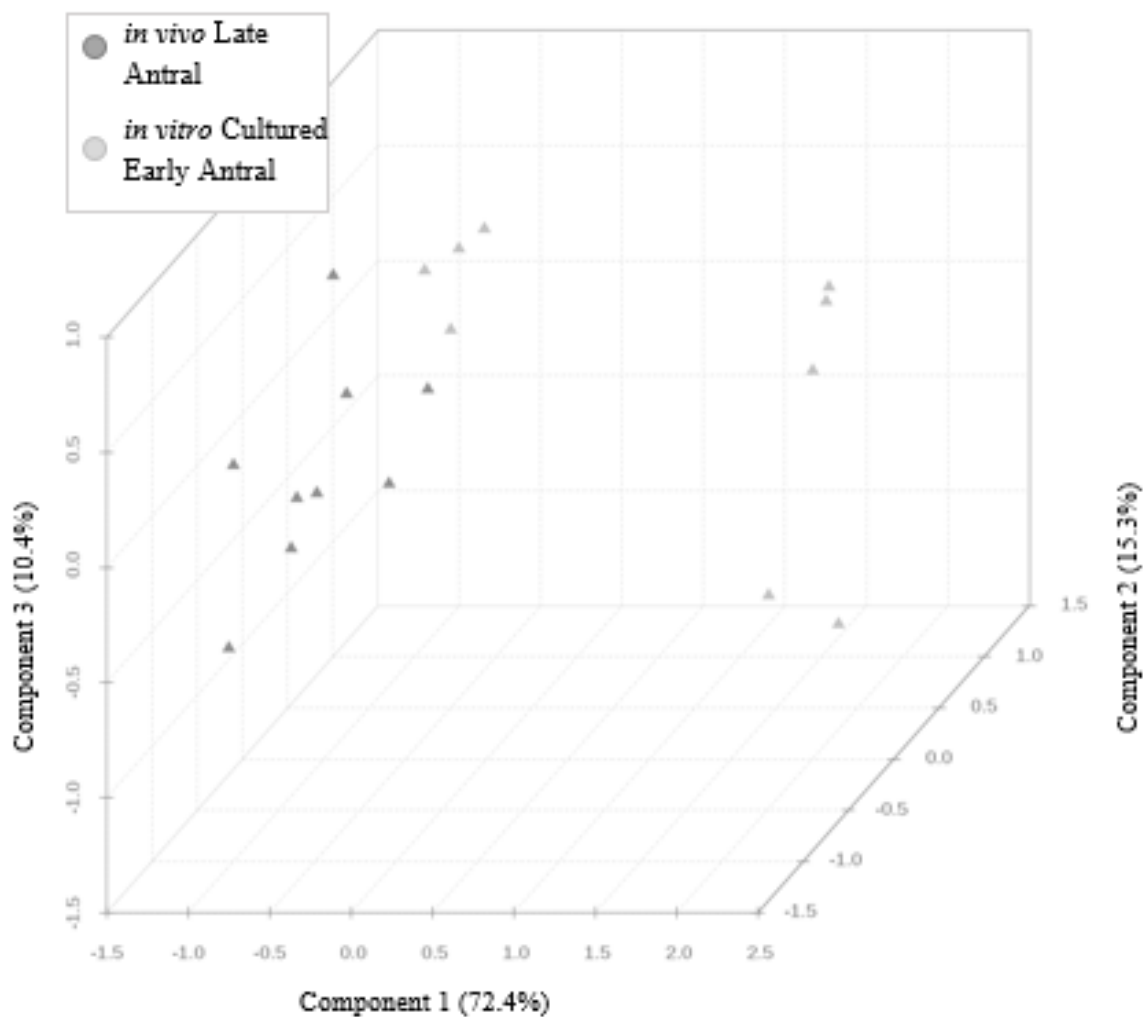


Figure 3.17: Three-dimensional PLS-DA of *in vitro* cultured (light gray) and *in vivo* derived late antral follicles (dark gray) after incubation with tracer media. The amount of variation between samples captured by each component is indicated in parenthesis.

3.5. Discussion

Most previous studies regarding follicle metabolism have focused on static measurements of metabolite concentrations, whether directly from follicular fluid or from the entire follicle, or on metabolite disappearance and appearance in spent media. Even in the most recent metabolomics studies of follicular fluid, only a limited picture of metabolism can be achieved – a single snapshot of the follicle in time is captured, without regards to the ebb and flow of metabolites through physiologic pathways. Understanding the metabolism of follicles will enable future research to innovate *in vitro* culture media to better accommodate the needs of follicles. As previous research has shown, even simply altering glucose concentrations in culture media can have catastrophic results on the developmental capacity of female gametes (Sutton *et al.*, 2010). To address these shortcomings, the objective of the current study was to utilize stable isotope tracers to track the flux of glucose carbon through follicles of different developmental stages and developmental environments.

In order to address this objective, a follicle culture media was formulated with 50% unlabeled glucose and 50% [U-¹³C₆] glucose tracer. After twenty-four hours of individual incubation in the media, consistent labeling of follicles can be achieved (as determined previously), while minimizing the effect on the follicles. While the flux of metabolites through pathways in follicles has not been directly analyzed previously, flux in oocytes has been minimally explored. For those oocytes which undergo *in vitro* maturation (as COCs), glycolysis is highly active in granulosa cells and pyruvate and lactate, the resulting metabolites, are metabolized through the Krebs cycle, followed by oxidative phosphorylation (Seeves and Gardner, 1999). Sutton *et al.* (2010), asserted that pentose

phosphate pathway activity in the cumulus granulosa cells and oocyte are low, although oocytes have a higher potential for pentose phosphate pathway activity. Activity of glucose-6-phosphate dehydrogenase, the first step of carbon allotment into the pentose phosphate cycle, has been qualitatively assessed in oocytes, pre-maturation, and low activity linked to higher quality oocytes (Mohammadi-Sangcheshmeh *et al.*, 2011).

Four main pathways of glucose metabolism in cumulus-oocyte complexes have been proposed: the polyol pathway, hexosamine pathway, the pentose phosphate pathway and glycolysis (Sutton *et al.*, 2010). The pentose phosphate pathway and glycolysis in whole follicles were quantitatively evaluated with this research.

3.5.1. Non-Invasive Analysis of Follicle Metabolism

3.5.1.1. Glycolysis

When moles of [M+n] Glycine were calculated and normalized to 100 moles of [M+0] tracee, there was a significant difference ($P = 0.0014$) detected between the labeling of [M+2] Glycine in early and late antral follicles derived *in vivo*, as well as between *in vitro* cultured early antral follicles and *in vivo* derived late antral follicles ($P = 0.0069$) (**Table 3.14**). The [M+2] labeling pattern is only observed when glucose carbon is metabolized strictly through glycolysis to 3-phosphoglycerate, then to serine, and then to glycine, indicating that flux through glycolysis significantly increases as follicles develop from the early to late antral stage. There was no significant difference between early antral follicles derived *in vivo* and those cultured *in vitro*.

Table 3.14: (A) Moles of tracer per 100 moles of tracee, as detected in early and late antral follicles (n=9), (B) Moles of tracer per 100 moles of tracee, as detected in early antral follicles derived *in vivo* and cultured *in vitro* (n=9), (C) Moles of tracer per 100 moles of tracee, as detected in late antral follicles and *in vitro* cultured early antral follicles (n=8)¹

A	Follicle Stage		<i>P</i> ²
	Early Antral (<i>in vivo</i>)	Late Antral (<i>in vivo</i>)	
Flux/Intermediate			
[M+2] Glycine	0.33 ± 0.01	0.66 ± 0.07	0.0014*
[M+3] Alanine	30.19 ± 1.60	51.18 ± 1.48	< 0.0001*
[M+3] Lactate	0.43 ± 0.18	0.40 ± 0.04	0.8292
[M+2] Glutamate	2.37 ± 0.49	2.18 ± 0.25	0.4989
[M+3] Glutamate	0.96 ± 0.07	0.90 ± 0.11	0.6173
[M+3] Serine	0.17 ± 0.02	0.75 ± 0.09	0.0003*
[M+2] Proline	1.84 ± 0.70	1.82 ± 0.50	0.9803

B	Follicle Stage		<i>P</i> ²
	Early Antral (<i>in vivo</i>)	Early Antral (<i>in vitro</i>)	
Flux/Intermediate			
[M+2] Glycine	0.34 ± 0.01	0.38 ± 0.01	0.0686
[M+3] Alanine	31.44 ± 1.33	28.65 ± 1.07	0.0880
[M+3] Lactate	0.42 ± 0.18	0.47 ± 0.13	0.8268
[M+2] Glutamate	2.40 ± 0.16	1.04 ± 0.14	< 0.0001*
[M+3] Glutamate	0.97 ± 0.07	0.38 ± 0.04	<0.0001*
[M+3] Serine	0.17 ± 0.02	0.13 ± 0.01	0.2476
[M+2] Proline	1.96 ± 0.72	0.99 ± 1.93	0.5976

C	Follicle Stage		P ²
	Early Antral (<i>in vitro</i> cultured)	Late Antral (<i>in vivo</i>)	
[M+2] Glycine	0.38 ± 0.06	0.68 ± 0.06	0.0069*
[M+3] Alanine	28.40 ± 1.17	52.00 ± 1.17	<0.0001*
[M+3] Lactate	0.47 ± 0.11	0.40 ± 0.11	0.6633
[M+2] Glutamate	1.07 ± 0.23	2.29 ± 0.23	0.0071*
[M+3] Glutamate	0.39 ± 0.11	0.95 ± 0.11	0.0071*
[M+3] Serine	0.17 ± 0.02	0.13 ± 0.01	0.0005*
[M+2] Proline	0.73 ± 1.5	2.00 ± 1.50	0.5701

¹Values reported as the mean, plus or minus the standard error, expressed as moles per 100 moles of tracee

²P-value after pairwise t-test. Starred (*) values indicate a significant difference between groups based on P <0.05 significance level; crossed (†) values indicate erroneous significance detection

Much as with [M+2] glycine, [M+3] alanine is only produced when [U-¹³C₆] glucose is taken up by the follicle and metabolized directly through glycolysis to pyruvate. 51.18 (±1.48) moles of [M+3] alanine were present per 100 moles of tracee in late antral follicles, while only 30.19 (±1.60) moles of [M+3] alanine were present per 100 moles of tracee in early antral follicles. These findings were reflected in the comparison between *in vivo* derived late antral follicles and *in vitro* cultured early antral follicles. Again, these findings reflect a significant increase (P <0.0001) in [M+3] alanine, therefore glycolytic activity and glucose contribution to the pyruvate pool, in late antral follicles over early antral follicles. Conversely, no significant difference was detected between *in vivo* derived early antral and *in vitro* cultured early antral follicles (**Table 3.14**).

There were no significant changes in [M+3] lactate abundance across developmental stages or environmental conditions (**Table 3.14**). This finding is surprising

as lactate is generally accepted to be in isotopic equilibrium with the pyruvate pool; therefore, similar results in labeling patterns between lactate and alanine would be expected. It appears that there is compartmentalization of the pyruvate pool (mitochondrial vs. cytosolic) in follicles. If that is the case, severe dilution of the tracer could occur independently in the lactate pool given an influx of alternative endogenous carbon sources -- for example, via metabolism of glycerol to lactate. In bovine follicles, triglycerides are at highest concentrations in small follicles and decreased concentrations in large, late antral follicles (Leroy *et al.*, 2004b). If triglycerides are metabolized, glycerol and fatty acids are released, and glycerol can be converted to lactate. It would follow that triglyceride concentrations would be depleted in large follicles as more lactate is being produced, which is consistent with current and previous results.

While serine labeling was measured, erratic results were obtained. Given the presence of serine in the culture medium, it would be expected that severe dilution of the tracer would occur. Additionally, as tracer ([M+3] serine) abundances decrease, the accuracy with which they can be determined is diminished. After correction for natural labeling, error in the serine labeling patterns is compounded, giving highly negative, as well as impossibly high results for tracer abundances. While additional testing is warranted, these results suggest that serine does not serve as a reliable indicator of the 3-phosphoglycerate pool or for glycolytic activity.

As discussed previously, pyruvate is in isotopic equilibrium with alanine and lactate; therefore, the contributions of glucose carbon to the pyruvate carbon pool can be estimated by correcting the [M+3] enrichments of alanine and lactate for the abundance of [M+6] glucose in the media. There are no significant differences in the contributions of

glucose carbon to the cytosolic pyruvate pool (approximated by lactate) in any of the groups. Glucose carbon comprised a higher proportion of the mitochondrial pyruvate pool in late antral versus early antral follicles, *in vivo* derived and *in vitro* cultured. This could reflect an increased glycolytic flux in late antral follicles, or a decrease in contributions of alternative carbon sources (e.g., amino acid catabolism).

3.5.1.2. Urea Cycle

No significant differences in proline labeling were detected among groups, either between follicles of different developmental stages or between environmental conditions (**Table 3.14**). Slightly negative values for [M+3] proline are likely a combined result of low [M+3] abundances as well as imperfect background fitting, which causes error in the natural isotope corrections. Interestingly however, [M+2] proline labeling tends to be lower than [M+2] glutamate abundance in early and late antral follicles derived *in vivo* ([M+2] proline being about 83% of the [M+2] glutamate) (**Figure 3.18**). Proline is typically in isotopic equilibrium with glutamate; however, tracer dilution in proline would occur if the cells had an active urea cycle. During this process, arginine is converted to ornithine via arginase, which results in the release of urea, then ornithine can form proline. Urea was annotated in metabolomic analysis of feline follicles but was inconsistent. However, urea has been detected in the follicles of several species in previous studies. In bovine follicles, urea is higher in small and mid-size follicles (early antral stage) than in late antral stage follicles. This is indicative of a highly functioning urea cycle (arginase activity) in early antral follicles, with lower activity in late antral follicles, which mirrors tracer dilution results. Results are inconclusive, however, feline follicles should be

evaluated for a functioning urea cycle. It would not be surprising to find that feline follicles do in fact exhibit high arginase activity, given the uncontrolled, high functionality of the urea cycle in adult felids (Morris *et al.*, 2002).

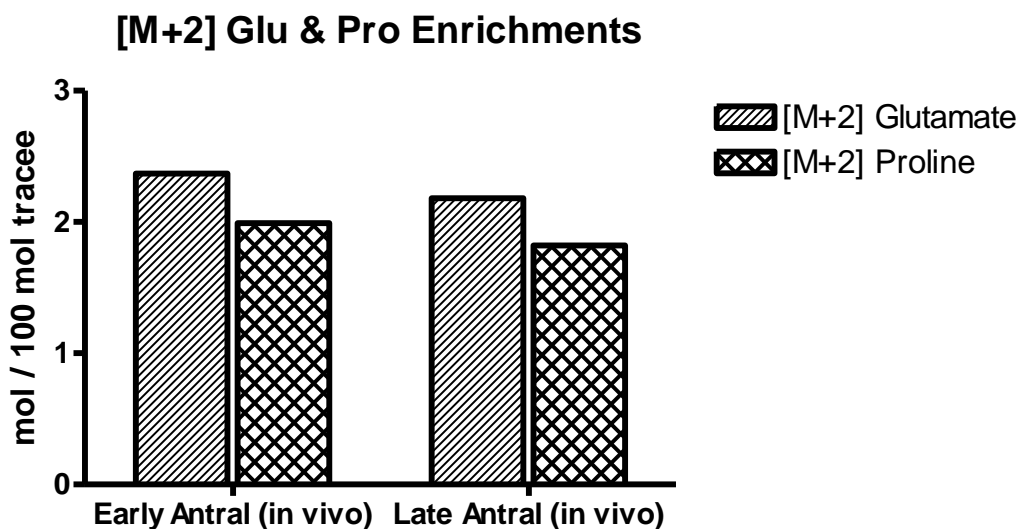


Figure 3.18: [M+2] glutamine and proline enrichments for early antral and late antral follicles derived *in vivo*. [M+2] proline enrichment consistently tends to be about 83% of [M+2] glutamate enrichment.

3.5.1.3. TCA Cycle, PPP, and PEPCK-c

[M+2] Glutamate can result from one of two metabolic courses. It can result from the entrance of [M+2] Acetyl CoA into the TCA Cycle, in which [M+2] α -Ketoglutarate is produced in the first turn (which can then be metabolized to [M+2] glutamate). It can also result from pyruvate carboxylase activity, converting [M+3] pyruvate to [M+3] oxaloacetate. Oxaloacetate exhibits two positional isotopomers due to its equilibrium with

malate. If [M+3]_{C1-C3} oxaloacetate forms α -ketoglutarate, [M+2] α -ketoglutarate will result on the first turn of the cycle; however, if [M+3]_{C2-C4} oxaloacetate proceeds, it will form [M+3] α -ketoglutarate on the first turn of the cycle and [M+2] α -ketoglutarate on the second turn. This pathway, which results in [M+3] α -ketoglutarate formation, is the only pathway which will result in [M+3] glutamate production. No significant differences in [M+2] or [M+3] glutamate abundances are observed in *in vivo* derived early and late antral follicles. However, altering the follicle environment results in a decrease in both [M+2] and [M+3] glutamate in *in vitro* cultured early antral follicles as compared to *in vivo* derived early and late antral follicles (**Table 3.14**). This suggests that there is decreased entrance of glucose carbon into the TCA cycle in *in vitro* cultured early antral follicles. Metabolomics data suggests that TCA activity remains constant in feline follicles. It follows that alternative anapleurotic carbon sources are utilized in these follicles, possibly including fatty acid oxidation.

Evaluation of the abundances of alanine isotopomers can elucidate the main pathways of glucose carbon metabolism. Again, [M+3] alanine can only result when [U-¹³C₆] labeled glucose is metabolized through glycolysis to pyruvate. [M+1] and [M+2] alanine result primarily from activity of the pentose phosphate pathway, where a single glucose carbon is lost as carbon dioxide when ribulose-5-phosphate is formed, and carbon rearrangements occur. These two isotopomers can also result from phosphoenolpyruvate (PEP) synthesis via PEP carboxykinase (cytosolic) (PEPCK-c), which can then be converted to pyruvate. Therefore, a ratio of [M+1] and [M+2] to [M+3] alanine can give a crude estimate of PPP/PEPCK-c to glycolytic activity. This ratio, 0.09, 0.08, and 0.10, for early antral, late antral, and *in vitro* cultured early antral follicles respectively, did not

change between *in vivo* derived early and late antral follicles or between *in vivo* derived and *in vitro* cultured early antral follicles; however, there was a change detected between late antral follicles and *in vitro* cultured early antral follicles. For feline follicles, there does not appear to be a shift in the comparative glycolytic activity to pentose phosphate activity between developmental stages in the cat, or early antral follicles in different environmental conditions. Instead, in accordance with previous reports, there is a consistently higher glycolytic flux than PPP flux. However, given the heightened glycolytic activity in late antral follicles, a matched increase in PPP and PEPCK-c activity would be expected to maintain the ratio. For early and late antral follicles, as compared to preantral follicles, the increase in follicle diameter is due largely to an increase in the amount of follicular fluid produced, rather than a large increase in cell proliferation. Without increased cell proliferation, activity of the PPP would not be expected to increase, as its two main functions are to produce reducing equivalents and pentoses for nucleic acids. However, during this time course, oocytes are growing and accumulating mRNAs which will be utilized by early embryos until embryonic genome activation, which could account for the higher PPP flux observed in follicles. Conversely, when late antral follicles are compared to *in vitro* cultured early antral, there is a marked difference between the flux through the PPP and PEPCK-c as compared to glycolysis. It appears that in *in vitro* cultured early antral follicles there is a disproportionate shift in glucose flux through the PPP and PEPCK-c. The case has been made that in embryos, those with the quietest metabolisms are the most viable to continue growth and development (Leese *et al.*, 2008). It may be possible that the same is true in follicles, and that these *in vitro* cultured early

antral follicles (which achieved minimal growth in culture, see Chapter 2), are not as able to continue development due to their overactive metabolisms (PPP and PEPCK-c fluxes).

Previous reports by Berthold *et al.* (1994), have utilized the abundances of [M+3] aspartate and [M+2] and [M+3] glutamate to calculate the enrichment of acetyl CoA. Aspartate was not accurately detected for the media assessed, most likely because of its low abundance in samples or low derivatization efficiency; however, a rough estimate for [M+3] aspartate can be calculated from [M+3] glutamate. Given that [M+3] glutamate can only derive from oxaloacetate labeled at carbons 2, 3, and 4, and that oxaloacetate's two positional isotopomers are in equilibrium, [M+3] aspartate is at least two times higher than [M+3] glutamate. If oxaloacetate is at perfect equilibrium, [M+3] glutamate is half of [M+3] aspartate. Using this information and the equation established by Berthold *et al.*, it was determined that acetyl CoA enrichment is similar in *in vivo* derived early and late antral follicles, while there appears to be a slight decrease in enrichment in *in vitro* cultured early antral follicles as compared to their *in vivo* derived counterparts. The decrease in glucose contribution to the acetyl CoA pool would most likely due to an increased contribution of acetyl CoA from fatty acid oxidation in these follicles. More interesting to note is the large difference in glucose contribution to the pyruvate pool as opposed to the acetyl CoA pool. Further work is needed to determine what contributions the pyruvate pool is making to the metabolisms in feline follicles, as it appears that very little of pyruvate is converted to acetyl CoA for entrance to the TCA cycle.

A visual summary of the metabolic differences between *in vivo* derived early antral follicles, *in vivo* derived late antral follicles, and *in vitro* cultured early antral follicles is depicted in **Figure 3.19, 3.20, and 3.21.**

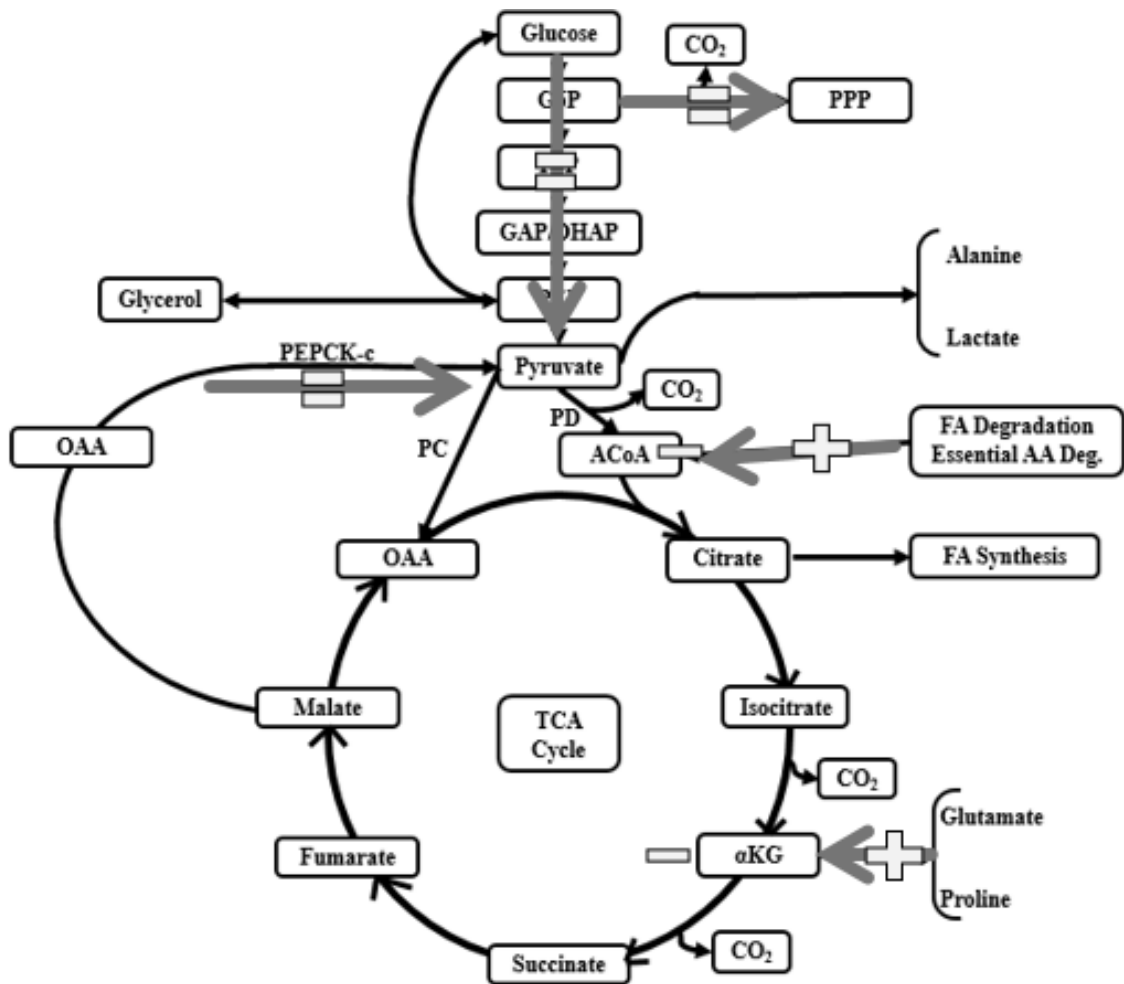


Figure 3.13: Comparison of metabolism through the central carbon pathway in *in vivo* derived early antral follicles as compared to *in vitro* cultured early antral follicles. Gray arrows (\rightarrow) indicate a flux (e.g., flux through glycolysis), plus signs (+) indicate an increase in *in vitro* cultured early antral follicles over *in vivo* derived early antral follicles, minus signs (-) indicate a decrease in *in vitro* cultured early antral follicles as compared to *in vivo* derived early antral follicles, and an equal sign (=) indicates equivalence. There is an equivalent glycolytic flux, as well as a maintained ratio of PPP and PEPCK-c flux to glycolysis in *in vitro* cultured early antral follicles. Enrichments of acetyl CoA ([M+2]) and α -ketoglutarate ([M+2] and [M+3] glutamate) are decreased in *in vitro* cultured early antral follicles, indicating an increase in contribution to these pools by alternative anapleurotic substrates.

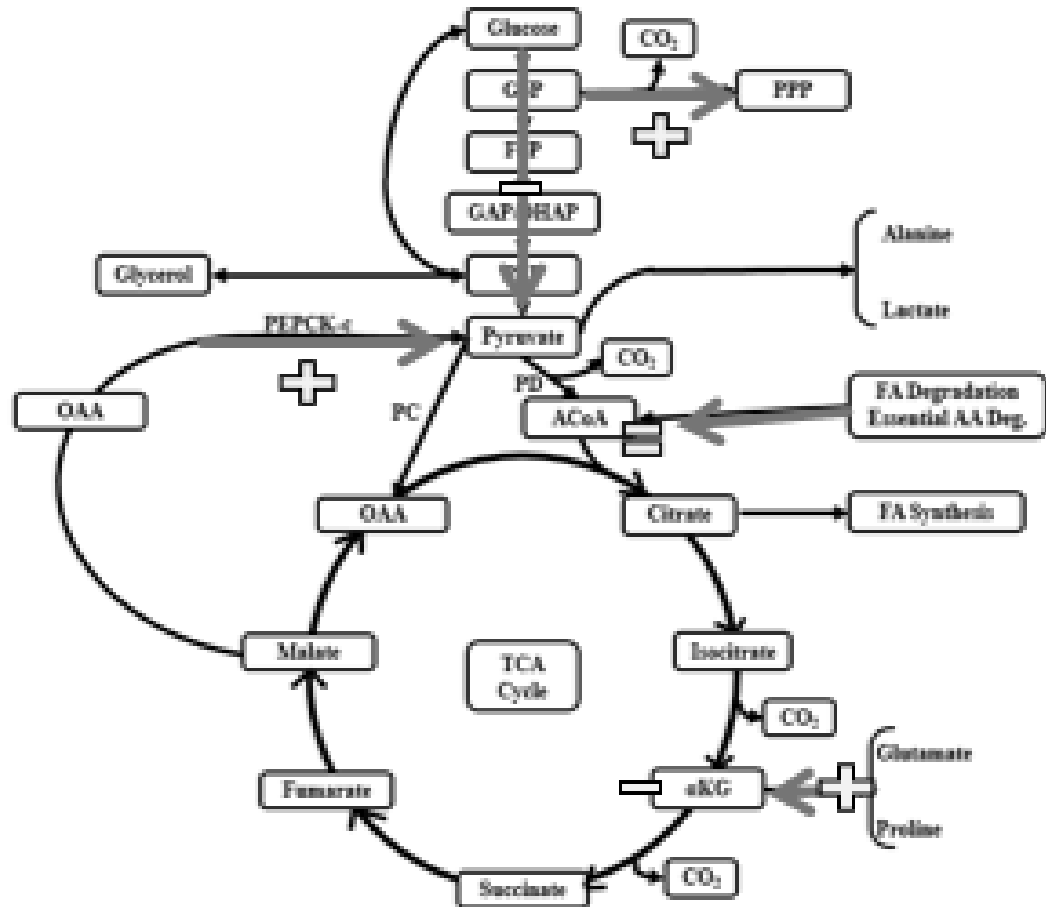


Figure 3.14: Comparison of metabolism through the central carbon pathway in *in vivo* derived late antral follicles as compared to *in vitro* cultured early antral follicles. Gray arrows (→) indicate a flux (e.g., flux through glycolysis), plus signs (+) indicate an increase in *in vitro* cultured early antral follicles over *in vivo* derived late antral follicles, minus signs (-) indicate a decrease in *in vitro* cultured early antral follicles over *in vivo* derived late antral follicles, and an equal sign (=) indicates equivalence. There is a decrease in glycolytic flux, but an increase in the ratio of PPP and PEPCK-c flux to glycolysis in *in vitro* cultured early antral follicles as compared to late antral follicles. Enrichment of acetyl CoA ([M+2]) is equivalent between groups, while α-ketoglutarate ([M+2] and [M+3] glutamate) is decreased in *in vitro* cultured early antral follicles, indicating an increase in contribution to this pool by alternative anapleurotic substrates.

3.5.1.4. Partial Least Squares Analysis based on results from spent media

Tight clustering of late antral follicles derived *in vivo*, discriminant from early antral follicles derived *in vivo* and from *in vitro* cultured early antral follicles, in both 2D and 3D PLS-DA suggests that the variability in the metabolism in late antral follicles, with regards to glucose metabolism, are low. This could provide a good model to assess follicle class via metabolic evaluation. Assessment of atretic follicles, as opposed to healthy follicles, using these evaluation measures could provide insight into markers for good versus poor quality follicles and oocytes. Indistinct clustering of early antral follicles derived directly from the ovary and those subjected to *in vitro* culture suggest that there is large variation in the metabolism of these two groups, and that their metabolisms do not greatly differ from one another. There appears to be a decreased ability of early antral follicles to progress to the late antral stage when cultured *in vitro* (as suggested by the minimal growth observed in *in vitro* cultured early antral follicles, observed during the metabolomics study), it does not appear to be due to a fundamental difference in glucose carbon metabolism of the two groups of early antral follicles, but rather an inability of the *in vitro* cultured early antral follicles to shift to the metabolism expressed by late antral follicles.

3.5.2. Direct Analysis of Follicle Metabolism

Direct analysis of feline follicles did not offer many significant differences in flux and glucose carbon contributions to intermediate pools. Glucose contribution to the pyruvate pool (as assessed via alanine labeling) was higher in late antral follicles as compared to *in vitro* cultured early antral follicles. This result is in line with the results

obtained from analysis of the spent media. The difference in glucose contributions to the pyruvate pool may have been detected, while other differences were not, given that alanine enrichment was the highest among those amino acids monitored (potentially allowing it to be accurately detected even with the smaller sample size). Conversely, glucose's contribution to the acetyl CoA pool was lower in late antral follicles as compared to *in vitro* cultured early antral follicles, which was not reflected in the analysis of spent media. While it would be expected that similar enrichment patterns would be observed in spent media and their corresponding follicle samples, and that similar differences between groups would be observed during direct and indirect assessment, it appears that this is not the case. Due to very small amounts of available material for processing, it is possible that abundances were too near the threshold of detection for the GC-MS platform for accurate quantification of ions. Any deviations from the true abundance of ions would have been compounded through natural isotope abundance correction, and the subsequent calculations. It is possible that collection of higher numbers of follicles, especially at the early antral stage, may be required for analysis with this platform. However, because analysis of spent media provides a more clinically valuable avenue for analysis, that is, the media can be tested and the follicles and oocytes are left intact for culture and use in ARTs, further research should be carried out to determine if fluxes determined through analysis of spent media correlate to maturation, fertilization, and developmental potential of oocytes and embryos.

Chapter 4: Concluding Remarks and Future Directions

Feline follicles of different developmental stages and environmental conditions were considered in this study. Fundamental differences in metabolite profiles and carbon metabolism were observed among early antral and late antral follicles, suggesting that follicles which successfully progress through folliculogenesis undergo metabolic shifts in order to do so. Furthermore, while it seems that early antral follicles cultured *in vitro* have a lower capacity than those derived *in vivo* to grow to the late antral stage (suggested by the minimal growth of *in vitro* cultured early antral follicles, as described in Chapter 2) the difference is not due to a fundamental metabolic difference in the early antral follicles themselves, but rather an inability to shift to the metabolism which marks late antral follicles. Further research is needed in order to truly understand the metabolism of these dynamic structures. Isolation of oocytes from follicular cells (granulosa and theca), as well as isolation of follicular fluid from these two cellular pools will provide a more specific, targeted view of metabolism. As of yet, metabolite profiles are confounded because of the numerous cell types present in samples.

The metabolomics and fluxomics procedures refined for this study can easily be applied to gamete and embryo evaluation, providing essential metabolic information which could be used to define viable follicles, gametes, and embryos for model species. The

increased understanding of metabolism in these structures will also allow for refinement of present ARTs (e.g., culture media formulation), and potentially make possible the culture of preantral follicles to the late antral stage. Further research regarding preantral follicle metabolism using metabolomic and fluxomic technologies, followed by development of effective IVC methods can unlock access to follicles and oocytes which are currently unavailable (Gupta and Nandi, 2012). Effective culture methods for most species are only available for antral follicles, which severely limits quantities available for use, and effectively wastes thousands of preantral follicles and their oocytes which are ultimately lost to atresia. Once culture methods for preantral follicles are developed, thousands of additional oocytes per animal will be available for embryo production (Gutierrez *et al.*, 2000). This outcome has already been realized and employed with limited success in mice (Hasegawa *et al.*, 2004 and 2006).

While there are many facets to breeding exotic species which need to be addressed, including reproductive physiology, cyclicity of females, and behavior, there is a basic need for development of efficient ART's, which is only possible with better understandings of gamete, follicle, and embryo metabolism. This is an imperative to the effort to perpetuate genes, to maintain and increase genetic variability, and to allow for gamete rescue. Even with comprehensive conservation plans, genetic diversity is limited because of the limited number of individuals. When even a single individual is lost because of injury, disease, or natural death, ARTs provide an opportunity for gamete rescue. Post-mortem collection of follicles from African Black Rhinoceros have been carried out, and showed limited success in producing cleavage stage embryos. With further assessment of follicle and oocyte

metabolism, it may be possible to refine culture techniques to increase efficiency (Stoops *et al.*, 2011).

Finally, ART's for livestock and exotic species need to be improved to allow for selection of the most viable oocytes and embryos to decrease the need for multiple embryo transfer. This will improve safety for recipient animals and decrease the wastage of invaluable eggs and embryos.

APPENDICES

Appendix 1: Mass Isotopomer Distributions for monitored amino acids, standardized as moles [M+n] per 100 moles of [M+0], reported as an average \pm standard error. Tables A-C report values for the spent tracer media for early antral follicles derived *in vivo* and cultured *in vitro* and late antral follicles derived *in vivo*. Tables D-E report values for follicular samples.

A	Glycine		Alanine			Lactate		
	[M+1]	[M+2]	[M+1]	[M+2]	[M+3]	[M+1]	[M+2]	[M+3]
Early Antral Follicles (<i>in vivo</i>)	2.33 \pm 0.21	0.34 \pm 0.01	0.81 \pm 0.07	1.92 \pm 0.11	30.56 \pm 1.48	0.06 \pm 0.04	-0.25 \pm 0.01	0.40 \pm 0.16
Late Antral Follicles (<i>in vivo</i>)	1.68 \pm 0.30	0.66 \pm 0.07	1.24 \pm 0.10	2.91 \pm 0.11	51.18 \pm 1.48	0.03 \pm 0.02	-0.27 \pm 0.07	0.40 \pm 0.04
Early Antral Follicles (<i>in vitro</i>)	2.71 \pm 0.19	0.38 \pm 0.01	0.92 \pm 0.07	2.00 \pm 0.09	28.65 \pm 1.07	0.08 \pm 0.03	-0.24 \pm 0.02	0.47 \pm 0.13

B	Serine			Glutamate				
	[M+1]	[M+2]	[M+3]	[M+1]	[M+2]	[M+3]	[M+4]	[M+5]
Early Antral Follicles (in vivo)	0.12±0.01	0.00±0.01	0.16±0.02	0.72±0.06	2.37±0.15	0.96±0.07	0.02±0.01	-0.39±0.02
Late Antral Follicles (in vivo)	0.86±0.16	0.43±0.10	0.75±0.09	0.71±0.10	2.18±0.26	0.90±0.11	0.04±0.01	0.02±0.00
Early Antral Follicles (in vitro)	0.13±0.01	0.01±0.01	0.13±0.01	0.37±0.08	1.05±0.14	0.38±0.04	-0.92±0.18	0.04±0.07

C	Proline				
	[M+1]	[M+2]	[M+3]	[M+4]	[M+5]
Early Antral Follicles (in vivo)	1.30±0.41	1.99±0.65	-2.32±0.25	-0.04±0.05	0.15±0.01
Late Antral Follicles (in vivo)	0.71±0.68	1.82±0.50	-1.09±0.40	-0.29±0.06	0.09±0.02
Early Antral Follicles (in vitro)	1.16±1.27	0.99±1.93	-2.03±0.42	0.00±0.11	0.13±0.03

D	Glycine		Alanine			Lactate		
	[M+1]	[M+2]	[M+1]	[M+2]	[M+3]	[M+1]	[M+2]	[M+3]
Early Antral Follicles <i>(in vivo)</i>	49.10±26.63	2.15±0.48	0.29±0.31	0.73±0.51	22.80±2.48	-0.33±0.29	-0.59±0.54	0.47±0.25
Late Antral Follicles <i>(in vivo)</i>	43.98±10.68	1.88±0.19	0.90±0.10	1.94±0.18	35.30±2.91	0.01±0.04	-0.24±0.04	0.81±0.16
Early Antral Follicles <i>(in vitro)</i>	92.62±2.69	4.72±0.23	1.14±0.57	1.56±0.28	22.61±2.91	-0.55±0.33	0.02±0.35	1.07±0.32

E	Glutamate				Proline				
	[M+2]	[M+3]	[M+4]	[M+5]	[M+1]	[M+2]	[M+3]	[M+4]	[M+5]
Early Antral Follicles <i>(in vivo)</i>	11.91± 0.98	5.01±0.75	-0.14± 0.08	0.04±0.03	6.86± 0.99	72.92± 29.14	3.50± 3.65	-1.47± 0.93	5.82± 3.75
Late Antral Follicles <i>(in vivo)</i>	5.65±0.76	2.08±0.36	0.05±0.03	0.06±0.01	20.08± 18.19	6.78± 8.45	1.84± 1.66	-0.67± 0.35	1.10± 0.52
Early Antral Follicles <i>(in vitro)</i>	11.64± 0.73	3.81±0.14	-0.15± 0.07	0.06±0.21					

REFERENCES

- Aerts JMJ, Bols PEJ. Ovarian follicular dynamics: a review with emphasis on the bovine species. Part I: folliculogenesis and pre-antral follicle development. *Reproduction in Domestic Animals*. 2010; 45: 171-179.
- Aerts JMJ, Bols PEJ. Ovarian follicular dynamics: a review with emphasis on the bovine species. Part II: antral development, exogenous influence and future prospects. *Reproduction in Domestic Animals*. 2010; 45: 180-187.
- Anastasiou D, Cantley LC. Breathless cancer cells get fat on glutamine. *Cell Research*. 2012; 22: 443-446.
- Apparicio M, Ferreira CR, Tata A, Santos VG, Alves AE, Mostachio GQ, Pires-Butler EA, Motheo TF, Padilha LC, Pilau EJ, Gozzo FC, Eberlin MN, Lo Turco EG, Luvoni GC, Vicente WRR. Chemical composition of lipids present in cat and dog oocyte by matrix-assisted desorption ionization mass spectrometry (MALDI-MS). *Reproduction in Domestic Animals*. 2012; 47: 113-117.
- Arya BK, Ul-Haq A, Chaudhury K. Oocyte quality reflected by follicular fluid analysis in poly cystic ovary syndrome (PCOS): a hypothesis based on intermediates of energy metabolism. *Medical Hypotheses*. 2012; 78: 475-478.
- Aydiner F, Yetkin CE, Seli E. Perspectives on emerging biomarkers for non-invasive assessment of embryo viability in assisted reproduction. *Current Molecular Medicine*. 2010; 10: 1875-5666.
- Bender K, Walsh S, Evans A, Fair T, Brennan L. Metabolite concentrations in follicular fluid may explain differences in fertility between heifers and lactating cows. *Society for Reproduction and Fertility*. 2010; 139: 1047-1055.
- Berisha B, Schams D. Ovarian function in ruminants. *Domestic Animal Endocrinology*. 2005; 29: 305-317.
- Bequette BJ, Sunny NE, El-Kadi SW, Owens SL. Application of stable isotopes and mass isotopomer distribution analysis to the study of intermediary metabolism of nutrients. *Journal of Animal Science*. 2006; 84: E50-E59.
- Berthold HK, Wykes LJ, Jahoor F, Klein PD, Reeds PJ. The use of uniformly labelled substrates and mass isotopomer analysis to study intermediary metabolism. *Proceedings of the Nutrition Society*. 1994; 53: 345-354.
- Biggers JD, Summers MC. Choosing a culture medium: making informed choices. *Fertility and Sterility*. 2008; 90: 473-483.

Biggers JD, Whittingham DG, Donahue RP. The pattern of energy metabolism in the mouse oocyte and zygote. *Proc Natl Acad Sci USA* 1967; 58: 560-567.

Bonnet A, Bevilacqua C, Benne F, Bodin L, Cotinot C, Liaubet L, Sancristobal M, Sarry J, Terenina E, Martin P, Tosser-Klopp G, Mandon-Pepin B. Transcriptome profiling of sheep granulosa cells and oocytes during early follicular development obtained by laser capture microdissection. *BMC Genomics*. 2011; 12: 417-431.

Botros L, Sakkas D, Seli E. Metabolomics and its application for non-invasive embryo assessment in IVF. *Molecular Human Reproduction*. 2008; 14: 679-690.

Brinster RL. Oxidation of pyruvate and glucose by oocytes of the mouse and rhesus monkey. *Journal of Reproduction and Fertility*. 1971; 24: 187-191.

Brison DR, Houghton FD, Falconer D, Roberts SA, Hawkhead J, Humpherson PG, Lieberman BA, Leese HJ. Identification of viable embryos in IVF by non-invasive measurement of amino acid turnover. *Human Reproduction*. 2004; 19: 2319-2324.

Bristol-Gould S, Woodruff TK. Folliculogenesis in the domestic cat (*Felis catus*). *Theriogenology*. 2006; 66: 5-13.

Byskov AG. The role of the rete ovarii in meiosis and follicle formation in the cat, mink and ferret. *Journal of Reproduction and Fertility*. 1975; 45: 201-209.

Campbell BK, Onions V, Guo L, Scaramuzzi RJ. The effect of monosaccharide sugar and pyruvate on the differentiation and metabolism of sheep granulosa cells *in vitro*. *Reproduction*. 2010; 140: 541-550.

Carnevale EM, Frank-Guest BL, Stokes JE. Effect of equine oocyte donor age on success of oocyte transfer and intracytoplasmic sperm injection. *Animal Reproduction Science*. 2010; 121S: S258-S259.

Cheng Y, Kawamura K, Takae S, Deguchi M, Yang Q, Kuo C, Hsueh AJW. Oocyte-derived r-spondin2 promotes ovarian follicle development. *The Journal of the Federation of American Societies for Experimental Biology*. 2013; 27: 2175-2184.

Chun SY and Hsueh AJ. Paracrine mechanisms of ovarian follicle apoptosis. *Journal of Reproductive Immunology*. 1998; 39: 63-75.

Cooper G. Meiosis and Fertilization. *The Cell*.

Cortezzi SS, Cabral EC, Trevisan MG, Ferreira CR, Setti AS, Paes de Almeida Ferreira Braga D, de Cassia Savio Figueira R, Iaconelli A, Eberlin MN, Borges E. Prediction of embryo implantation potential by mass spectrometry fingerprinting of the culture medium. *Reproduction*. 2013; 145: 453-462.

Cortvrindt R, Hu Y, Smitz J. Recombinant luteinizing hormone as a survival and differentiation factor increases oocyte maturation in recombinant follicle stimulating hormone supplemented mouse preantral follicle culture. *Human Reproduction*. 1998; 13: 1292-1302.

Cortvrindt R, Smitz J, Van Steirteghem AC. Assessment of the need for follicle stimulating hormone in early preantral mouse follicle culture *in vitro*. *Human Reproduction*. 1997; 12: 759-768.

d' Anglemont de Tassigny X, Colledge WH. The role of kisspeptin signaling in reproduction. *American Physiological Society*. 2010; 25: 207-217.

D'Alessandro A, Gederica G, Palini S, Bulletti C, Zolla L. A mass spectrometry-based targeted metabolomics strategy of human blastocoele fluid: a promising tool in fertility research. *Molecular BioSystems*. 2012; 8: 953-958.

da Silveira JC, Veeramachaneni DNR, Winger QA, Carnevale EM, Bouma GJ. Cell-secreted vesicles in equine ovarian follicular fluid contain miRNAs and proteins: a possible new form of cell communication within the ovarian follicle. *Biology of Reproduction*. 2012; 86: 1-10.

de Castro e Paula LA, Andrzejewski J, Julian D, Spicer LJ, Hansen PJ. Oxygen and steroid concentrations in preovulatory follicles of lactating dairy cows exposed to acute heat stress. *Theriogenology*. 2008; 69: 805-813.

DeHaven CD, Evans AM, Dai H, Lawton K. Software techniques for enabling high-throughput analysis of metabolomic datasets. *Metabolomics*. 167-192.

De la Luz-Hdez K. Metabolomics and mammalian cell culture. *Metabolomics*. 2012; 3-18.

Dell' Aquila ME, Cho YS, Martino NA, Uranio MF, Rutigliano L, Hinrichs K. OMICS for the identification of biomarkers for oocyte competence, with special reference to the mare as a prospective model for human reproductive medicine. *Meiosis – Molecular Mechanisms and Cytogenetic Diversity*. 2012; 257-282.

Demeestere I, Delbaere A, Gervy C, Van Den Bergh M, Devreker F, Englert Y. Effect of preantral follicle isolation technique on *in vitro* follicular growth, oocyte maturation and embryo development in mice. *Human Reproduction*. 2002; 17: 2152-2159.

Demeestere I, Centner J, Gervy C, Englert Y, Delbaere A. Impact of various endocrine and paracrine factors on *in vitro* culture of preantral follicles in rodents. *Reproduction*. 2005; 130: 147-156.

Des Rosiers C, Fernandez CA, David F, Brunengraber H. Reversibility of the mitochondrial isocitrate dehydrogenase reaction in the perfused rat liver. *The Journal of Biological Chemistry*. 1994; 269: 27179-27182.

Diercks AK, Schwab A, Rittgen W, Kruspel A, Heuss E, Schenkel J. Environmental influences on the production of pre-implantation embryos. *Theriogenology*. 2010; 73: 1238-1243.

Doherty L. Optimizing the agilent technologies 6890 series GC for high performance MS analysis. 2003.

Dunn WB, Broadhurst D, Begley P, Zelena E, Francis-McIntyre S, Anderson N, Brown M, Knowles JD, Halsall A, Haselden JN, Nicholls AW, Wilson ID, Kell DB, Goodacre R, HUSERMET Consortium. Procedures for large-scale metabolic profiling of serum and plasma using gas chromatography and liquid chromatography coupled to mass spectrometry. *Nature Protocols*. 2011; 6: 1060-1083.

Durlinger AL, Gruijters MJ, Kramer P, Karels B, Kumar TR, Matzuk MM, Rose UM, de Jong FH, Uilenbroek JT, Grootegoed JA, Themmen AP. Anti-Mullerian hormone attenuates the effects of FSH on follicle development in the mouse ovary. *Endocrinology*. 2001; 142: 4891-4899.

Ealy AD, Drost M, Hansen PJ. Developmental changes in embryonic resistance to adverse effects of maternal heat stress in cows. *Journal of Dairy Science*. 1993; 76: 2899-2905.

Eppig JJ, Schroeder AC. Capacity of mouse oocytes from preantral follicles to undergo embryogenesis and development to live young after growth, maturation, and fertilization *in vitro*. *Biology of Reproduction*. 1989; 41: 268-276.

Eppig JJ and O'Brien MJ. Development *in vitro* of mouse oocytes from primordial follicles. *Biology of Reproduction*. 1996; 54: 197-207.

Eppig JJ, Hosoe M, O'Brien MH, Pendola FM, Requena A, Watanabe S. Conditions that affect acquisition of developmental competence by mouse oocytes *in vitro*: GSH, insulin, glucose and ascorbic acid. *Molecular and Cellular Endocrinology*. 2000; 163: 109-116.

Erickson BH. Development and radio response of the prenatal bovine ovary. *Journal of Reproduction and Fertility*. 1966; 11: 91-105.

Erickson BH. Development and senescence of the postnatal bovine ovary. *Journal of Animal Science*. 1966; 25: 800-805.

Fair T. Follicular oocyte growth and acquisition of developmental competence. *Animal Reproduction Science*. 2003; 78: 203-216.

- Fan TWM, Kucia M, Jankowski K, Higashi RM, Ratajczak J, Ratajczak MZ, Lane AN. Rhabdomyosarcoma cells show an energy producing anabolic metabolic phenotype compared with primary myocytes. *Molecular Cancer*. 2008; 7: 79-98.
- Feldman EC, Nelson KW. *Canine and feline endocrinology and reproduction*. Philadelphia, PA: WB Saunders Co. 1996; 741-768.
- Feng X, Page L, Ruben J, Chircus L, Colletti P, Pakrasi HB, Tang YJ. Bridging the gap between fluxomics and industrial biotechnology. *J Biomed Biotech*. 2010; 13.
- Ferreira C, Saraiva S, Catharino R, Garcia J, Gozzo F, Sanvido G, Santos L, Lo Turco E, Pontes J, Basso A, Bertolla R, Sartori R, Guardieiro M, Perecin F, Meirelles F, Sangalli J, Eberlin M. Single embryo and oocyte lipid fingerprinting by mass spectrometry. *Journal of Lipid Research*. 2010; 51: 1218-1227.
- Ferreira C, Eberlin M, Hallett JE, Cooks RG. Single embryo lipid analysis by desorption electrospray ionization and mass spectrometry. *Journal of Mass Spectrometry*. 2012; 47: 29-33.
- Fiehn O, Kopka J, Trethewey RN, Willmitzer L. Identification of uncommon plant metabolites based on calculation of elemental compositions using gas chromatography and quadrupole mass spectrometry. *Analytical Chemistry*. 2000; 72: 3573-3580.
- Fiehn O, Kopka J, Dormann P, Altmann T, Trethewey RN, Willmitzer L. Metabolite profiling for plant functional genomics. *Nature Biotechnology*. 2000; 18: 1157-1161.
- Folmes CDL, Nelson TJ, Martinez-Fernandez A, Arrell DK, Lindor JZ, Dzeja PP, Ikeda Y, Perez-Terzic C, Terzic A. Somatic oxidative bioenergetics transitions into pluripotency-dependent glycolysis to facilitate nuclear reprogramming. *Cell Metabolism*. 2001; 14: 264-271.
- Fortune JE. The early stages of follicular development: activation of primordial follicles and growth of preantral follicles. *Animal Reproduction Science*. 2003; 78: 135-163.
- Fouladi-Nashta AA, Campbell KHS. Dissociation of oocyte nuclear and cytoplasmic maturation by the addition of insulin in cultured bovine antral follicles. *Reproduction*. 2006; 131: 449-460.
- Gardner D, Lane M, Stevens J, Schoolcraft W. Noninvasive assessment of human embryo nutrient consumption as a measure of developmental potential. *Fertility and Sterility*. 2001; 76: 1175-1180.
- Goodrowe KL, Howard JG, Schmidt PM, Wildt DE. Reproductive biology of the domestic cat with special reference to endocrinology, sperm function and in vitro fertilization. *Journal of Reproduction and Fertility (Supp)*. 1989; 39: 73-90.

Gougeon A, Chainy GB. Morphometric studies of small follicles in ovaries of women at different ages. *Journal of Reproduction and Fertility*. 1987; 81: 433-442.

Grassian AR, Metallo CM, Coloff JL, Stephanopoulos G, Brugge JS. Erk regulation of pyruvate dehydrogenase flux through PDK4 modulates cell proliferation. *Genes & Development*. 2011; 25: 1716-1733.

Gudermuth DF, Newton L, Daels P, Concannon P. Incidence of spontaneous ovulation in young, group-housed cats based on serum and faecal concentrations of progesterone. *Journal of Reproduction and Fertility (Supp)*. 1997; 51: 177-184.

Guerin P, Rosset E, Rey M, Febvay G, Bruyere P, Corrao N, Neto V, Buff S. Amino acids in cat fallopian tube and follicular fluids. *Theriogenology*. 2012; 77: 558-562.

Gupta PSP, Nandi S. Isolation and culture of preantral follicles for retrieving oocytes for the embryo production: present status in domestic animals. *Reproduction in Domestic Animals*. 2012; 47: 513-519.

Gutierrez CG, Ralph JH, Telfer EE, Wilmut I, Webb R. Growth and antrum formation of bovine preantral follicles in long-term culture in vitro. *Biology of Reproduction*. 2000; 62: 1322-1328.

Hachey D, Parsons WR, McKay S, Haymond MW. Quantitation of monosaccharide isotopic enrichment in physiologic fluids by electron ionization or negative chemical ionization GC/MS using di-o-isopropylidene derivatives. *Analytical Chemistry*. 1999; 71: 4734-4739.

Hansen PJ. Effects of heat stress on mammalian reproduction. *Philosophical Transactions of the Royal Society B*. 2009; 364: 3341-3350.

Harris SE, Leese HJ, Gosden RG, Picton HM. Pyruvate and oxygen consumption throughout the growth and development of murine oocytes. *Mol Reprod Dev* 2009; 76: 231-238.

Hasegawa A, Hamada Y, Mehandjiev T, Koyama K. In vitro growth and maturation as well as fertilization of mouse preantral oocytes from vitrified ovaries. *Fertility and Sterility*. 2004; 81: 824-830.

Hasegawa A, Mochida N, Ogasawara T, Koyama K. Pup birth from mouse oocytes in preantral follicles derived from vitrified and warmed ovaries followed by in vitro growth, in vitro maturation, and in vitro fertilization. *Fertility and Sterility*. 2006; 86: 1182-1192.

Hayashi M, McGee EA, Min G, Klein C, Rose UM, van Duin M, Hsueh AJ. Recombinant growth differentiation factor-9 (GDF-9) enhances growth and differentiation of cultured early ovarian follicles. *Endocrinology*. 1999; 140: 1236-1244.

- Hemmings KE, Leese HJ, Picton HM. Amino acid turnover by bovine oocytes provides an index of oocyte developmental competence in vitro. *Biology of Reproduction*. 2012; 86: 1-12.
- Hildahl J, Taranger GL, Norberg B, Haug TM, Weltzien FA. Differential regulation of GnRH ligand and receptor genes in the brain and pituitary of atlantic cod exposed to different photoperiod. *General and Comparative Endocrinology*. 2013; 180: 7-14.
- Hiller K, Metallo CM, Kelleher JK, Stephanopoulos G. Nontargeted elucidation of metabolic pathways using stable-isotope tracers and mass spectrometry. *Analytical Chemistry*. 2010; 82: 6621-6628.
- Hirose M, Kamoshita M, Fujiwara K, Kato T, Nakamura A, Wojcikiewicz RJ, Parys JB, Ito J, Kashiwazaki N. Vitrification procedure decreases inositol 1,4,5-trisphosphate receptor expression, resulting in low fertility of pig oocytes. *Animal Science Journal*. 2013; 84: 693-701.
- Houghton FD, Hawkhead JA, Humpherson PG, Hogg JE, Balen AH, Rutherford AJ, Leese HJ. Non-invasive amino acid turnover predicts human embryo developmental capacity. *Human Reproduction*. 2002; 17: 999-1005.
- Iyer VV, Sriram G, Fulton DB, Zhou R, Westgate ME, Shanks JV. Metabolic flux maps comparing the effect of temperature on protein and oil biosynthesis in developing soybean cotyledons. *Plant, Cell, & Environment*. 2008; 31: 506-517.
- Jain M, Nilsson R, Sharma S, Madhusudhan N, Kitami T, Souza AL, Kafri R, Kirschner MW, Clish CB, Mootha VK. Metabolite profiling identifies a key role for glycine in rapid cancer cell proliferation. *Science Magazine*. 2012; 336: 1040-1044.
- Jemmett JE, Evans JM. A survey of sexual behavior and reproduction of female cats. *Journal of Small Animal Practice*. 1977; 18: 31-37.
- Jewgenow K, Goritz F. The recovery of preantral follicles from ovaries of domestic cats and their characterisation before and after culture. *Animal Reproduction Science*. 1995; 39: 285-297.
- Johnson J, Canning J, Kaneko T, Pru JK, Tilly JL. Germline stem cells and follicular renewal in the postnatal mammalian ovary. *Nature*. 2004; 428: 145-150.
- Kajiwara M, Mizutani M, Matsuda R, Hara KI, Kojima I. A new biosynthetic pathway of porphyrins from isopropanol. *Journal of Fermentation and Bioengineering*. 1994; 77: 626-629.
- Katz-Jaffe MG, McReynolds S. Proteomic/metabolomic analysis of embryos: current status for use in ART. *Biennial Review of Infertility*. 2011; 2: 245-253.

- Kidder GM, Vanderhyden B. Bidirectional communication between oocytes and follicle cells: ensuring oocyte developmental competence. *Can J Physiol Pharmacol.* 2010; 88: 399-413.
- Kikuchi N, Andoh K, Abe Y, Yamada K, Mizunuma H, Ibuki Y. Inhibitory action of leptin on early follicular growth differs in immature and adult female mice. *Biology of Reproduction.* 2001; 65: 66-71.
- Knight PG, Glister C. TGF-beta superfamily members and ovarian follicle development. *Reproduction.* 2006; 132: 191-206.
- Koek MM, Muilwijk B, van der Werf MJ, Hankemeier. Microbial metabolomics with gas chromatography/mass spectrometry. *Analytical Chemistry.* 2006; 78: 1272-1281.
- Koek M, Bakels F, Engel W, van den Maagdenberg A, Ferrari M, Coulier L, Hankemeier T. Metabolic profiling of ultrasmall sample volumes with GC/MS: from microliter to nanoliter samples. *Anal Chem.* 2010; 82: 156-162.
- Kouremenos KA, Harynuk JJ, Winniford WL, Morrison PD, Marriott PJ. One-pot microwave derivatization of target compounds relevant to metabolomics with comprehensive two-dimensional gas chromatography. *Journal of Chromatography B.* 2010; 878: 1761-1770.
- Kromer J, Quek L-E, Nielsen L. ¹³C-Fluxomics: a tool for measuring metabolic phenotypes. *Aus Biochem* 2009; 4: 17-20.
- Lawler DF, Johnston SD, Hegstad RL, Keltner DG, Owes SF. Ovulation without cervical stimulation in domestic cats. *Journal of Reproduction and Fertility (Suppl).* 1993; 47: 57-61.
- Lee WNP, Sorou S, Bergner EA. Glucose isotope, carbon recycling and gluconeogenesis using [U-¹³C₆]glucose and mass isotopomer analysis. *Biochemical Medicine and Metabolic Biology.* 1991; 45: 298-305.
- Leese HJ, Baumann CG, Brison DR, McEvoy TG, Sturmey RG. Metabolism of the viable mammalian embryo: quietness revisited. *Molecular Human Reproduction.* 2008; 14: 667-672.
- Leese HJ, Sturmey RG, Baumann CG, McEvoy TG. Embryo viability and metabolism: obeying the quiet rules. *Human Reproduction.* 2007; 22: 3047-3050.
- Leroy JLMR, Vanholder T, Delanghe JR, Opsomer G, Van Soom A, Bols PEJ, Dewulf J, de Kruif A. Metabolic changes in follicular fluid of the dominant follicle in high-yielding dairy cows early post partum. *Theriogenology.* 2004; 62: 1131-1143.

Leroy JLMR, Vanholder T, Delanghe JR, Opsomer G, Van Soom A, Bols PEJ, de Kruif A. Metabolite and ionic composition of follicular fluid from different-sized follicles and their relationship to serum concentrations in dairy cows. *Animal Reproduction Science*. 2004; 80: 201-211.

Leroy JLMR, Van Soom A, Opsomer G, Goovaerts IGF, Bols PEJ. Reduced fertility in high-yielding dairy cows: are the oocyte and embryo in danger? Part II. Mechanisms linking nutrition and reduced oocyte and embryo quality in high-yielding dairy cows. *Reproduction in Domestic Animals*. 2008; 43: 623-632.

Lofstedt RM. The estrous cycle of the domestic cat. *Compendium on Continuing Education for the Practising Veterinarian*. 1982; 4: 52-58.

Lucy MC. The bovine dominant ovarian follicle. *Journal of Animal Science*. 2007; 85: E89-E99.

Lucy MC. Regulation of ovarian follicular growth by somatotropin and insulin-like growth factors in cattle. *Journal of Dairy Science*. 2000; 83: 1635-1647.

Madla S, Miura D, Wariishi H. Optimization of extraction method for GC-MS based metabolomics for filamentous fungi. *Journal of Microbial & Biochemical Technology*. 2012; 4: 5-9.

Malandain E, Rault D, Froment E, Baudon S, Desquilbet L, Begon D, Chastant-Maillard S. Follicular growth monitoring in the female cat during estrus. *Theriogenology*. 2011; 76: 1337-1346.

McEvoy, TG, Coull, GD, Broadbent PJ, Hutchinson JSM, Speake BK. Fatty acid composition of lipids in immature cattle, pig and sheep oocytes with intact zona pellucida. *Journal Reproduction and Fertility*. 2000; 118: 163-170.

McGee EA, Spears N, Minami S, Hsu SY, Chun SY, Billing H, Hsueh AJ. Preantral ovarian follicles in serum-free culture: suppression of apoptosis after activation of the cyclic guanosine 3',5'-monophosphate pathway and stimulation of growth and differentiation by follicle-stimulating hormone. *Endocrinology*. 1997; 138: 2417-2424.

McGee EA, Smith R, Spears N, Nachtigal MW, Ingraham H, Hsueh AH. Mullerian inhibitory substance induces growth of rat preantral ovarian follicles. *Biology of Reproduction*. 2001; 64: 293-298.

McNatty KP, Smith P, Moore LG, Reader K, Lun S, Hanrahan JP, Groome NP, Laitinen M, Ritvos O, Juengel JL. Oocyte-expressed genes affecting ovulation rate. *Molecular and Cellular Endocrinology*. 2005; 234: 57-66.

- McRae C, Sharma V, Fisher J. Metabolite profiling in the pursuit of biomarkers for IVF outcome: the case for metabolomics studies. *International Journal of Reproductive Medicine*. 2013; 2013: 1-16.
- Merchant-Larios H, Chimal-Monroy. The ontogeny of primordial follicles in the mouse ovary. *Progress in Clinical Biological Research*. 1989; 296: 55-63.
- Meredith S, Dudenhoefter G, Jackson K. Classification of small type B/C follicles as primordial follicles in mature rats. *Journal of Reproduction and Fertility*. 2000; 119: 43-48.
- Metallo CM, Walther JL, Stephanopoulos G. Evaluation of ^{13}C isotopic tracers for metabolic flux analysis in mammalian cells. *Journal of Biotechnology*. 2009; 144: 167-174.
- Mitchell LM, Kennedy CR, Hartshorne GM. Effects of varying gonadotropin dose and timing on antrum formation and ovulation efficiency of mouse follicles *in vitro*. *Human Reproduction*. 2002; 17: 1181-1188.
- Mohammadi-Sangcheshmeh A, Held E, Ghanem N, Rings F, Salilew-Wondim D, Tesfaye D, Sieme H, Schellander K, Hoelker M. G6PDH-activity in equine oocytes correlates with morphology, expression of candidate genes for viability, and preimplantative *in vitro* development. *Theriogenology*. 2011; 76: 1215-1226.
- Morris JG. Idiosyncratic nutrient requirements of cats appear to be diet-induced evolutionary adaptations. *Nutrition Research Reviews*. 2002; 15: 153-168.
- Mu F, Williams RF, Unkefer CJ, Unkefer PJ, Faeder JR, Hlavacek WS. Carbon-fate maps for metabolic reactions. 2007; 23: 3193-3199.
- Mukaida T, Oka C, Goto T, Takahashi K. Artificial shrinkage of blastocoeles using either a micro-needle or a laser pulse prior to the colling steps of vitrification improves survival rate and pregnancy outcome of vitrified human blastocysts. *Human Reproduction*. 2006; 21: 3246-3252.
- Naib A, Wallace M, Brennan L, Fair T, Lonergan P. Metabolomic analysis of bovine pre-implantation embryos. *Reproduction, Fertility and Development*. 2009; 22: 230.
- Nandi S, Kumar VG, Manjunatha BM, Ramesh HS, Gupta PSP. Follicular fluid concentrations of glucose, lactate and pyruvate in buffalo and sheep, and their effects on cultured oocytes, granulosa and cumulus cells. *Theriogenology*. 2008; 69: 186-196.
- Nayudu PL and Osborn SM. Factors influencing the rate of preantral and antral growth of mouse ovarian follicles *in vitro*. *Journal of Reproduction and Fertility*. 1992; 95: 349-362.

- Nel-Themaat L, Nagy ZP. A review of the promises and pitfalls of oocyte and embryo metabolomics. *Placenta*. 2011; 32: S257-S263.
- Nishimoto H, Hamano S, Hill GA, Miyamoto A, Tetsuka M. Classification of bovine follicles based on the concentrations of steroids, glucose and lactate in follicular fluid and the status of accompanying follicles. *Journal of Reproduction and Development*. 2009; 55: 219-224.
- Niwa T. Procedures for MS analysis of clinically relevant compounds. *International Journal of Clinical Chemistry*. 1995; 241: 75-152.
- Owen OE, Kalhan SC, Hanson RW. The key role of anaplerosis and cataplerosis for citric acid cycle function. *The Journal of Biological Chemistry*. 2002; 277: 30409-30412.
- Paczkowski M, Silva E, Schoolcraft WB, Krisher PL. Comparative importance of fatty acid beta-oxidation to nuclear maturation, gene expression, and glucose metabolism in mouse, bovine, and porcine cumulus oocyte complexes. *Biology of Reproduction*. 2013; 88: 111, 1-11.
- Paik MJ, Kim KR. Sequential ethoxycarbonylation, methoximation and tert-butyltrimethylsilylation for simultaneous determination of amino acids and carboxylic acids by dual column gas chromatography. *Journal of Chromatography A*. 2004; 1034: 13-23.
- Palazoglu M, Fiehn O. Metabolite identification in blood plasma using GC/MS and the agilent fiehn GC/MS metabolomics RTL library. 1-8.
- Parrott JA, Skinner MK. Direct actions of kit-ligand on theca cell growth and differentiation during follicle development. *Endocrinology*. 1997; 138: 3819-3827.
- Parrott JA, Skinner MK. Kit-ligand/stem cell factor induces primordial follicle development and initiates folliculogenesis. *Endocrinology*. 1999; 140: 4262-4271.
- Pasikanti KK, Ho PC, Chan ECY. Gas chromatography/mass spectrometry in metabolic profiling of biological fluids. *Journal of Chromatography B*. 2008; 871: 202-211.
- Pepling ME, Spradling AC. Mouse ovarian germ cell cysts undergo programmed breakdown to form primordial follicles. *Developmental Biology*. 2001; 234: 339-351.
- Pérez-Crespo M, Pintado B, Gutiérrez-Adan A. Scrotal heat stress effects on sperm viability, sperm DNA integrity, and the offspring sex ratio in mice. *Molecular Reproduction and Development*. 2008; 75: 40-47.
- Pinero-Sagredo E, Nunes S, de los Santos MJ, Celda B, Esteve V. NMR metabolic profile of human follicular fluid. *NMR in Biomedicine*. 2010; 23: 485-495.

Quennell JH, Mulligan AC, Tups A, Liu X, Phipps SJ, Kemp CJ, Herbison AE, Grattan DR, Anderson GM. Leptin indirectly regulates gonadotropin-releasing hormone neuronal function. *Endocrinology*. 2009; 150: 2805-2812.

Raghu HM, Nandi S, Reddy SM. Effect of insulin, transferrin and selenium and epidermal growth factor on development of buffalo oocytes to the blastocyst stage *in vitro* in serum-free, semidefined media. *The Veterinary Record*. 2002; 151: 260-265.

Ratts VS, Flaws JA, Kolp R, Sorenson CM, Tilly JL. Ablation of bcl-2 gene expression decreases the numbers of oocytes and primordial follicles established in the post-natal female mouse gonad. *Endocrinology*. 1995; 136: 3665-3668.

Revelli A, Piane LD, Casano S, Molinari E, Massobrio M, Rinaudo P. Follicular fluid content and oocyte quality: from single biochemical markers to metabolomics. *Reproductive Biology and Endocrinology*. 2009; 7: 40-52.

Reynaud K, Cortvrindt R, Smits J, Driancourt MA. Effects of kit ligand and anti-kit antibody on growth of cultured mouse preantral follicles. *Molecular Reproduction and Development*. 2000; 56: 483-494.

Rieger D, Loskutoff NM. Changes in the metabolism of glucose, pyruvate, glutamine and glycine during maturation of cattle oocytes *in vitro*. *Journal of Reproduction and Fertility*. 1994; 100: 257-262.

Roessner U, Wagner C, Kopka J, Trethewey RN, Willmitzer L. Simultaneous analysis of metabolites in potato tuber by gas chromatography-mass spectrometry. *The Plant Journal*. 2000; 23: 131-142.

Runft LL, Watras J, Jaffe LA. Calcium release at fertilization of *xenopus* eggs requires type I IP₃ receptors, but not SH2 domain-mediated activation of PLC γ or G_q-mediated activation of PLC β . *Developmental Biology*. 1999; 214: 399-411.

Sakkas D, Morita H, Yamashita N, Kato O, Botros L, Roos P, Seli E. Evaluation of embryo quality by metabolomics: a new strategy to aid single embryo transfer. *Journal of Mammalian Ova Research*. 2008; 25: 26-31.

Seli E, Botros L, Sakkas D, Burns DH. Noninvasive metabolomic profiling of embryo culture media using proton nuclear magnetic resonance correlates with reproductive potential of embryos in women undergoing *in vitro* fertilization. *Fertility and Sterility*. 2008; 90: 2183-2189.

Seli E, Robert C, Sirard M. OMICS in assisted reproduction: possibilities and pitfalls. *Molecular Human Reproduction*. 2010; 16: 513-530.

Sepulveda S, Garcia J, Arriaga E, Diaz J, Noriega-Portella L, Noriega-Hoces L. In vitro development and pregnancy outcomes for human embryos cultured in either a single medium or in a sequential media system. *Fertility and Sterility*. 2009; 91: 1765-1770.

Shehab-El-Deen MAMM, Leroy JLMR, Fadel MS, Saleh SYA. Biochemical changes in the follicular fluid of the dominant follicle of high producing dairy cows exposed to heat stress early post-partum. *Animal Reproduction Science*. 2010; 117: 189-200.

Shikanov A, Xu M, Woodruff TK, Shea LD. A method for ovarian follicle encapsulation and culture in a proteolytically degradable 3 dimensional system. *Journal of Visualized Experiments*. 2011; 49.

Shille VM, Lundstrom KE, Stabenfeldt GH. Follicular function in the domestic cat as determined by estradiol-17 beta concentrations in plasma: relation to estrous behavior and cornification of exfoliated vaginal epithelium. *Biology of Reproduction*. 1979; 21: 953-963.

Shimasaki S, Moore RK, Otsuka F, Erickson GF. The bone morphogenetic protein system in mammalian reproduction. *Endocrine Review*. 2004; 25: 72-101.

Smitz JE, Cortvrindt RG. The earliest stages of folliculogenesis in vitro. *Reproduction*. 2002; 123: 185-202.

Soanes KH, Achenbach JC, Burton IW, Hui JPM, Penny SL, Karakach TK. Molecular characterization of zebrafish embryogenesis via DNA microarrays and multiplatform time course metabolomics studies. *Journal of Proteome Research*. 2011; 10: 5102-5117.

Sobolevsky TG, Revelsky AI, Miller B, Oriedo V, Chernetsova ES, Revelsky IA. Comparison of silylation and esterification/acetylation procedures in GC-MS analysis of amino acids. *Journal of Separation Science*. 2003; 26: 1474-1478.

Songsasen N, Fickes A, Pukazhenthil BS, Wildt DE. Follicular morphology, oocyte diameter and localisation of fibroblast growth factors in the domestic dog ovary. *Reproduction in Domestic Animals*. 2009; 44: 65-70.

Songsasen N, Spindler RE, Wildt DE. Requirement for, and patterns of, pyruvate and glutamine metabolism in the domestic dog oocyte in vitro. *Mol Reprod Dev* 2007; 74: 870-877.

Songsasen N, Wesselowski S, Carpenter JW, Wildt DE. The ability to achieve meiotic maturation in the dog oocyte is linked to glycolysis and glutamine oxidation. *Molecular Reproduction & Development*. 2012.

Songsasen N, Woodruff TK, Wildt DE. In vitro growth and steroidogenesis of dog follicles are influenced by the physical and hormonal microenvironment. *Reproduction*. 2011; 142: 113-122.

Spindler RE, Pukazhenti BS, Wildt DE. Oocyte metabolism predicts the development of cat embryos to blastocyst *in vitro*. *Mol Reprod Dev* 2000; 56: 163-171.

Sriram G, Fulton DB, Iyer VV, Peterson JM, Zhou R, Westgate ME, Spalding MH, Shanks JV. Quantification of compartmented metabolic fluxes in developing soybean embryos by employing biosynthetically directed fractional ¹³C labeling, two-dimensional [¹³C, ¹H] nuclear magnetic resonance, and comprehensive isotopomer balancing. *Plant Physiology*. 2004; 136: 3043-3057.

Steeves TE, Gardner DK. Metabolism of glucose, pyruvate, and glutamine during the maturation of oocytes derived from pre-pubertal and adult cows. *Molecular Reproduction and Development*. 1999; 54: 92-101.

Stoops MA, O'Brien JK, Roth TL. Gamete rescue in the african black rhinoceros (*diceros bicornis*). *Theriogenology*. 2011; 76: 1258-1265.

Sturmey R, Reis A, Leese H, McEvoy T. Role of fatty acids in energy provision during oocyte maturation and early embryo development. *Reproduction in Domestic Animals*. 2009; 44: 50-58.

Sunny NE, Parks EJ, Browning JD, Burgess SC. Excessive hepatic mitochondrial TCA Cycle and gluconeogenesis in humans with nonalcoholic fatty liver disease. *Cell Metabolism*. 2011; 14: 804-810.

Sutton-McDowall ML, Gilchrist RB, Thompson JG. The pivotal role of glucose metabolism in determining oocyte developmental competence. *Reproduction* 2010; 139: 685-695.

Sutton ML, Gilchrist RB, Thompson JG. Effects of *in-vivo* and *in-vitro* environments on the metabolism of the cumulus-oocyte complex and its influence on oocyte developmental capacity. *Hum Reprod Update* 2003; 9: 35-48.

Tamanini C, De Ambrogi M. Angiogenesis in developing follicle and corpus luteum. *Reproduction in Domestic Animals*. 2004; 39: 206-216.

Telfer EE, McLaughlin M. In vitro development of ovarian follicles. *Seminars in Reproductive Medicine*. 2011; 29: 15-23.

Torrance C, Telfer E, Gosden RG. Quantitative study of the development of isolated mouse pre-antral follicles in collagen gel culture. *Journal of Reproduction and Fertility*. 1989; 87: 367-374.

Tsutsui T, Stabenfeldt GH. Biology of ovarian cycles, pregnancy and pseudopregnancy in the domestic cat. *Journal of Reproduction and Fertility (Supp)*. 1993; 47: 29-35.

- Uchikura K, Nagano, M, Hishinuma M. The effect of ovarian status and follicular diameter on maturational ability of domestic cat oocytes. *J Vet Med Sci.* 2011; 73: 561-566.
- van den Hurk R, Zhao J. Formation of mammalian oocytes and their growth, differentiation and maturation within ovarian follicles. *Theriogenology.* 2005; 63: 1717-1751.
- Wagner J, Fall CP, Hong F, Sims CE, Allbritton NL, Fontanilla RA, Moraru II, Loew LM, Nuccitelli R. A wave of IP₃ production accompanies the fertilization Ca²⁺ wave in the egg of the frog, *xenopus laevis*: theoretical and experimental support. *Cell Calcium.* 2004; 35: 433-447.
- Wallace M, Cottell E, Gibney M, McAuliffe FM, Wingfield M, Brennan L. An investigation into the relationship between the metabolic profile of follicular fluid, oocyte developmental potential, and implantation outcome. *Fertility and Sterility.* 2012; 97: 1078-1084.
- Want EJ, Cravatt BF, Siuzdak G. The expanding role of mass spectrometry in metabolite profiling and characterization. *A European Journal of Chemical Biology.* 2005; 6:1941-1951.
- West ER, Xu M, Woodruff TK, Shea LD. Physical properties of alginate hydrogels and their effects on in vitro follicle development. *Biomaterials.* 2007; 28: 4439-4448.
- White KL, Pate BJ, Sessions BR. Oolemma receptors and oocyte activation. *Systems Biology in Reproductive Medicine.* 2010; 56: 365-375.
- Xia J, Mandal R, Sinelnikov IV, Broadhurst D, Wishart DS. MetaboAnalyst 2.0 – a comprehensive server for metabolomic data analysis. *Nucleic Acids Research.* 2012; 1-7.
- Xia J, Psychogios N, Young N, Wishart DS. MetaboAnalyst: a web server for metabolomic data analysis and interpretation. *Nucleic Acids Research.* 2009; 37: W652-W660.
- Xia J, Wishart DS. Web-based inference of biological patterns, functions and pathways from metabolic data using MetaboAnalyst. *Nature Protocols.* 2011; 6: 743-760.
- Yamamoto K, Otoi T, Koyama N, Horikita, N, Tachikawa S, Miyano T. Development to live young from bovine small oocytes after growth, maturation and fertilization in vitro. *Theriogenology.* 1999; 52: 81-89.
- Zamboni N, Sauer U. Novel biological insights through metabolomics and ¹³C-flux analysis. *Curr Opin Microbiol* 2009; 12: 553-558.